



**Gas Hydrate and Acoustically Laminated Sediments:
Potential Environmental Cause of
Anomalously Low Acoustic Bottom Loss
in Deep-Ocean Sediments**

MICHAEL D. MAX

*Acoustics Media Characterization Branch
Acoustics Division*

February 9, 1990

REPORT DOCUMENTATION PAGE			Form Approved OMB No. 0704-0188	
<small>Public reporting burden for this collection of information is estimated to average 1 hour per response, including the time for reviewing instructions, searching existing data sources, gathering and maintaining the data needed, and completing and reviewing the collection of information. Send comments regarding this burden estimate or any other aspect of this collection of information, including suggestions for reducing this burden, to Washington Headquarters Services, Directorate for Information Operations and Reports, 1215 Jefferson Davis Highway, Suite 1204, Arlington, VA 22202-4302, and to the Office of Management and Budget, Paperwork Reduction Project (0704-0188), Washington, DC 20503.</small>				
1. AGENCY USE ONLY (Leave blank)	2. REPORT DATE February 9, 1990	3. REPORT TYPE AND DATES COVERED Final		
4. TITLE AND SUBTITLE Gas Hydrate and Acoustically Laminated Sediments: Potential Environmental Cause of Anomalously Low Acoustic Bottom Loss in Deep-Ocean Sediments			5. FUNDING NUMBERS	
6. AUTHOR(S) Max, M. D.				
7. PERFORMING ORGANIZATION NAME(S) AND ADDRESS(ES)			8. PERFORMING ORGANIZATION REPORT NUMBER NRL Report 9235	
9. SPONSORING/MONITORING AGENCY NAME(S) AND ADDRESS(ES) Office of Naval Research Arlington, VA 22217-5000			10. SPONSORING/MONITORING AGENCY REPORT NUMBER	
11. SUPPLEMENTARY NOTES				
12a. DISTRIBUTION/AVAILABILITY STATEMENT Approved for public release; distribution unlimited.			12b. DISTRIBUTION CODE	
13. ABSTRACT (Maximum 200 words) <p>Gas hydrates (clathrates) are solid, icelike crystalline compounds formed from mixtures of water and certain gas molecules. They are an important secondary geological attribute of deep-ocean sediments, whose presence has been detected only recently. They are stable under medium-to-high hydrospheric pressures and low temperatures typical of ocean basin near-surface sediments, and they form in blankets up to 1100-m thick at the top of the sediment column. They have been identified in virtually all ocean basins, continental shelves, and deep lakes. Because of the extreme pressure in the deep-ocean basins and the generally low temperatures at which hydrates are stable, gas produced in deep-ocean, near-surface sediment or rising into it from below, will be transformed into gas hydrate. P-wave acoustic velocity of gas hydrates appears to be in the 2.5 to 4.5 km/s range, although sediment-gas hydrate is more commonly in the 2.3 to 3.4 km/s range. The presence of hydrates and the velocity structure they impart to bottom sediments can radically alter overall geoacoustic response.</p> <p>Three environmental cases have been modeled for 10 Hz, 50 Hz, and 1 kHz; unhydrated sediment, hydrated sediment, and hydrated sediment with bottom-simulating reflector (BSR) caused by subjacent free gas. At frequencies below 350 ± 50 Hz, there is a direct relationship between reflection-loss coefficient and frequency; lower frequencies show lower loss. Above 400 Hz, the effect of gas hydrates is less, and reflection loss is less frequency-dependent.</p>				
14. SUBJECT TERMS Gas hydrate, Anomalous low-bottom loss Acoustic-impedance enhancement Abysal sediments Energy resource Bottom-simulating reflector (BSR)			15. NUMBER OF PAGES 73	
			16. PRICE CODE	
17. SECURITY CLASSIFICATION OF REPORT UNCLASSIFIED	18. SECURITY CLASSIFICATION OF THIS PAGE UNCLASSIFIED	19. SECURITY CLASSIFICATION OF ABSTRACT UNCLASSIFIED	20. LIMITATION OF ABSTRACT SAR	

CONTENTS

1.0 INTRODUCTION	1
1.1 Acoustic Bottom Interaction and the Need To Reassess Concepts of the Physical State of Sediments in the Seafloor	1
2.0 GAS IN SEA BOTTOM SEDIMENTS	3
2.1 Occurrence and Distribution of Gas in the Sea Bottom	3
2.2 Physical States of Gas in the Seafloor and their Physical Effects on Acoustic Propagation	4
2.3 Nature of Gas Hydrates	5
2.4 Recognition of Gas Hydrate	7
2.5 Formation of Gas Hydrate	9
2.6 Extent and Distribution of Gas Hydrate	14
2.7 Physical Properties of Gas Hydrates	20
2.8 Acoustic Effects of Gas and Gas Hydrates	21
2.8.1 Acoustic Turbidity, Gas Blanking, Wipeout, Smear	21
2.8.2 Amplitude Anomalies, Bright Spots, Pull-Downs	22
2.8.3 Nature of the Bottom-Simulating Reflector (BSR)	24
2.9 The Hydrate Layer; the Need for More Information	26
2.10 Inherent Stability of the Gas Hydrate Blanket	28
2.11 Hydrated Sediments with BSR and PBSR	29
2.12 Possible Alteration in Sediment Surface Owing to the Presence of Gas and Gas Hydrate	29
3.0 ACOUSTICALLY LAMINATED SEDIMENTS	30
3.1 Implications of Acoustic Structure in Bottom Sediments	30
3.2 Acoustic Impedance, Acoustic Structure, and Reflection Coefficients Within the Bottom	30
3.2.1 Primary Factors	30
3.2.2 Secondary Factors	31
3.3 Naturally Occurring Frequency Dependence of Bottom Loss	34
4.0 NAVY GEOACOUSTIC BOTTOM-LOSS CHARACTERIZATION	36
4.1 Predicting Geoacoustic Response Through Modeling	36
4.2 Primary and Secondary Geological Attributes	37
4.3 Geoacoustic Physical Parameters and their Representation as Physical Models	38

5.0	GEOPHYSICAL AND GEOACOUSTIC MODEL OF DEEP-OCEAN SEDIMENTS CONTAINING GAS HYDRATE	40
5.1	Purpose of Modeling	40
5.2	Source of Velocity Profiles	43
5.2.1	Unhydrated Sediment as Reference	43
5.2.2	Hydrated Sediments	44
6.0	TRANSMISSION LOSS CAUSED BY THE PRESENCE OF GAS HYDRATE AND PBSR	46
6.1	Geoacoustic Modeling and Prediction of Bottom Loss	46
6.2	Results of the Model Predictions for Transmission Loss	47
6.2.1	Environmental Situation 1—Generalized Hydrate Layer	47
6.2.2	Environmental Situation 2—Thoroughly Saturated Layer and Shallow PBSR	53
6.3	Gas Hydrate and PBSR Bottom Loss Effect: Conclusions	53
6.4	Frequency Dependence of Low Grazing Angle Loss	53
6.5	Modeling of the Bottom-Interaction Effects Caused By the Presence of the Gas Hydrate Layer	56
7.0	DETERMINING THE SEISMOACOUSTIC CHARACTER OF THE GAS HYDRATE LAYER AND THE NEED FOR IN SITU MEASUREMENT	57
8.0	SIGNIFICANCE OF IN SITU GAS AND GAS HYDRATES AND THEIR GEOACOUSTIC-ENVIRONMENTAL IMPLICATIONS: CONCLUSIONS	59
9.0	ACKNOWLEDGMENTS	60
10.0	REFERENCES	60

GAS HYDRATE AND ACOUSTICALLY LAMINATED SEDIMENTS: POTENTIAL ENVIRONMENTAL CAUSE OF ANOMALOUSLY LOW ACOUSTIC BOTTOM LOSS IN DEEP-OCEAN SEDIMENTS

1.0 INTRODUCTION

1.1 Acoustic Bottom Interaction and the Need to Reassess Concepts of the Physical State of Sediments in the Seafloor

Acoustic energy transmission in the sea generally becomes weaker with increasing distance from any source of interest. This diminution of signal occurs because the propagating energy travels outward in all directions from the source and, at the first arrival of any wave front, naturally spreads the energy over a broader area and a greater volume. These spreading losses can be related to spherical and then cylindrical spreading curves as the water volume becomes filled (Urick 1975) with respect to ray-path variation induced by the nonlinear sound speed profile in a water mass. Apart from minor special cases, transmission loss tends to be proportional to distance from the source.

Although water-volume scattering losses may occur because of propagation through anomalous water masses such as gas or plankton-rich water or through large schools of fish, these losses tend to be stratified or otherwise localized within the water column. Water-body fronts and thermoclines that refract acoustic energy do not necessarily diminish sound levels in the water; water-column temperature, density, and salinity variations (Hurdle 1986) usually cause a repositioning of wave propagation phenomena such as convergence zones and also often form shadow zones. This report does not explain the often rapidly changing acoustic properties within the water column or the sea surface, however, but concentrates on less transient properties of the sea bottom and subbottom.

Bottom loss is a general term that describes a reduction of acoustic propagation energy attributable to interaction with the bottom environment (bottom is used throughout to refer to both bottom and subbottom). Bottom-interaction effects on acoustic transmission are more dramatic than the variation seen in water volume alone, because the bottom is more complicated in its physical parameters and their dispositions. Acoustic energy interacting with the bottom usually introduces surprising propagation and reflection phenomena that have proven difficult to predict.

In shallow water, a number of environmental parameters control bottom loss, which either do not occur or are more significant to acoustic propagation than they are in deep water. Subsea permafrost, hardground surfaces, soil zones in variable degrees of alteration, glacial effects, a wide variety of acoustic basement roughness, different materials, and complexly disposed sequences of oriented impedance contrasts are common in shallow water and rare to absent in deep-ocean basins. Also, accentuated transmission loss is caused by intensive bottom interaction because of the narrowness of the sound duct; acoustic energy in shallow water encounters these rock and sediment materials

of vastly differing acoustic-interaction character more often, thus enhancing their effect. *Asymmetrical fine-scale morphology and subbottom disposition of oriented geological components are often azimuthally variable and introduce quite different responses from place to place with intensive bottom-acoustic interaction. Shallow-water geoacoustics, however, and are not considered in detail in this report.*

The focus here is deep-water-sediment geoacoustic response. The intent is not to review primary geoenvironmental factors, such as particular rock and sediment variations (type, sedimentology, geochemistry) and dispositions (mapping different sediments) within the sea-floor or any particular site. The intent is to examine two important and subtle secondary or diagenetic geoenvironmental factors that induce significant variations from the expected geoacoustic response, especially in deep-sea sediments. Bottom-acoustic character of deep-water sediments may be more strongly affected by secondary geoacoustic parameters than by primary parameters. Recognizing the significance of secondary geoenvironmental attributes should cause a widespread reassessment of the overall seismoacoustic character of ocean floor sediments and radically change the ways in which these properties are currently estimated.

Methane and related gases in the seafloor occur as free gas, as gas solution in fluid, and at high pressures typical of deep oceans, and gas molecules bond with water to form crystalline solids. These solids are gas hydrates—important secondary geoenvironmental attributes of the seafloor. They occur commonly within ocean-bottom sediments and are more common in more porous and permeable materials. Their presence in the seafloor has recently become known, and their extent and variability in the world's oceans remain to be established. Nonetheless, what is known about hydrates suggests that their presence radically alters the geoacoustic character of host sediments—at least in the uppermost part of the sediment column of greatest importance in bottom-acoustic interaction and acoustic transmission relevant to Navy interests.

Hydrates are ephemeral in nature. While they are the stable form of methane in the deep oceans, normal sampling of the seafloor sediments has not revealed their presence, because they invert to gas and dissipate during recovery to the surface. Also, where they have been recovered, they have been treated as a local scientific curiosity, and their widespread nature has not generally been realized. Although their acoustic character is known, application of this knowledge has not been made available in a manner that is relevant to Navy needs. This report demonstrates the probable widespread development of gas hydrates, examines their physical properties, and determines their seismoacoustic character to quantify these bottom-acoustic variations relevant to Navy acoustic interests.

Gas hydrates act in two ways to alter bottom-acoustic interaction. First, they can accentuate acoustical lamination, which will strongly affect the **reflective character** of the sediment by lowering bottom loss. Second, thick hydrate development probably introduces strongly upward refracting velocity profiles and lowers attenuation; this allows for significant **refraction** and overall lower loss. Both effects are impossible to predict by extrapolating existing laboratory measurements of deep-sea-sediment primary geoenvironmental parameters to the sea-bottom environment. It is likely that bottom-acoustic interaction will be predictable only when the full range of primary and secondary geoenvironmental parameters are taken into account.

2.0 GAS IN SEA-BOTTOM SEDIMENTS

2.1 Occurrence and Distribution of Gas in the Sea Bottom

Although many gases occur naturally on the sea bottom (such as carbon dioxide, helium, and sulfur dioxide), the gases that are of primary interest here are low density hydrocarbons (such as methane through propane (natural gas)), which are commonly found in sea-bed sediments and hydrate. Gas can be produced biogenically on or just below the seafloor from the natural decay of debris that incessantly drifts down to the seafloor. It also may be derived by petrogenic gas produced through thermal distillation of primitive hydrocarbons in the marine sediments caused by elevated temperatures and pressures resulting from burial, tectonism, or abnormal heat flow. This is the dominant formation mechanism of most methane gas found in rocks and sediments. Natural gas also can be produced through igneous and volcanic processes when melt rock from the depths crystallizes and fractionates as it responds to changes in temperature and pressure and leaves a liquid-gas residue. Seafloor metamorphism may also evolve gas.

The likelihood of sedimented areas in the seafloor to evolve gas is determined by a number of circumstances. The detailed chemistries and the nature of the organic residues in the sediments are often as important as the bulk organic-carbon materials present; lipids and carbohydrates, for instance, have a greater potential to produce gas and hydrocarbons than does cellulose. Factors that favor gas generation in sediments include:

- Sediments with high and irregular rates of sedimentation, where a high degree of raw organic carbon materials is incorporated rather than being oxidized in the water column or on the sea bottom,
- Sediments with a high degree of biogenic material, and particularly sediments with a high proportion of material derived originally on land areas or continental shelves (Romankevich 1984), and
- Sediments overlying the lithosphere, which has moderate-to-high geothermal gradients that will act to generate or stimulate gas generation. High-geothermal gradients may also serve to thin the hydrate zone and thus allow more of the sediment section to contain gas.

Gas can be mobilized within sediment by diapirs, mud volcanos, and seismic shocks and then is naturally driven upward through buoyancy. Gas commonly migrates in the interstitial spaces of seafloor sediment. Some rocks can also hold gas but because the porosities of rock are small in comparison with sediments, this is inconsequential in grossly affecting acoustic-bottom interaction. Direct observation of gas rising from the seafloor is often seen in the water column as concentrations of gas bubbles (McCartney and Bary 1965; Nelson et al. 1978; Zonenshayn et al. 1987; and Hovland and Judd 1988). These water-column anomalies are often associated with subsurface geological features, such as faults or diapirs, and with acoustic evidence for gas presence in the subjacent sediments.

Pockmarks in the seafloor are collapse features that are associated with sudden exhalation of gas; these are observed by side-scan sonar in the shallow water of the Barents and North Seas (Hovland 1982; Solheim and Larsson 1987) and on virtually all low-to-mid-latitude continental shelves. A few surveys have found pockmarks in the deep oceans and in the polar regions (Hovland and Judd 1988). Zonenshayn et al. (1987) record pockmark fields associated with gas blowouts and relic

vertical-gas-channel pits associated with subbottom caverns and grottoes in 800-m water depths in the Sea of Okhotsk. Blowouts are often associated with the formation of carbonate cement and nodular crusts as a result of the methane oxidation in the presence of dissolved calcium carbonate.

Pockmarks in ocean sediments at depths of 4400 to 4800 m along the Blake Outer Spur (off the southeast coast of the United States) that are usually attributed to gas venting in shallower water are regarded as probably having been formed by venting subsurface water (Paull and Dillon, 1981); owing to high pressure and low-ambient-bottom temperatures (2.2°C), gas hydrate would be expected to form in the presence of gas (Hovland and Judd 1988). Cratering in deep ocean areas such as the Gulf of Mexico (Prior et al. 1989), however, has been attributed to the sudden release of large quantities of petrogenic gas by diapiric piercement or by fracturing of a gas hydrate trap rock in the uppermost sediments. Because free gas often exists beneath the hydrate layer, and gas blowout inevitably produces cratering, the presence of cratering and collapse structures can probably be used to widely infer the presence of both gas and gas hydrate in seabed sediments, regardless of water depth.

Gas in shallow-water sea-bed sediments has been investigated thoroughly by the hydrocarbon exploration industry because of economic and safety considerations. In the first instance, gas in appreciable and recoverable deposits is a valuable energy source (U.S. Department of Energy (DOE) 1987). The estimated gas hydrate reserves in the Gulf of Mexico alone are estimated to be 200 to 2000 trillion cubic feet (Bennet 1988). Second, shallow gas deposits introduce important variations in physical properties of the seabed sediments; shallow gas is usually associated with engineering difficulties and is a safety hazard in platform siting and drilling procedures. Regardless, investigations have revealed many physical characteristics that are of substantial interest to the Navy in assessing and predicting bottom-acoustic interaction.

2.2 Physical States of Gas in the Seafloor and Their Effects on Acoustic Propagation

Methane is found in many physical states in the sea bottom. Low-density hydrocarbons, especially methane, are found

- (1) as concentrations of free gas that displace fluids and induce high attenuation and lower sound speeds;
- (2) dissolved in fluids with varying degrees of gas saturation that affect attenuation and sound speeds;
- (3) dissolved in bituminous masses that may impart a variable viscosity and scattering potential; and,
- (4) as solids in the form of a gas-water crystalline or pseudocrystalline compound (gas hydrate) that strongly raises the acoustic velocity and lowers attenuation of sediments that they occur within.

The characteristic high pressures and low temperatures found in deep-sea bottoms make hydrate the thermodynamically stable phase of methane and its related hydrocarbons. Because the stable form of methane and its related short-chain hydrocarbons are not gas in the deep ocean seafloor, but components in crystalline solids, the seismoacoustic properties of sediments where hydrates develop can be expected to be radically different from the properties of unhydrated sediment.

2.3 Nature of Gas Hydrates

Gas hydrates are solid, icelike compound substances in which cubic crystalline lattices are formed by water and a variety of gas molecules. In appearance, gas hydrates are clearly defined transparent-to-translucent crystals, whose forms and crystal geometry depend on the state of hydrate formation and the nature of the entrapped gas. Gas, primarily methane, is held within this lattice and thermodynamically stabilizes the compound crystals through hydrogen bonding. These compounds can form and become stable at temperatures well above the freezing point of water. Hydrates are non-stoichiometric, forming when enough gas molecules are enclosed to thermodynamically stabilize the hydrate. However, this allows gas to be entrapped up to saturation within the lattice up to saturation. One volume of water commonly binds from 70 to 220 volumes of gas. Voids in the atomic lattice of hydrate become increasingly occupied at lower temperatures and higher pressures. Gas hydrate volume is determined by gas composition, reservoir water mineralization, geothermal gradient, and pressure. Water molecules as hydrates and voids are under pressure from the entrapped gases that are bound in the structure.

These substances are termed "clathrates," from the Latin word *clathratus*, which means enclosed by bars of grating (Barrer and Stuart 1957). Methane, ethane, and propane are the most common host gases currently recognized as forming hydrates in the seafloor. Naturally occurring gases that are not hydrogen-carbon based dissolve in fluids but do not commonly appear to form hydrates even though they have the potential to do so (Fig. 1). These preliminary stability fields for the gas hydrate species may alter substantially as more crystallographic and physical research in the gas hydrate field is carried out. Makogon (1988) states that all gases whose molecule size is smaller than about 7 Å—except hydrogen, helium, and neon—can form hydrated clathrates.

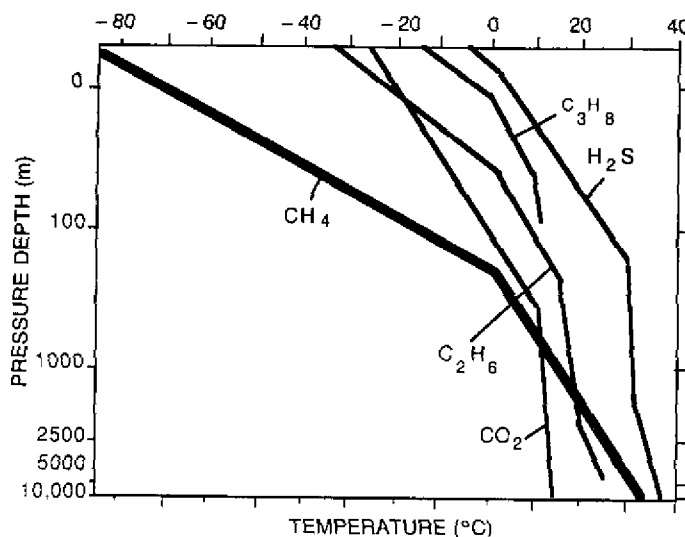


Fig. 1 — Conditions of hydrate formation for different gases. From Makogon (1988). Replotted with temperature in normal scale and pressure-depth in meters recalculated from logarithmic absolute pressure scale. 0 is atmospheric pressure at sea level. CH₄, methane; C₂H₆, ethane; C₃H₈ propane; C₄H₁₀, butane, the most dense of the paraffin gases probably has a diffusion rate too slow to allow formation as a clathrate. No stability data, probably exists, along with pentane, as a fluid at depth; CO₂, carbon dioxide; H₂S, hydrogen sulphide.

The most common hydrated gas appears to be the lightest paraffin methane, although ethane, propane, and some butane also have been identified in hydrate specimens (Fig. 2). Two different crystalline structures in the cubic system may form, but only Structure I gas hydrates are expected in nature. Structure II hydrates, which are less densely packed structures that accommodate varying gas molecule atomic radii, only occur if the gas is rich in propane and isobutane relative to methane (Davidson 1973; Kvenvolden 1988). Other polymers in the naphthene series also occur in hydrates but are more rare (Table 1). Structure II hydrates may occur at near atmospheric temperatures and pressures (Matthews, private communication) and are not as pressure dependent in their thermodynamic stability range as Structure I hydrates. Brooks and Bryant (1985) discuss molecular structure and the geochemistry of the gas hydrate water system.

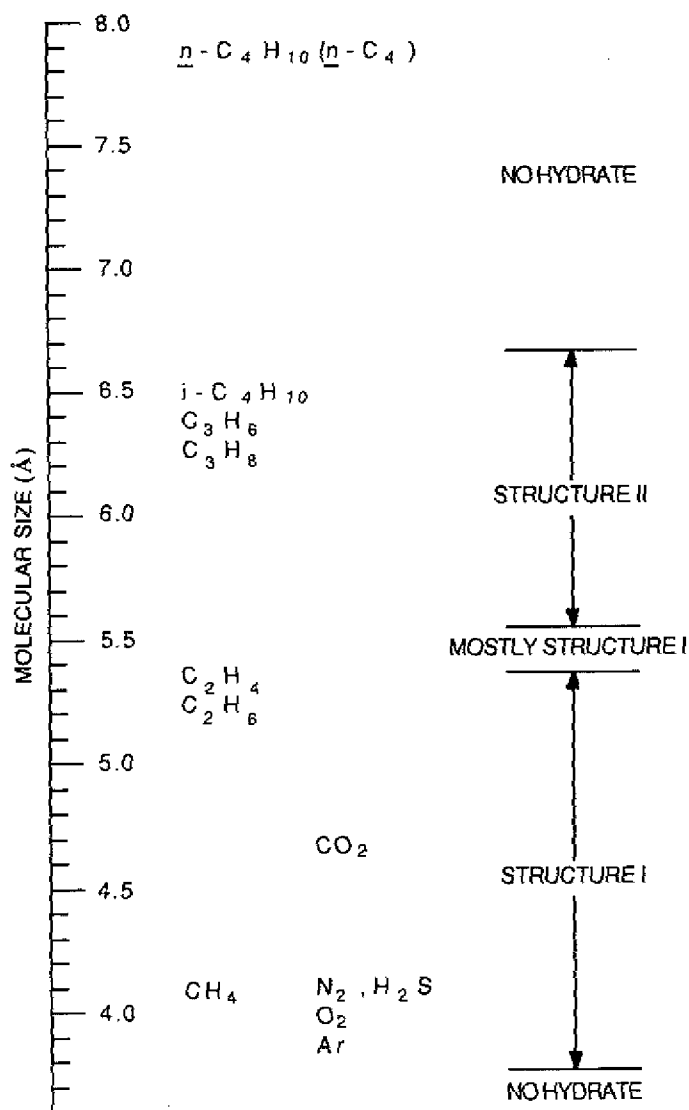


Fig. 2 — Diagram of paraffin series natural gas and other gases in relation to atomic size of molecules. The largest allowable size of gas molecules that can be incorporated in the natural gas clathrate series is 6.7 Å. Structure I shows body centered cubic lattices; Structure II shows face centered lattices (diamond packing). After Davidson (1973) and Hand et al. (1974).

Table 1 — Composition of Gases Recovered from Pressure-Core Barrels at Site 533 (DSDP/IPOS Leg 76). C₁, methane; C₂, ethane; C₃, propane; C₄, butane; C₅, pentane. Oxygen, hydrogen sulfide, nitrogen, etc. occurred but were not analyzed. Because of the difficulty of handling the very high pressure specimens, the percentage of hydrate in pore spaces was not determined.

Core No.	Cylinder No.	Interval (m)	C ₁ (%)	C ₂ (ppm)	C ₃ (ppm)	i-C ₄ (ppm)	n-C ₄ (ppm)	i-C ₅ (ppm)	n-C ₅ (ppm)	CO ₂ (%)
23	3,4	332.5-340.3	76	102	4.2	1.8	0.5	0.8	0.6	1.5
23	12	"	96	171	5.8	1.9	0.7	1.2	0.5	0.9
23	13	"	95	143	5.7	1.5	0.5	0.8	1.1	0.4
23	14	"	90	179	5.7	3.0	0.7	1.6	0.3	5.0
23	15	"	90	181	8.5	4.5	0.0	0.5	0.2	4.7
26	6	361.0-368.8	7.0	13	0.7	0.2	0.2	0.2	0.1	0.04
29	3	392.2-399.0	94	234	6.1	1.5	0.6	0.3	0.2	0.2
29	9	"	97	242	8.0	1.6	0.7	0.5	0.3	0.5
29	FR	"	96	237	11.9	2.5	1.5	1.3	0.6	1.8
29	LB-1	"	97	237	12.5	4.0	1.6	1.7	0.8	0.3
29	LB-3	"	94	230	15.8	4.5	2.0	2.2	1.5	1.9
29	LB-6	"	94	223	18.5	5.5	2.4	2.7	1.3	2.4

2.4 Recognition of Gas Hydrate

Gas hydrates were virtually unrecognized as a naturally occurring component of rocks and sediments prior to 1970, and little published information was available prior to 1980. Malone (1983) has an extensive reference list about the early recognition and other aspects of clathrates. The study of gas hydrates to date has been driven largely by their potential as a major energy resource. The lack of research into their disposition, physical properties, and other attributes since 1983 (DOE 1987) reflects the low cost of other, more readily available sources of hydrocarbon energy and the lack of government interest. Economic assessment of hydrates and gas concentrated below gas hydrate is recent and is currently proceeding at a very low level. Very few scientific publications have focused on economic assessments of gas hydrate or gas trapped below hydrates.

Gas hydrates formed from natural gas were known as academic chemical curiosities for 100 years before they came to the attention of scientists during the 1930s when clogged gas and oil pipelines were found to be obstructed by white crystalline masses identified as hydrates of natural gas. Applied research into the nature of these crystals was conducted to solve the economic problems they caused. These low-pressure gas hydrates had large proportions of heavier gas, such as ethane and butane, that are stable at lower pressures than methane hydrate. Pipeline clogging by hydrates was solved by adding liquid methanol alcohol to the pipeline, which retards the formations of hydrate crystals in much the same way that antifreeze in water systems blocks the formation of ice by drying or removing water from the fluid prior to transport (DOE 1987).

Gas hydrates are a recently recognized natural phenomena that was thought to be a peculiar feature of subareal permafrost terrains in the Arctic (Collett 1983; Makogon 1988). Gas hydrate in the

oceans was originally identified on continental shelves where subsea permafrost extends out from land beneath the sea floor to the edge of the continental shelf. The compound hydrate/water-ice permafrost horizon was identified in Arctic regions of northern Alaska, Canada, and Siberia in drill cores and seismic shocks during the 1950s and 1960s. Hydrates have since been identified in the Barents Sea, where it is thought to have formed independently of the presence of permafrost (Solheim and Larsson 1987) and in other continental shelves and slopes at moderate depths where the formation of permafrost could never have taken place. In the deep-oceans, where it may be almost ubiquitous, hydrates must have formed independently from water-ice and are no longer regarded as an ice-related phenomenon found only in permafrost terrane.

In 1972, the ARCO and EXXON Corporations first recovered a pressurized specimen of naturally occurring gas hydrate from a depth of 666 m from a Prudhoe Bay, Alaska, exploration well (Collett 1983). Makogon (1981) reported that the Messoyakha hydrocarbon field in western Siberia had methane reserves in the form of gas hydrates on the order of hundreds of billions of cubic meters. Komar (1986) reports that a single Soviet gas hydrate discovery in Siberia has the potential to supply European energy demands for centuries (IARPC 1987). Significant quantities of gas hydrates have since been detected in many permafrost regions and on the continental shelves of the USSR and North America (Kvenvolden and McMenamin 1980).

The recognition of gas hydrate in deep-ocean sediments was a major contribution of the deep-sea drilling projects; this confirmed the earlier tentative identification from seismic reflection records (Kvenvolden and Barnard 1982; Kvenvolden and McDonald 1982; and Paull and Dillon 1981). An acoustically more transparent zone in the upper sediment that later was positively identified as gas hydrate provided the important drilling target. The presence of gas hydrates had been put forward as a likely explanation of the unexpected upper-sediment seismic response (Stoll et al. 1971; Bryan and Markle 1966; and Markle et al. 1970). Prior to the drilling, however, there was no consensus about what might be causing the mysterious acoustic character. Lancelot and Ewing (1973) are regarded as the first to confirm gas hydrates in ocean-floor sediments from drilling that could be correlated with seismic records.

During the initial drilling, several attributes of the target horizon became apparent. First, unexpectedly great quantities of gas were liberated, and drilling mud was blown all over the drill ship. Second, drill targets interpreted from the seismic record could only be correlated with the drill core if ridiculously high velocities were used for the (hydrate) upper sediment, acoustically imaged blanket (Ewing, private communication). Subsequently, pressurized cores were taken, and both the crystalline structure and chemical content were analyzed; the presence of gas hydrates in deep-ocean sediments was confirmed.

Hydrates from the deep-oceans have been recovered by direct sampling with a pressurized core barrel of 5.8 m in length and 5.8 cm in diameter (Kvenvolden et al. 1982). The hydrate specimens were maintained at in situ pressures (of ~ 34.4 MPa) and temperatures at or below ocean bottom and subbottom ambient (Table 1). Only gas composition was analyzed; other information, such as hydrate percentages of porosity, degree of hydrate saturation and the acoustic velocity and its structure was not investigated because of the difficulty of handling the very high-pressure cores.

2.5 Formation of Gas Hydrate

Formation of gas hydrates in oceans is a world-wide phenomenon because gas hydrates are predominantly affected in their formation and stability field by the elevated pressures that are a common feature of deep-ocean basins. Gas hydrate stability is less sensitive to slight changes in normal bottom water temperature.

Gas produced within the deep-water subbottom by any mechanism tends either to vent into the water column from where it may eventually find its way into the atmosphere or be bound in some manner within the seabottom sediments and rocks. Methane gas is produced both biogenically (bacteriological decay) and thermogenically (petrogenetically) as deposited sediments become heated during burial. Because of its low density, methane is extremely buoyant and has the potential to migrate upward rapidly or upward and laterally when obstructed from its direct upward migration by a geological "cap."

Undersaturated gas hydrate, which is produced by the initial crystallization process, is lighter than water. If hydrates form in the water column, they will rise and degrade to gas. Unidentified particles that were regarded as possibly being gas-hydrate crystals with a density similar to the ambient water have been observed, however, during deep-diving operations (Markle, private communication).

Gas hydrates have been widely recognized on continental slopes and in continental rise sediments, but their presence in abyssal depths is less well substantiated because of inappropriate survey and sampling techniques. Abyssal plains, for instance, are not usually the subject of seismic surveys of the resolution necessary to predict the presence of possible hydrates; the general bedding parallel reflectors in these sediments would also camouflage their presence. In addition, organic detritus descending to abyssal depths may have been bacteriologically degraded with consequent gas production in the water before it can become incorporated in the bottom. Close examination of seismic records, however, can reveal the presence of gas hydrate where its presence may be obscured by other seismoacoustic signals (Cooper et al. 1986).

Empirical data suggest that the strongest acoustic reflectivities (low bottom loss) occur in abyssal plain areas where the presence of gas hydrate is regarded as the most likely cause of the anomalous acoustic return (Edgar, private communication). In addition, both the presence of gas hydrate and acoustically laminated bottom are already recognized in Navy documentation as likely causes for this anomalous response (Monet et al. 1983), but a relationship between the presence of gas and gas hydrate and the enhancement of laminated acoustic structure has not been proposed previously. Because gas hydrate is now known or inferred to be so potentially widespread as a secondary geological attribute of deep-ocean sediments, its physical properties, especially those that affect the transmission of acoustic energy, are very important.

Gas hydrate can form and accumulate at any place having suitable gases, appropriate thermodynamic conditions, and unbound water. Areas of abnormally high heat flow, hydrothermal activity, and low methane production, for instance, are unsuitable for hydrate formation; the majority of the ocean-basin areas, which are moderately to thickly sedimented, appear to have suitable conditions for sediment formation. The thermodynamics of hydrate formation are such (Godbole and Kamath 1987) that water-saturated solutions of methane and more dense paraffin series gas will form hydrates slowly enough to allow sufficient gas to diffuse through a porous sediment so that broad zones in which hydrate is stable can be suffused with the highly diffusible natural gas.

Hydrate zones can form in a variety of ways. Gas and water permeability through gas hydrate can be very low. An early formed hydrate layer in sediment may comprise an excellent diagenetic cap to continuing upward migration of as yet unhydrated gas. Gas hydrates can thus be selfregenerating deposits in sediments because early-formed hydrate will act to trap subsequently formed gas and gas migrating from below and allow it to hydrate. Hydrate in the deep-oceans probably has formed by upward gas migration into a zone of methane hydrate stability. Existing hydrate deposits also could be part of a preexisting gas reservoir that was frozen in situ; this situation would be confined to permafrost terrane. Gas hydrates coexist with both water-ice and water at relatively low containing pressures in the near-shore area of the North Slope of Alaska (Lachenbruch et al. 1988) and reflect the original conditions of formation.

The optimum conditions for formation of gas hydrate are found in thickly sedimented areas of the deep ocean where significant quantities of gas can be produced petrogenetically in the lower part of the sedimentary column. The nature of the sediments must allow the gas to percolate upward, driven by buoyancy, where it enters the zone of hydrate stability and becomes fixed. A thickly sedimented area that has a rapid rate of sedimentation involving rapid turbidite-fan buildup, for instance, will tend to trap more gas-producing potential than slowly depositing pelagic sediments. Gas-producing potential can be obtained where the fine sediment is derived from a continental source and contains a high proportion of biological material. Such areas as the Alaska basin, the northern North Atlantic and base of slope and abyssal areas off the southeast coast of the United States and the Gulf of Mexico are theoretically very suitable for gas production; large deposits of gas hydrates have been recognized in these areas. The full extent of gas hydrate development, however, has not been established.

Certain problems of local sediment chemistries that may have a bearing on the likelihood of gas formation (Romankevich 1984) and subsequent hydrate nucleation and crystal growth have not been fully assessed. For instance, we do not know if foraminiferal ooze will have a greater propensity to nucleate hydrate because of the high surface test area than either phyllosilicate- (clay) or tectosilicate (quartz feldspar)-based sediment. In addition, diagenetic changes within sediment may be controlled by the position of the base of the gas hydrate layer, which will induce strong reducing conditions. Nodular horizons of ankerite, siderite, and other mixed carbonates have been found in drill core in the highly saturated lower part of the hydrate (Ewing, private communication). These diagenetic minerals may contribute to the higher velocity of the hydrate layer. Below the hydrate, clays, rather than carbonates, will predominate. It follows that a long-term, stable, gas hydrate base may introduce diagenetic alteration at particular horizons that survive the rise of the base of the hydrate, which compensates for further sedimentation and becomes part of the stable geological record.

Gas hydrate formation is an exothermic reaction similar to the crystallization of water to ice. Thus the process of hydrate formation is accompanied by the release of heat and the process of degradation is accompanied by the absorption of heat or as a response to decreasing pressure. At 0°C, the heat of phase conversion is about 420 kJ/kg and at >0°C, ~140 kJ/kg (Makogen 1988). The heat-release amount depends on the composition of hydrated and unhydrated gas and pressure, temperature, and salinity of the water. In addition, buffering may affect reaction rates. Increased ambient pressure allows more gas to fill the hydrate lattice because the molecular pressure in a fully saturated lattice may reach several kbar. Increased gas amounts exert an outward pressure on the lattice (on the order of 1.26 to 1.32 cm³) and, without high ambient pressures, saturation takes place with lower gas volumes. Thus it can be expected that gas hydrates at different depths will have different bottom-acoustic responses.

The general thermodynamic conditions for methane-hydrate formation, for example, are strongly influenced by pressure (Katz et al. 1959) (Figs. 3 and 4). Where higher molecular-weight gases—such as ethane and propane—are part of the mixture, a common feature of ocean-sediment gases (Table 1), the hydrate stability field expands considerably. One-percent propane in the gas mixture can reduce the pressure at which the hydrate forms by nearly 40% (Brown 1962). Although hydrates are icelike and bond water molecules, their formation in the deep oceans is expected at temperatures above the freezing point of water, although they will form at colder temperatures as well.

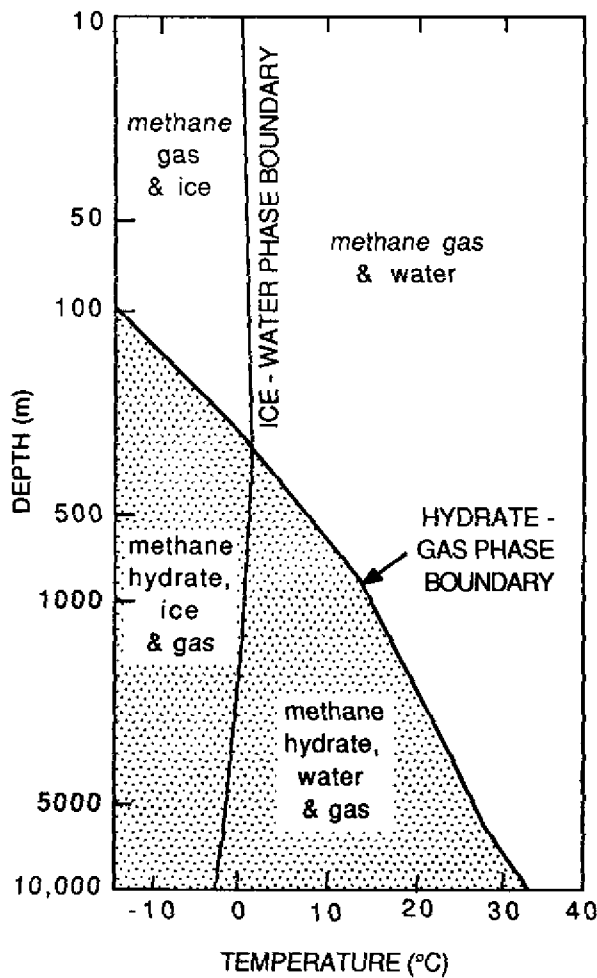


Fig. 3 — Phase boundary diagram showing the water-ice-gas-hydrate stability fields (using fresh water). From Kvenvolden and McMenamin (1980) and Collett (1983), attributed to redrawing from Katz et al. (1959). Addition of NAC_1 to water mixture shifts the curve to the left; addition of CO_2 , H_2S , ethane, and propane to the mixture shifts the boundary to the right, and increases the area of the hydrate stability field.

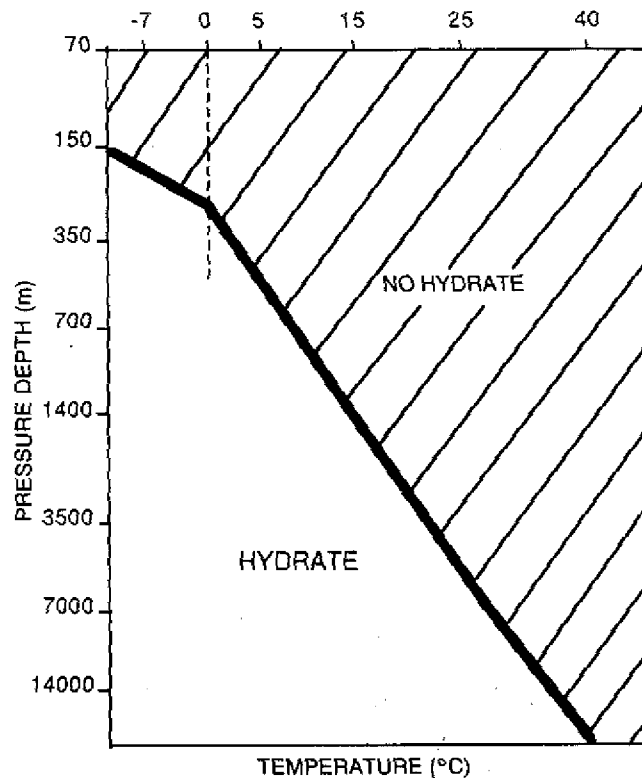


Fig. 4 — Simplified stability conditions for methane hydrate formation in a fresh water-gas mixture after Jeffrey (1969). Hydrate stability curve in sea water is slightly to the left.

In the deep oceans, the water mass is stable, with temperatures worldwide usually below 4°C (Sverdrup et al. 1961). Antarctic and Arctic waters both tend to sink and flow into abyssal regions because of their high density and relatively high salinity. The steady-state inflow of these dense, refrigerated waters provides a continuous mechanism for extracting heat from the seafloor. When water becomes heated naturally at ridge plumes and elsewhere, it rises and is further replaced by polar-water inflow. In the North Atlantic (Fig. 5), the Northern Pacific (Fig. 6), and the Arctic Oceans (important areas of Navy interest), a thick layer of refrigerated bottom water may be below 0°C for most of the year. Along north-south lines from Alaska, the Barents Sea, and the northern Indian Ocean to Antarctica, the deeper, more saline water is consistently <2 or 2.5°C below 2000 m (Couper 1983).

In the Norwegian-Greenland Sea (Johannessen 1986), subzero temperatures can exist in a large part of the water column. Figure 7 shows temperatures recorded on the north side of the Faeroe Ridge (Sverdrup et al. 1961). The existence of subfreezing temperatures may further accelerate the formation of gas hydrate and water-ice and gas hydrate mixtures. The subzero, supercooled, dense, highly saline water that spills into the Norwegian-Greenland Sea comes from the Arctic basin with only minor amounts flowing from the continental-shelf water mass (Swift 1986).

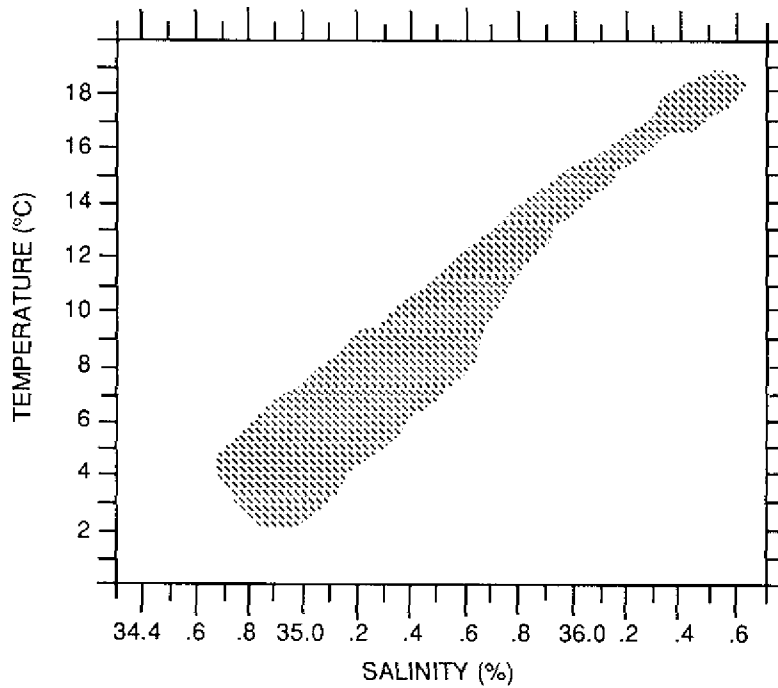


Fig. 5 — Patterned area shows simplified temperature-salinity diagram for the North Atlantic from 10 sites, each incorporating sampling at various depths. Redrawn from Sverdrup et al. (1961, Fig. 183).

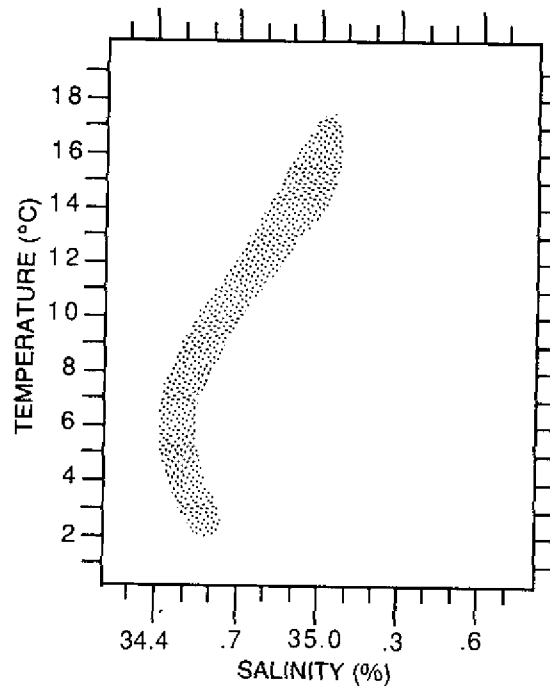


Fig. 6 — Patterned area shows simplified temperature-salinity diagram for the North Pacific region from 22 sites, each incorporating sampling at various depths. Redrawn from Sverdrup et al. (1961, Fig. 196).

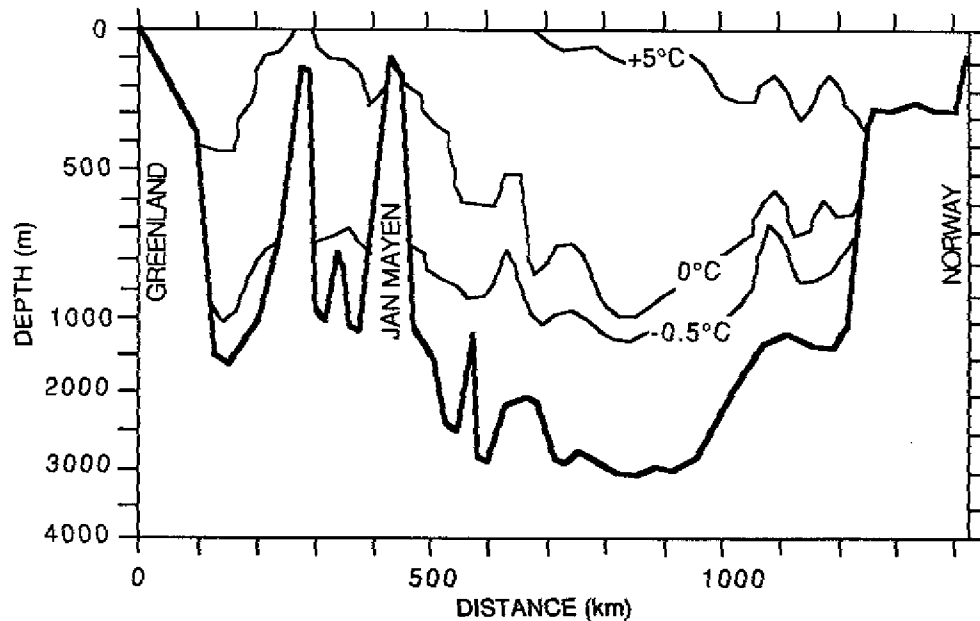


Fig. 7 — Simplified diagram showing vertical temperature section in °C across the Norwegian Sea in winter 1968. Note change in vertical exaggeration at 1,000 m. Redrawn from A. Johannessen (1986, Fig. 9(a)) derived from data in Dietrich (1969).

2.6. Extent and Distribution of Gas Hydrate

Gas hydrates are potentially stable on 25% of the Earth's land area and in 90% of the seafloor (Carson and Katz 1942). Gas hydrates can form and remain stable over a wide range of temperatures (100 to 400 K) and pressure ($1 \cdot 10^{-6}$ to $2 \cdot 10^{-3}$ MPa). The stability field of gas hydrate plus ice plus water show stability in permafrost continental shelves while, at oceanic depths, gas hydrate plus water are stable at elevated temperatures because of the high pressure (Fig. 4).

The likelihood of gas hydrates, however, is predicated on the likelihood of gas generation, which itself is dependent on the availability of organic carbon material in sediments. Although paleogeographic reconstructions of organic carbon in sediments are not available, which would give definite information on the likelihood of gas production, Romankevich (1984) gives the distribution of organic carbon in the upper sediment (0 to 5 cm) layer. Extrapolation of this depositional zonation back into the tertiary is possible because the world's oceans have had the same configuration since the time the Atlantic plate margin spread into the Arctic Ocean and established the present interocean water circulation patterns, about 30 million years ago (Vogt 1985). The oceans of the northern hemisphere (particularly the Arctic Ocean, the North Atlantic basin north of Iceland, and the Greenland-Iceland-UK transocean ridge), form the largest contiguous area in which organic carbon is being deposited. Broad areas of the northwest and northern Pacific areas, and to a lesser extent, the eastern Pacific—from the Americas to about 20° south—and elsewhere adjacent to continents, are also important areas of organic-carbon deposition (Premuzic 1980; Romankevich 1984). Central ocean areas, especially in the South Pacific, contain a minimum of organic carbon deposits.

On continental shelves, information on gas hydrates and their stability comes from those Arctic areas that are active hydrocarbon exploration provinces (Barker et al. 1982). For example, Lachenbruch et al. (1988) have shown detailed relationships between permafrost and gas hydrates and their developments at depths that are the current model for the north-slope area of Alaska. Although permafrost seen in a number of wells is developed to a depth of about 600 m, gas hydrates are developed to depths in excess of 1000 m where they are stable at up to $+12^{\circ}\text{C}$ (Fig. 8). The gas hydrate thickness mapped by Lachenbruch et al. (1988) increases from land onto the continental shelf. Assumptions for thermal gradients can be used to estimate both a thermal profile and a configuration for the hydrate stability zone (HSZ) (Holder et al. 1987; Kamath et al. 1987). In the Barents Sea, where subsea permafrost was not developed (Elverhoi and Solheim 1987), positive impedance "reflectors" currently identified as either local permafrost or gas pockets (Solheim and Larsson 1987) may actually be gas hydrate.

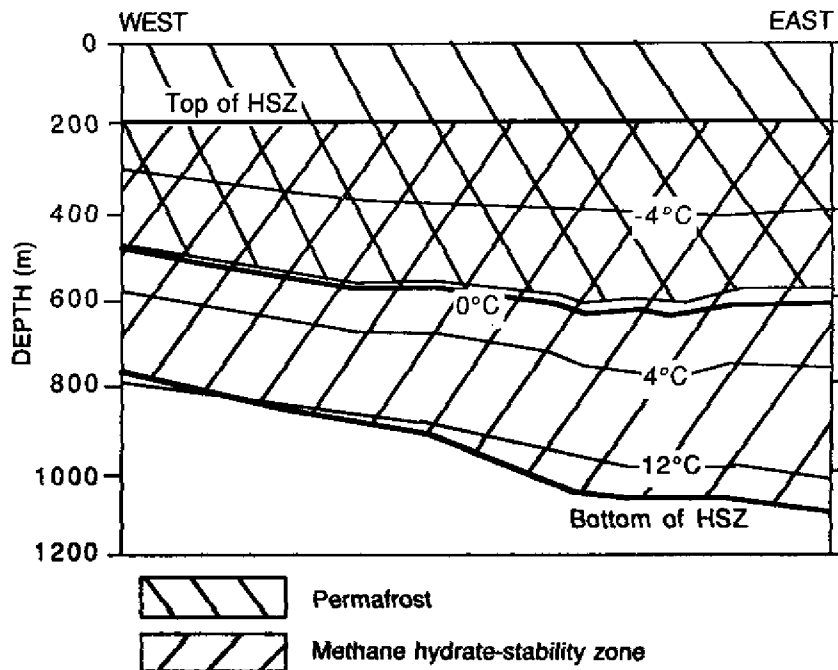


Fig. 8 — Cross section through 10 near-shore wells from the north slope of Alaska showing permafrost and gas hydrate stability zones (Lachenbruch et al. (1988)). Wells obliquely approach the seacoast from west to east with the eastern-most well being just into the marine area (65 km across).

In the deep oceans, most evidence for the presence of gas hydrates comes from seismic surveys; core analyses and geophysical drill-hole measurements provide some control. Bottom trawling near diapir-generated gas seeps in the Gulf of Mexico recovered amalgamated concentrations of nodules consisting of gas hydrates and sedimentary clasts with interspersed layers and solid masses (>150 mm thick) of both petrogenic and biogenic origin (Brooks et al., in press). Because the inversion of hydrate to gas is a thermally driven reaction, hydrate retrieved rapidly enough from the seafloor can be brought to the surface where it can be preserved in liquid nitrogen, even at atmospheric pressure. Gas-filled mounds sealed by hydrate-bonded sediments have been identified from drill cores in the

Gulf of Mexico (Prior et al. 1989). Widespread high level gas in the Sea of Okhotsk (Zonenshayn et al. 1987) implies a saturated gas hydrate blanket.

Gas hydrates have been recognized in what would normally be considered to be cold-bottom water areas, such as in the Arctic (Bily and Dick 1974; Grantz et al. 1976; and Grantz et al. 1982); in the Antarctic (Hitchon 1974); in the North Atlantic (Bugge 1983); in the central Atlantic (Ewing et al. 1966; Tucholke et al. 1977; Paull and Dillon 1981; Galate and Goodman 1982; Pinet et al. 1981; Dillon and Popenoe 1988; and Paull et al. 1989); in the South Atlantic (Flood 1989; Manley and Flood, in press); in the California margin (Field and Kvenvolden 1985; and Krason and Ciesnik 1986); in the North Pacific (Scholl and Creager 1973); in the Aleutian basin and trench and in shallower basins of the Bering Sea (Cooper et al. 1986; and Krason and Ciesnik 1987); off Japan (Aoki et al. 1982); and in the Pacific (Kvenvolden and Cooper 1987).

Gas hydrates have also been identified in the abyssal depths of warmer oceans, such as in the Gulf of Mexico and the Caribbean (Edgar, private communication; Von Huene 1980; Brooks and Bryant 1985; Hovland and Judd 1988; and Prior et al. 1989); off western Central America (Finlay and Krason 1986); off 22 other locations, such as the northern Australian shelf, New Zealand, and the Brazilian continental slope (Manley and Flood 1988); in the Arabian Sea and west of South Africa (Kvenvolden and Barnard 1983); in the northwest Indian Ocean (Fowler et al. 1985; and White 1985). Malone (1983) and Kvenvolden (1988) give additional information. Bernstein et al. (1988) show 0.5-s thick two-way travel (twt) at 7 and 5-s twt depth in laminated sediments of both the back and forearc basins in the warm-bottom water area of the Solomon Sea, where polar water can be expected to have a minimal influence. In the Atlantic, large deposits of gas hydrate have been acoustically imaged as far south as the Bahama outer ridge and spur areas (Grow et al. 1979; and Dillon, et al. 1982). Gas hydrates may be widespread in the deep-water sediment of the Black Sea (Ciesnik and Krason 1987) and might also be expected in other deep, restricted bodies of water.

With increasing sediment-depth temperature, the local geothermal gradients become important, because the intersection of the geothermal-gradient curve and the hydrate-phase boundary establish the gas hydrate, gas-stability boundary (Fig. 9). Hydrates can be expected to form ubiquitously and at considerable depths in deep ocean sediments (Fig. 10). Theoretically, the thickness of the potential gas hydrate zone increases with increasing depth at constant geothermal gradients (Fig. 11). A single, long-seismic line in the vicinity of the Blake outer ridge, off the southeast coast of the United States, clearly images the gas hydrate horizon, which thins from almost 1-s twt time at a depth of slightly greater than 6 s to <0.2-s twt at a depth of ~0.5-s twt (Bryan and Markel 1966, Fig. 14; and Markel and Bryan 1983).

The maximum thickness of gas hydrates recognized on land is up to 1700 m, and in the ocean, gas hydrate zones up to 1100 m have been identified. The gas hydrate upper-boundary zone (HFZ) is 100 to 200 m on land, and in the continental shelves of the Arctic Ocean, the upper surface of the hydrate is commonly near or at the surface below 200 to 400-m water depth. The depth of the acoustically imaged base of the gas hydrate blanket increases with water depth (Fig. 12). Gas hydrates recovered from different Deep-Sea Drilling Project holes in which temperatures were measured confirm the relatively high-temperature stability under high pressure (Fig. 13). Many gas hydrates identified in deep oceans have little or no lithologic or sediment cover and extend downward into the sediment from centimeters of the sediment surface. Occasionally a surface layer of amalgamated gas hydrate nodules occur near persistent gas seeps.

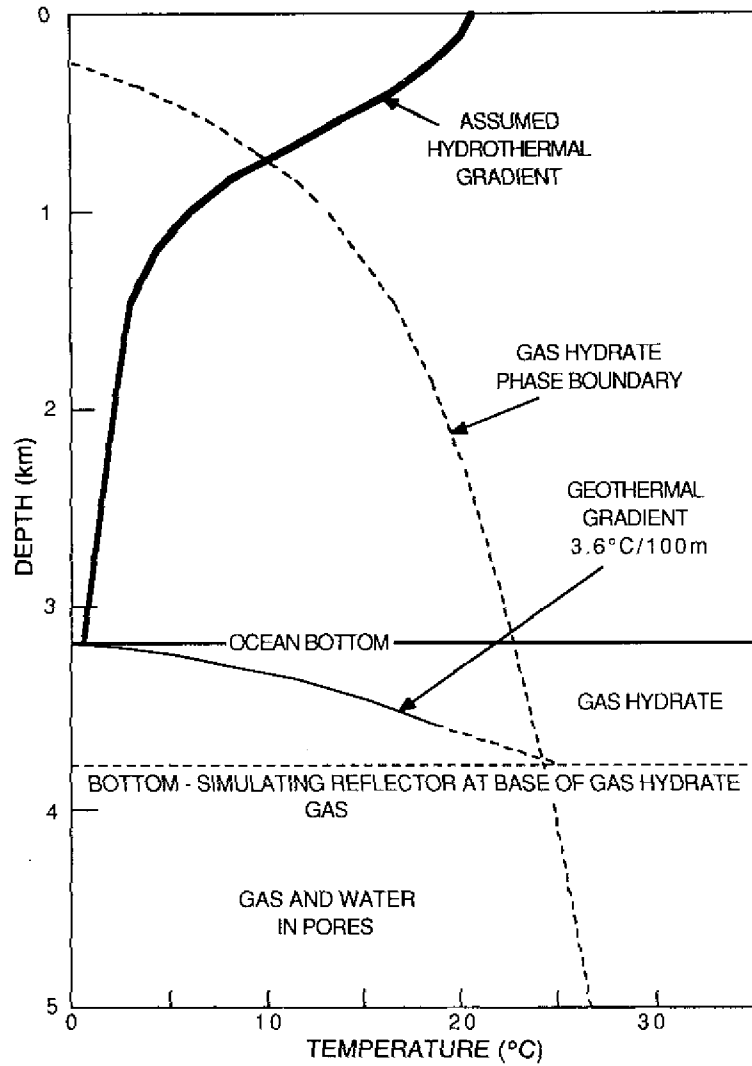


Fig. 9 — The gas hydrate zone in relation to thermal gradients in water and sediments. (Fig. 12 from DSDP leg 76 shipboard party, attributed to Kvenvolded and Barnard, supplied by T. Edgar.)

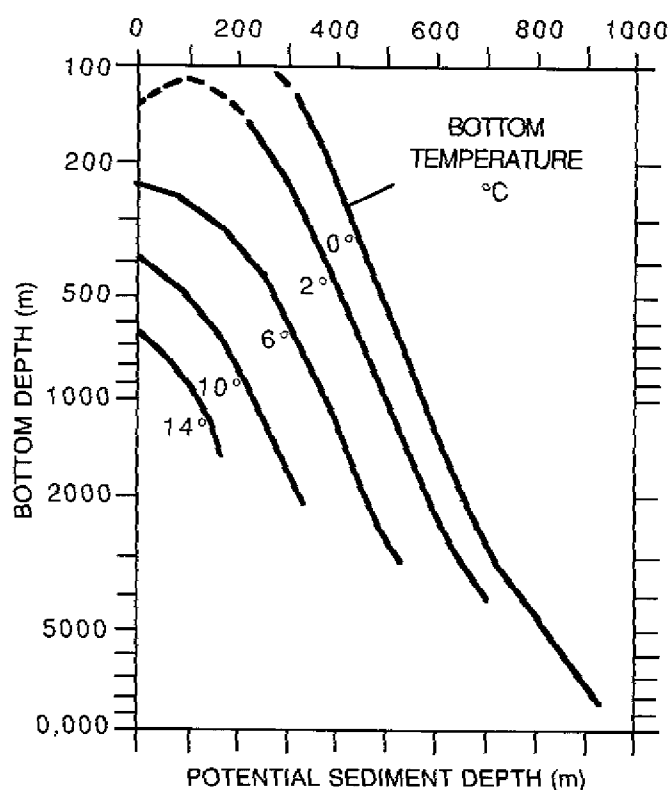


Fig. 10 — Potential depth of hydrate formation in sediments. Hydrate is stable under the depth (pressure)—sediment depth to the left of each isotherm for bottom temperature in a sediment column of average heat flow (Jhaveri and Robinson (1965) and Daniels and Vidmar (1982)).

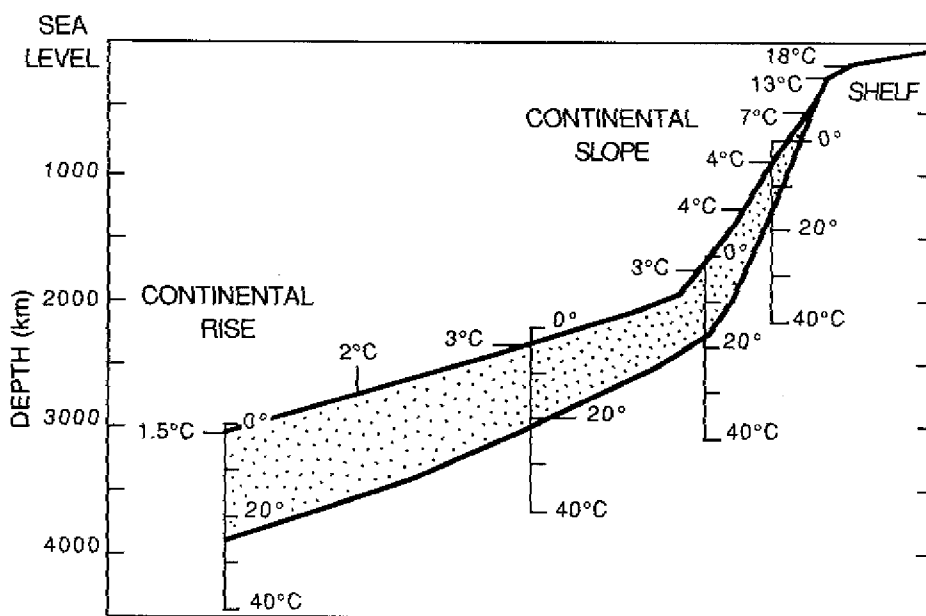


Fig. 11 — The thickness of gas hydrate zone increases with depth and temperature (Fig. 2 of Kvenvolden and Barnard 1982). Patterned zone is potential gas hydrate zone.

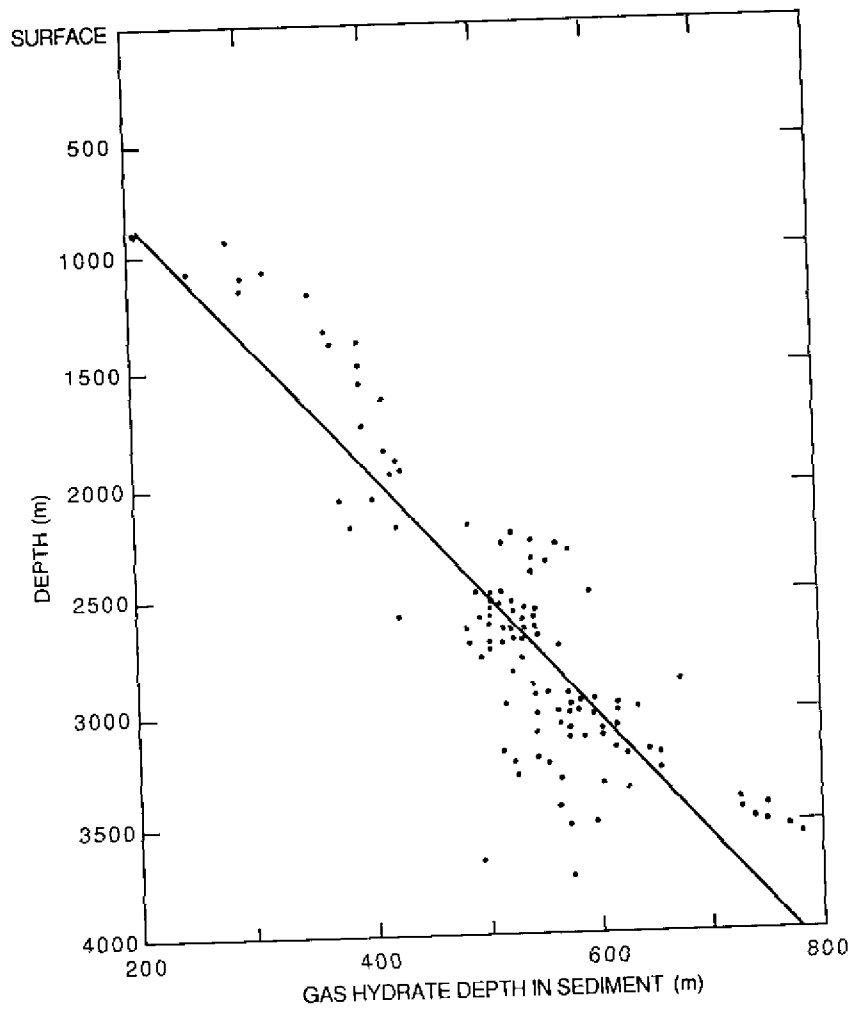


Fig. 12 — Subbottom base depth of gas hydrate layer compared with water depth. Variation from the best fit line is regarded as a function of velocity variation within the gas hydrate zone, which could not be compensated for in detail (from Dillon and Paull, 1983).

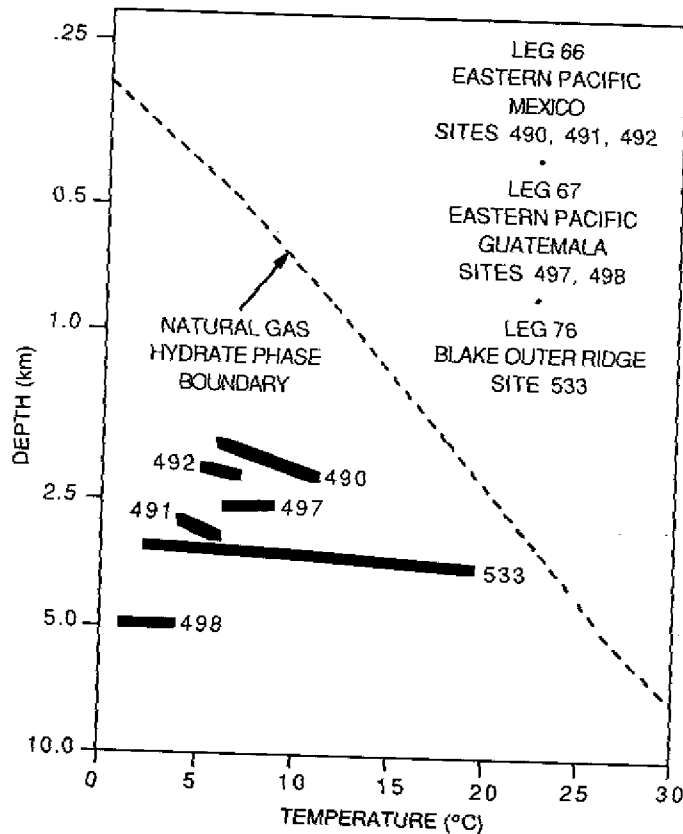


Fig. 13 — Depth and temperature summaries for Deep Sea Drilling Program (DSDP) sites at which solid gas hydrate was recovered. Depth is total depth of water plus sediment. Sheridan et al. (1982) established temperature gradient for site 533; Shipley and Didyk (1982) established gradients for sites 490, 491, and 492. Pressure-temperature data for sites 497 and 498 are from Harrison and Curiale (1982).

Shipley et al. (1979) note widespread evidence of bottom-simulating reflectors that identify the anomalously high-acoustic-velocity layer formed by gas hydrate. Continued examination of seismic data suggest an almost pervasive gas hydrate development in deep-ocean sediments, especially in light of recent work indicating that hydrates can be present even where their presence is difficult to interpret from reflection seismic records.

Although gas hydrates have not been recognized everywhere in the deep oceans, they have been positively identified over broad, thickly sedimented areas below 1-km water depth wherever they have been searched for. The recognition of natural gas hydrates has now extended to virtually all ocean basins. It is likely that some hydrate, at some level of saturation, occurs in virtually all deep-ocean sediment.

2.7 Physical Properties of Gas Hydrates

The density of gas hydrates varies from 0.8 to 1.2 g/cm³, which brackets the range of first formed, unsaturated to virtually complete saturation. Molecular pressure of gas in the hydrate lattice

can reach several kilobars with increasing saturation. Heat conduction in gas hydrates is considerably lower than that of ice, probably because heat buildup is enhanced by the high specific heat of methane. The critical temperature of methane is -82.6°C at 45.44 atm pressure (Dean 1974). At 200 K, methane-hydrate heat conduction is 8 times lower than that of ice. It is possible that gas hydrates, once formed, might form thermal high anomalies in the ocean floor without the hydrate becoming unstable and breaking down to a water-gas solution. Hydrate hardness is not well known; however available data (Makogon 1988) show that may be up to twice water-ice hardness. Fully bonded gas hydrate sediments are not common, however; therefore the hardness of the sediment layer would probably not be increased. A significant proportion of gas hydrate in sediment would cause an increase in ductility or rigidity that would affect the penetration of any foreign object that was emplaced by simple displacement of sediment, such as a gravity core barrel. Details of gas hydrate thermodynamics, reaction rates, and methane solubility and diffusability are discussed by Godbole and Kamath (1987).

Hydrates are mainly inferred from geophysical measurements both in drill holes and from acoustic methods. Hydrates characteristically induce high electric resistivities and are quite distinctive from unhydrated sediments (Pearson et al. 1983) on geophysical records of exploration boreholes in the Arctic continental shelves. Sound velocity in hydrates is substantially above that which would be expected in the sedimentary sequences without gas hydrates. Collett (1983) reports V_p -wave measurements of naturally occurring gas hydrates from drill holes at between 3.1 km/s and 4.4 km/s and Kvenvolden et al. (1982) found $V_p = 3.6$ km/s in *in situ*, down-hole measurements. Hydrate-sediment velocities are commonly in the 2.3 to 3.4 or 3.6 km/s range. Hydrates at lower temperatures support higher V_p velocities (Lawson et al. 1984). Structure I hydrates have higher V_p than Structure II hydrates; in general, the longitudinal velocity decreases with increasing mass or molecular weight of the host (Kieft et al. 1985). Velocity of seismoacoustic waves through porous rock saturated with gas hydrates can be 60% to 100% higher than through the same rock saturated with free gas. Virtually no experimental data concerning attenuation exists.

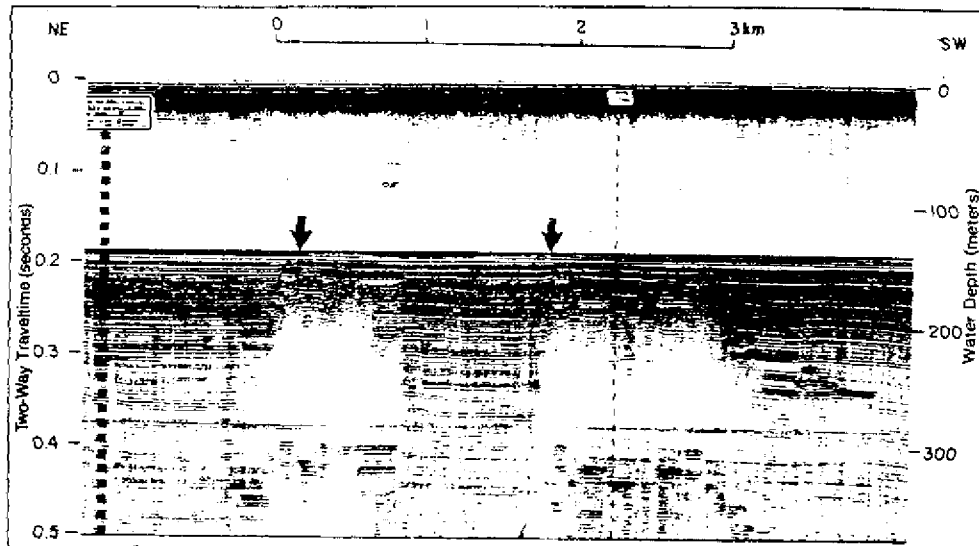
2.8 Acoustic Effects of Gas and Gas Hydrates

The effect of gas in sea-bottom sediments on acoustic propagation has been determined directly from high-resolution seismic-reflection surveys controlled by downhole geophysical logs and physical analyses of specimens. To date, almost 1000 well surveys have been examined. Acoustic anomalies related to gasified sediments that are commonly expressed on seismic records (Solheim and Larsson 1987) are particularly important to bottom-acoustic interaction. Fannin (1980), for instance, showed that gas content is a significant acoustic parameter of bottom-acoustic interaction; as little as 1% free gas by volume can significantly alter the acoustic response seen on seismic records.

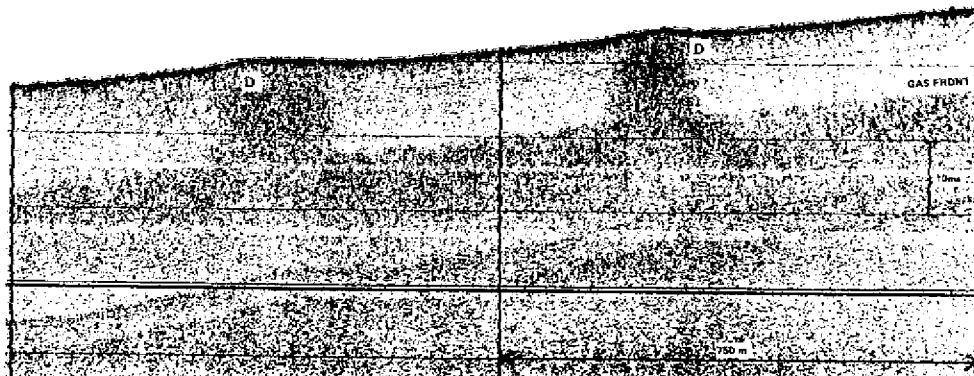
Seismics have been and will continue to be the most widely used method for detecting gas and gas hydrate (Elverhoi and Solheim 1987). The main effects of gas and gas hydrate on acoustic records are described next.

2.8.1 Acoustic Turbidity, Gas Blanking, Wipeout, Smear (Fig. 14)

These terms refer to acoustic loss of detail in the seismic record through absorption and scatter. Dark blanking (seismic smear) represents areas where energy is reflected in a disordered manner from gas in interstitial fluids, while light blanking (wipeout), which is more common, represents energy absorption or damping caused by selective absorption, especially at higher frequencies (Schramm et al. 1977; Rokoengen and Tegdan 1983). Wipeouts often occur at very shallow depths in shallow



(a)



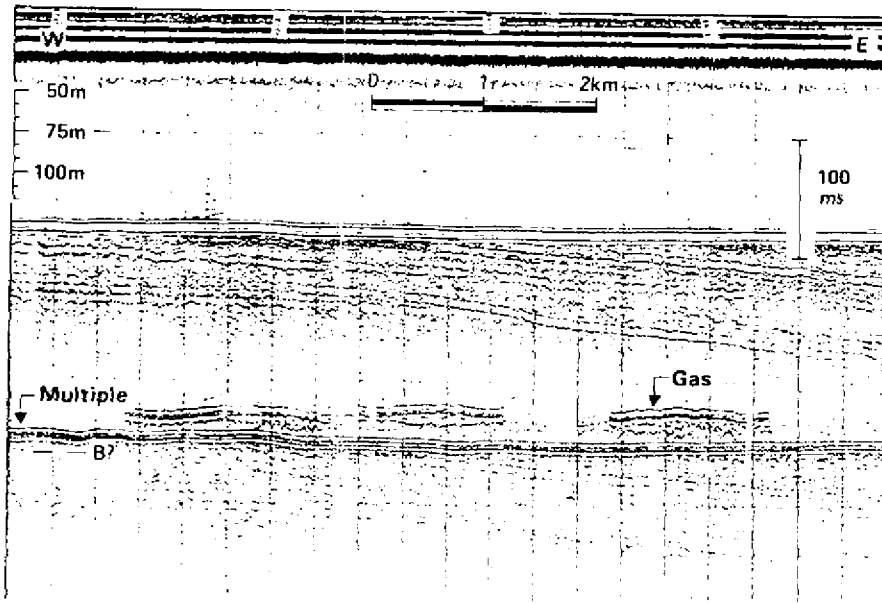
(b)

Fig. 14 — (a) Light gas blanking seen on a sparker profile from the Bering Sea (Fig. 2(a) from Solheim and Larsson (1987), after Carlson et al. (1985)); (b) Dark-blanking acoustic turbidity (from Fig. 4.4 of Howland and Judd (1988) attributed to 3.5 kHz subbottom profiler record, courtesy of R.J. Whittington, University of Wales, G.B. Note the "gas front," which rises into the "gas domes").

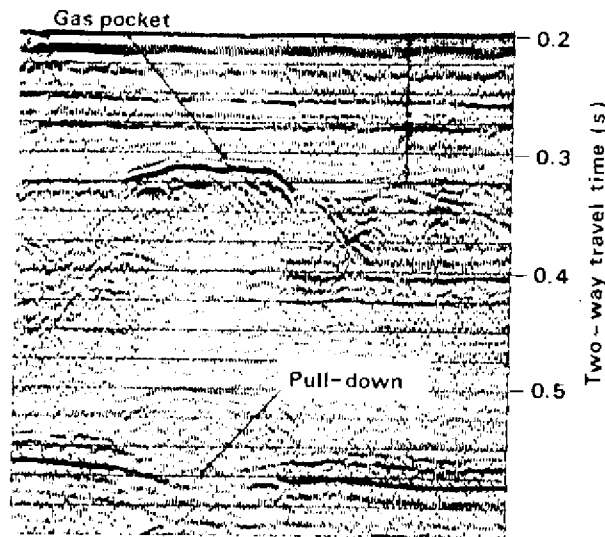
water where the presence of gas locally may be seasonal (Wingfield 1985). Energy encountering these gas-charged zones, which usually have diffuse margins, is either absorbed or not returned to the water column in a form useful for detecting the source.

2.8.2 Amplitude Anomalies, Bright Spots, Pull-Downs (Figs. 15)

Bright spots are the hydrocarbon-exploration industry term for seismic-record-amplitude anomalies that are attributable to the presence of stratified gas accumulations. These result from high-impedance contrasts between gas-charged and gas-poor strata. Passage of acoustic energy into lower acoustic impedance strata, which is a characteristic of gas charging, also induces a phase shift of the seismic signal. In addition to gas-induced seismic anomalies, the presence of gas throughout a stratigraphic section that would otherwise have significant impedance distinctions can cause masking through a diminution of the acoustic contrasts. These anomalies, because of the usually well-defined margins of the gas-charged zones, reflect coherent energy back into the water column.



(a)



(b)

Fig. 15 — (a) Bright spots in gentle culminations along a single horizon in a sparkler profile from the North Sea (from Fig. 2(b) of Solheim and Larsson (1987) after Rokoengen and Tegdan (1983)). False horizon labeled "multiple" is a repetition of the bottom interface. (b) Bright spot in multichannel seismic record from the North Sea showing enhanced amplitudes and subjacent reflector pull-down caused by the lower velocity of acoustic propagation through the gas pocket. Pull-down is a two-way travel time artifact (from Fig. 2(c) of Solheim and Larsson (1987) after Rodoengen and Tegdan (1983)). Note also slight wipe-out or diminishment of detail below the gas pocket.

MICHAEL D. MAX

The margins at and below gas accumulations show that other apparent reflectors appear to be pulled down (Fig. 16). This is a timescale effect caused by the acoustic energy passing through the lower-velocity gas-charged zone. These can often be the main indications on seismic records of the presence of moderate amounts of stratified gas.

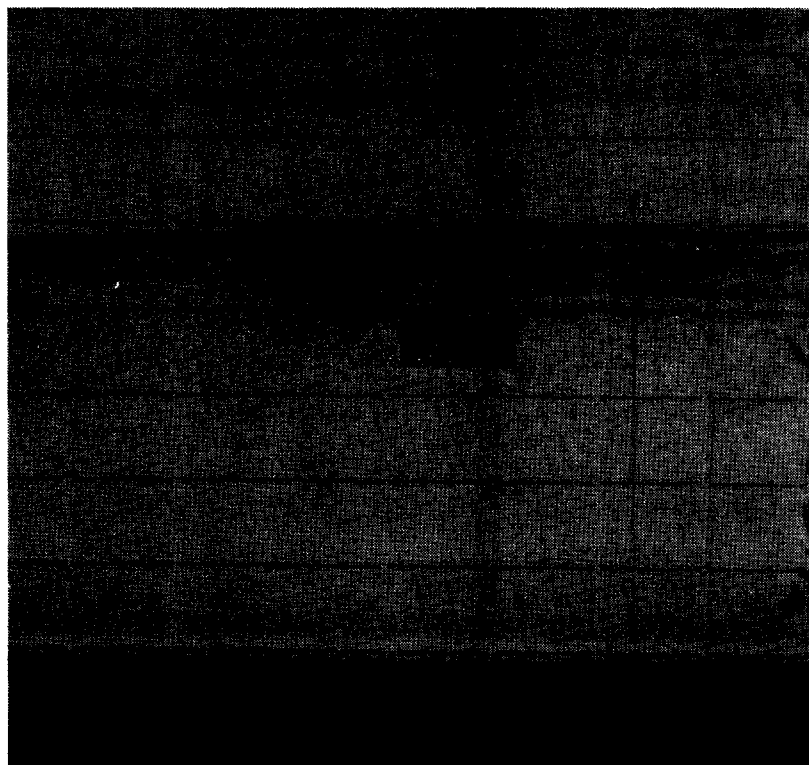
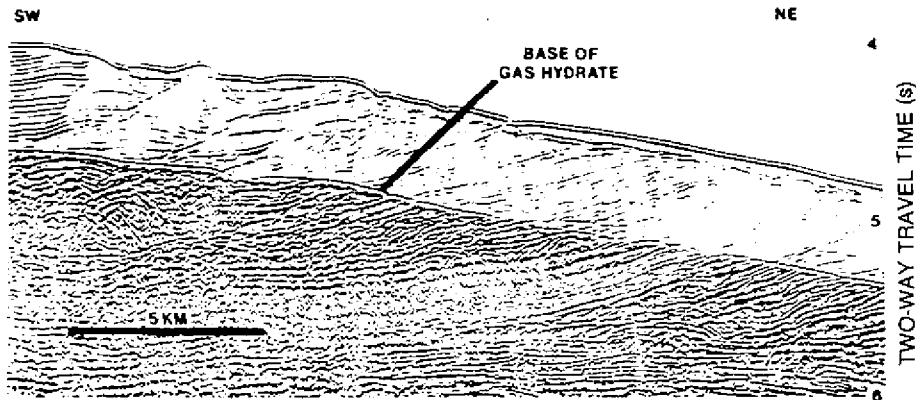


Fig. 16 — A 3.5 kHz depth-sounding record from the research vessel *Vema* along a short track across the Porcupine abyssal plain to the southwest of the European continental shelf (courtesy of the Lamont-Dougherty Geological Institute of Columbia University (of New York, U.S.A.)). Note marginal pull-down of apparent reflectors passing into the area containing the apparently translucent sediments. Apparent pull-down of reflectors in normal sediments is probably an artifact caused by the presence of low acoustic velocity gas in the wipeout.

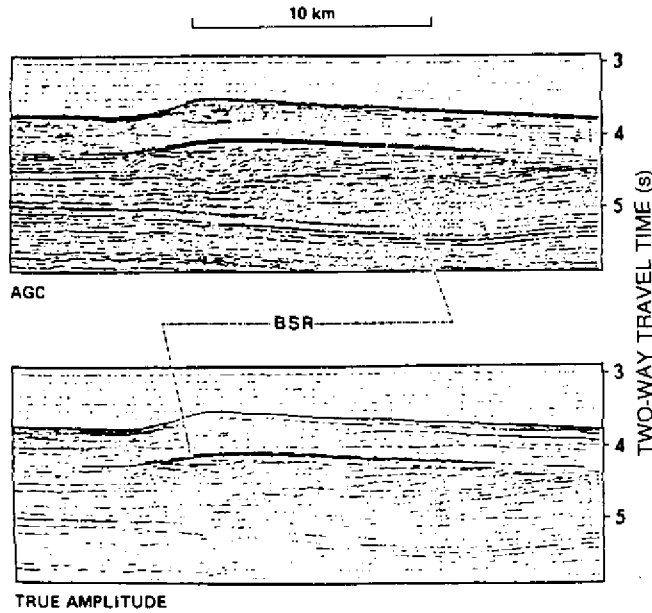
At the lateral termination of some gas deposits, secondary acoustic-signal generation, which is seen on the seismic record as diffraction patterns and hyperbolae, may also sometimes extract propagating acoustic energy.

2.8.3 Nature of the Bottom-Simulating Reflector (BSR) (Fig. 17)

The bottom-simulating reflector (BSR) is commonly imaged on seismic-reflection profiles as an impedance contrast or large reflection coefficient that is associated with the base of the gas hydrate blanket (Stoll et al. 1971; Stoll and Bryan 1979; and Judge 1982). The gas hydrate layer introduces a high acoustic-velocity character to sea-bottom sediments that would otherwise have a lower velocity structure. At the base of the hydrate, therefore, a negative-impedance contrast commonly exists between the hydrate and the subjacent-unhydrated sediment, although its presence is often masked by



(a)



(b)

Fig. 17 — (a) Bottom simulating reflector (PBSR) seen in 12-fold multichannel seismic reflection profile developed in continental slope sediment from the crest and eastern flank of Blake outer ridge, off the southeast coast of the United States, in which bedding is not parallel with the seafloor. The apparent lower amplitude above the gas hydrate reflector probably results from reduced-acoustic-impedance differences in the primary acoustically laminated sediment caused by gas hydrate presence. This reduced impedance, or wipeout blanked, serves to identify gas hydrate in the absence of a PBSR (from Solheim and Larsen (1987) after Shipley et al. (1979), Fig. 3). (b) Discontinuous PBSR seen in a sediment rise (from Fig. 5 of Daniels and Vidmar (1982) after Stoll and Bryan (1979)). Although the blanking effect of the hydrate layer can be followed across the section away from the knoll, it can be inferred to lie more widely at the surface than would be indicated from the presence of the PBSR alone. Gas presence in the area of the knoll may be an effect of a limited amount of free gas beneath the hydrate that migrated to the hydrate-induced culmination trap in the vicinity of the knoll. Note the presence of hyperbolic signals from the left termination of the PBSR. This may be an edge effect or may simply be associated with the presence of free gas. The same seismic section enhanced shows more hyperbolic signals generally beneath the gas (personal inspection of draft DSDP figure supplied by T. Edgar).

other bottom-parallel seismic events. Acoustic blanking is commonly seen in the hydrate zone, but the most convincing evidence for the presence of acoustically imaged, high velocity hydrate (rather than a low velocity gas-charged layer) is the presence of a bottom-simulating reflector that occurs at or near the base of the hydrate blanket.

Where free gas occurs beneath the hydrate layer, a much stronger negative-impedance contrast, the prominent-bottom-simulating reflector (PBSR) is formed. In this report, the presence of gas below the hydrate is indicated by PBSR.

The PBSR may not always be developed in association with a gas hydrate blanket, and hence its absence is not a proof of the absence of hydrate. The PBSR is usually subparallel to the seafloor and is difficult to identify on seismic records where sediments are dominantly bedded parallel with the seafloor because the PBSR is easily lost within the subparallel response of the other reflectors and the strong water-sediment surface-induced phase changes in the pulse-width band on the seismic record usually shown by parallel events immediately below the surface. In addition, gas hydrate might not be acoustically perceived if the base of the hydrate layer is sufficiently gradational with respect to subjacent gas, where a strongly downward-refracting-velocity profile may be formed that would cause a sound channel to form; in this case, there would be no strong impedance contrast and, hence, no PBSR. In relatively high-velocity marine sediments where no significant free gas underlays the hydrate layer, there also would not be a strong phase change, and the presence of hydrate might be difficult to infer from the seismic record. Kvenvolden and Bernard (1982) note that in the absence of a PBSR, the presence of a high-velocity layer in near-surface marine sediments is almost certainly indicative of the presence of gas hydrates. In the most dramatic cases of acoustically imaged hydrates, however, where the PBSR is developed within sediments that are not parallel with the seafloor, the PBSR stands out most clearly (Fig. 17(a)). The lateral continuation of a gas hydrate blanket in the absence of a PBSR away from a gas-trapping culmination can be clearly demonstrated from following the gas blanking effect within the layer itself, which has caused gas to become locally concentrated and form the impedance contrast necessary for a PBSR (Fig. 17(b)).

Within the gas hydrate zone, acoustic-transmission velocities are greater than would be expected from the normal marine sediments alone. Whereas the presence of free gas or significant quantities of gas dissolved in fluids may have the effect of diminishing or enhancing the return of acoustic energy to the water from the bottom through reflection, gas hydrates will almost always be associated with anomalously low bottom acoustic loss. The effect is complex because of the variable relationship between V_p and V_s depending on hydrate amounts and saturation (Daniels and Vidmar 1982) and the as-yet unmodeled possibility of developing sound channels associated with hydrate zones.

2.9 The Hydrate Layer; the Need for More Information

More needs to be known about the nature of the hydrate layer. Although the base of the hydrate can be identified when a PBSR is developed, this is primarily dependent on free gas existing below the hydrate. For predicting bottom-acoustic interaction, it will be necessary to obtain a clearer picture of the proportion of hydrate to interstitial fluid (degree cementing or bonding the sediment) and the degree of hydrate saturation with depth (which determines the density and acoustic velocity of individual crystals, and hence the crystal mesh). These aspects of hydrate development are currently little known.

Also, it is important to know the nature and depth at which the hydrate is commonly developed in the oceans to establish bottom-acoustic character. If the transition from water is to a fully hydrate-bonded sediment, then the bottom-acoustic response can be expected to be quite different from a hydrate layer with a gradational percent increase and increased saturation downward from the surface. A two-layer model for the velocity structure of hydrate from the Blake outer ridge (Fig. 18) is a simplistic representation of complex acoustic lamination (or an upward refracting profile) rather than the two layers within the hydrate. The profile (Fig. 22) shows the important seismoacoustic attributes of a gas hydrate/PBSR composite layer. First, the gas hydrate does induce a much higher acoustic velocity in the bottom and immediate subbottom sediment than would be considered normal in unhydrated sediment. Second, the velocity is higher in the lower part of the hydrate layer than in the upper part. Third, the presence of a gas-induced PBSR causes an important negative impedance contrast that may act, at very low frequencies, as a strongly downward-refracting horizon that would establish a sound channel.

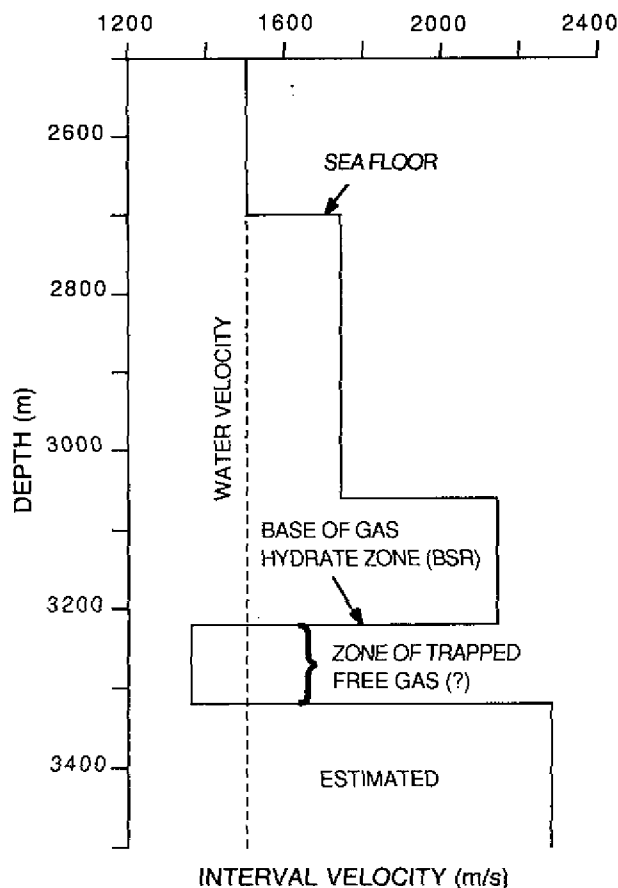


Fig. 18 — Velocity analysis of four-layer modeled-seismic-refraction data (attributed to Richard Wise of the United States Geological Survey). Drilling at PBSR site confirmed presence of gas hydrate as the environmental element that causes the anomalous velocity structure (figure supplied by T. Edgar.)

Although gas hydrate is stable at the surface, and indeed, within the water itself at depth, proof of its widespread or ubiquitous development as a surface layer is limited at present. Theoretically, however, there is reason to believe that gas hydrate formation is widespread. In every ocean basin where gas hydrate has specifically been looked for, for instance, it has been found. Its real extent is currently unknown. Normal core and dredge specimens can be expected to degas virtually all hydrate and gas on recovery to the sea surface, and thus the absence of hydrate in specimens from normal recovery programs does not bear on the problem of its existence. Gas hydrate has been recovered from within 6.5 m of the seafloor in sediment of the Black Sea (Yefremova and Zhishchenko 1975). Solid gas hydrates were recovered from 1.8 m below the bottom in 800 m of water in the Sea of Okhotsk; they were observed to decompose rapidly with effervescence in air (Zonenshain et al. 1987). Because their degradation is an endothermic reaction and they sublime, they are a complex, high-temperature analog of the more familiar substance, dry ice, which is solid carbon dioxide.

Large crystals of gas hydrate have been recovered from the immediate sea bottom in an area of high gas flow (Brooks et al., in press), but methane generation in less specialized environments may be insufficient to provide the volume of gas necessary for crystallizing hydrate on the seabed. A layer of fully saturated gas hydrate on or near the seabed surface would obviously affect bottom-acoustic interaction in a much different manner from that which would be expected in its absence.

2.10 Inherent Stability of the Gas Hydrate Blanket

The gas hydrate layer is a steady state, aggrading phenomenon in which gas produced in deep-sea sediment will tend to be trapped, reworked through gasification, and hydrated within the layer again. Even in areas with little gas production, once hydrate is formed, it should be held within the sediment in a surface-related layer regardless of the sediment rate. The thickness of the gas hydrate layer is essentially a function of water depth and the geothermal gradient, and the hydrate is stable only in the upper sediment. As sedimentation proceeds, the hydrate-layer base will move upward so that its thickness remains constant. Thus there is a balance between the sedimentation rate above the upper part of the sediment column and the rising geothermal gradient/hydrate stability curve (Fig. 9).

Where hydrate at the base of the layer becomes unstable owing to the rise in temperature from the upward-migrating heat expressed as the geothermal gradient, the hydrate inverts to free gas. The diffusion rate of methane is such that even small amounts of porosity in the lower hydrate layer allows the gas to rise into the hydrate layer, where it is again rehydrated. This attribute reworking of the hydrate layer with reinforced petrogenetically produced, upward-migrating gas by gasified hydrate explains why the bottom of the hydrate layer is everywhere more heavily crystallized with hydrate and why the lower hydrate layer has a tendency to be more thoroughly saturated. Rapidly produced gas at the base of the hydrate, combined with a completely hydrated and saturated lower part of the hydrate layer, causes a gas pocket to form. The hydrate layer now has the potential for great stability as an upper sediment phenomenon, even in areas with substantial sedimentation rates and only little or moderate gas production.

In the Aleutian and Bowers basins of the Bering Sea, Cooper et al. (1986) identified more than one BSR—an upper one—as being the base of the gas hydrate layer that is locally acting as a trap for subjacent free gas; it is identified from the existence of a series of velocity-amplitude anomalies (VAMPS) (Carlson et al. 1987) below gas blanking. The deeper BSR is correlated with the silica-diagenetic boundary between overlying and incompletely consolidated sediment and underlying more indurated mustone. There are a number of alternate interpretations for the cause of the deeper BSR.

First, although only one deeper BSR is identified, the seismic records can be interpreted (personal inspection) as having a number of discontinuous BSRs that may not reflect primary geological character. As the gas hydrate layer moves upward to accommodate intermittent sedimentation (or the heat flow changes regionally for some period of time), the base of the hydrate might be expected to maintain a stable position long enough to affect a local diagenetic alteration reflecting the transient geochemical transition from gas to gas hydrate. The hydrate, in other words, might induce diagenetic artifacts within the geological record, and these could be what are being imaged by seismics at the deeper BSR(s). This suggestion, as well as that of Cooper et al. (1986), remains to be tested.

2.11 Hydrated Sediments with BSR and PBSR

Predicting the likelihood of BSR development by extrapolating the proven relationship between the existence of PBSR and gas hydrate/gas interface may have an application in predicting geoacoustic transmission-loss anomalies in the deep-ocean floor and continental slopes. The bottom-simulating reflector has been identified as closely following the bathymetric profile, especially where broad or gentle swells, such as those that occur in the vicinity of sediment drifts or abyssal hills, are found. Because the hydrate layer forms a seal to the upward migration of gas, effectively filling void space and saturating the crystalline hydrate, it fulfills the definition of a cap rock to a potential reservoir of upward migrating gas and fluids. Beneath the swells and bathymetrically upstanding areas, continued upward and lateral migration of gas concentrates and there is a potential to form a gas reservoir. Figure 17(b) demonstrates that the contact between the base of the hydrate layer and the free gas beneath (Fig. 18), which forms the strong negative-impedance horizon, is laterally impersistent because not enough gas was produced to cause a PBSR everywhere beneath the hydrate blanket. This is thought to be the general case in the world's oceans because the PBSR has been observed to be laterally impersistent, even though the gas hydrate blanket is more persistent and, in fact, is probably never completely absent.

2.12 Possible Alteration in Sediment Surface Owing to the Presence of Gas and Gas Hydrate

In areas where gas seepage is common, isolated mounds and clusters of mounds up to 40-m high with surface hydrate-sediment mixtures have been identified (Prior et al. 1989). These mounds and concentric fault systems, which resemble scattered small hills on an otherwise smooth bottom, are individually about $1.5 \times 10^6 \text{ m}^2$ in area (in the Gulf of Mexico), where they have been imaged on side-scan sonar and transected by seismic sections. The shallow beds have been arched upward to form the hill; deeper beds appear to be unaffected by the arching. Prior et al. (1989) note that the exact formation mechanism is not known, but the hills are almost certainly associated with the upward migration of gas. The hills are unlikely to be mud-gas-fluid diapirs because the stratified structure is preserved and in a mass flow-laminated structure would be obliterated. Gas hydrate crystallization in the sediment would likely have formed the hill by a local expansion of sediment, water, and hydrate mixture. Prior et al. (1989) suggest that these hills on the seabed are a hydrate analog to the ice-cored pingos common in Arctic permafrost terrains.

Because these hydrate mounds and blowout craters are small features on the sediment plains of the ocean bottom, it is only recently that research tools such as deep-tow sidescan sonar and high-resolution deep-water-seismic profiling reveal their presence and their abundance, and distribution is unknown. Bottom-camera photography, which is widespread in the deep oceans, reveals too small an area to identify either a hill or a crater. If the formation of the hydrate hills is a common event, the roughness of the bottom will be much more highly variable on the small scale than it would be in

their absence. In addition, in areas where upward arching of bottom sediments is associated with an upward arching of the PBSR, gas will concentrate beneath the hills if there is a closure of the gas zone, and the gas will migrate from the lower areas. The arching process, then, may constitute a means of predicting the presence of PBSR in unsurveyed areas. In the Bering Sea, the velocity-amplitude anomalies (VAMPS) imaged on seismics are interpreted as showing the existence of gas traps held along the base of the hydrate layer (Cooper et al. 1986).

3.0 ACOUSTICALLY LAMINATED SEDIMENTS

3.1 Implications of Acoustic Structure in Bottom Sediments

Acoustic interaction in ocean-bottom sediments has traditionally been viewed in a simple manner for modeling bottom-interaction transmission loss. Although it is theoretically possible to accurately predict the effects of layered bottom interaction, local descriptions of the layered structure might not be available in enough detail to allow for accurate calculation, and the calculation process itself would be complicated and lengthy. Therefore, the aim of modelers has been to produce a generalized geoacoustical profile that would be a practical, flexible, and useful means for describing the geoacoustic properties of most sea floors (Vidmar et al. 1988).

Surface sediments are commonly referred to as having a uniform and predictable depth-dependent gradient in both acoustic velocity and density (Hamilton 1974; and Rutherford and Hawker 1978) even though it is well known that ocean-floor sediments rarely have near-ideal smooth velocity/depth profiles (Silva and Booth 1986). Especially above 800 Hz, seismics almost always show a highly reflective matrix of surface-parallel impedance contrasts (personal inspection). These laminated-impedance sediments are common in abyssal plains. Velocity "spikes" commonly occur on both positive and negative acoustic-velocity profiles, and often some of the "spiked" zones, which are associated with shear moduli (Trevorrow et al. 1987), can be up to tens of meters thick. These laminated or basically bottom-parallel acoustic structures may often result in developing sound channels where there are significant velocity reversals. On the smaller scale, acoustically laminated zones may form single sound ducts or multiple ducts that act as waveguides. Some sediments, especially in shallow water, commonly have waveguide attributes because of their depositional history. Acoustic lamination in sediments has the potential of being highly frequency dependent because of the often regular spacing of subparallel impedance surfaces.

Reflection and refraction are primary means of returning acoustic energy to the water column from bottom sediment in a form useful for Navy acoustics; scattered return is only rarely useful. In those areas where acoustic structure is increasingly complex and strongly contrasting, bottom-acoustic interaction tends to deviate progressively from the expected response of a simply modeled bottom.

3.2 Acoustic Impedance, Acoustic Structure, and Reflection Coefficients Within the Bottom

3.2.1 Primary Factors

Anisotropy within rocks and sediments can be caused by a number of primary geological factors: alignment of microcracks, nonisotropic porosity, orientation of acoustically anisotropic minerals, and alternate layering of rock or sediment with differing (elastic) properties or any other velocity-determining character. Preferred mineral orientation, especially of phyllosilicates (micas and clays), commonly occurs in sediments and can accentuate acoustic anisotropy dramatically with only minor compaction.

Sedimentary strata commonly have internal compositional structures that cause subparallel-acoustic impedance zones. In addition to deposition of pelagic and hemipelagic detritus in which the acoustic velocity does not vary, effusion of copper and other metals into the seawater from hydrothermal vents (Oberhnsli and Stoffers 1988) is very widespread in the oceans. These effusions result in dissemination of fine-grained metallic oxides and sulfides over broad areas of sediments well away from the hydrothermal sites at which the metal oxides and sulfides are concentrated. This submarine effusion of metallic reactants results in thin layers of relatively high-density acoustic velocity because these effusions tend to be fixed rapidly through chemical reaction with the seawater; because of their relatively high density, they sink rapidly and tend to compact more than the normal sediments. This manner of forming thin, high-acoustic-velocity layering is a general phenomenon associated with generating oceanic crust and subsequent ocean-basin sedimentation and has been recognized in one-time ocean sediments whose oceans have been obliterated by plate tectonics (Pfeifer et al. 1988).

Late primary or very early diagenetic alteration of the acoustic structure of ocean-basin sediments is also affected by manganese-nodule formation (Baturin 1988). These form from the interaction of seawater, which carries manganese and other metals that react in a similar manner, and the bottom and immediate subbottom, where the metals are fixed as oxides owing to the Eh-Ph contrast. Manganese and other metals fixed at the surface through direct geochemical effect are primary. Buried nodules dissolved with upward migration of the solutions to the surface where the metals are once again crystallized, however, are part of the cycle of nodule formation that results in a concentration of nodules at and just below the surface. Horizons of nodules become buried when sedimentation rates are abnormally high (Vogt 1986) and the nodules become buried or are otherwise separated from the surface-water circulation system.

3.2.2 Secondary Factors

Diagenetic or secondary geological modification of seafloor materials may also be important in establishing acoustic structure. Gas and gas hydrates in varying saturations have the potential to induce profound effects in sediments with strongly laminated high- and low-porosity zones, whereas with water saturation alone, impedance contrasts will not be as significant. Collett (1983), for instance, reports wells in the Prudhoe Bay region of Alaska that have multiple (up to four) zones of hydrate with unit thicknesses ranging from 2 to 28 m formed only in originally high-porosity sediments into which gas could migrate prior to hydration. Seismic reflections associated with diagenetic-acoustic anisotropy may be due to several factors including the contrast in acoustic impedance within a body, the contrast between bodies, and the affect of variable pore pressure.

So that anisotropic acoustic structure of rocks and sediments can be acoustically characterized to establish a model of minimum complexity for seabed materials, it is necessary to quantify responses in different materials. Physical properties of rocks offshore can be estimated using on-shore experimental data where acoustic impedance has been calculated for a number of samples from rock that extends onto the west European continental shelf (Chroston and Max 1988; and Max 1978). The specimens were triaxially tested at the University of East Anglia, England, to relate and quantify acoustic anisotropy in a rock with very fine scale (<1 cm) discontinuous foliation. Chroston and Max (1988) have a more complete discussion of the nature of acoustic variation, but anisotropic quantification in geological materials and their acoustic character are emphasized here.

Significant anisotropy was found (Fig. 19) with the higher velocities lying about in the foliation plane. Velocity differences were commonly 0.5 km s^{-1} , but ranged up to 0.8 km s^{-1} . Percentage

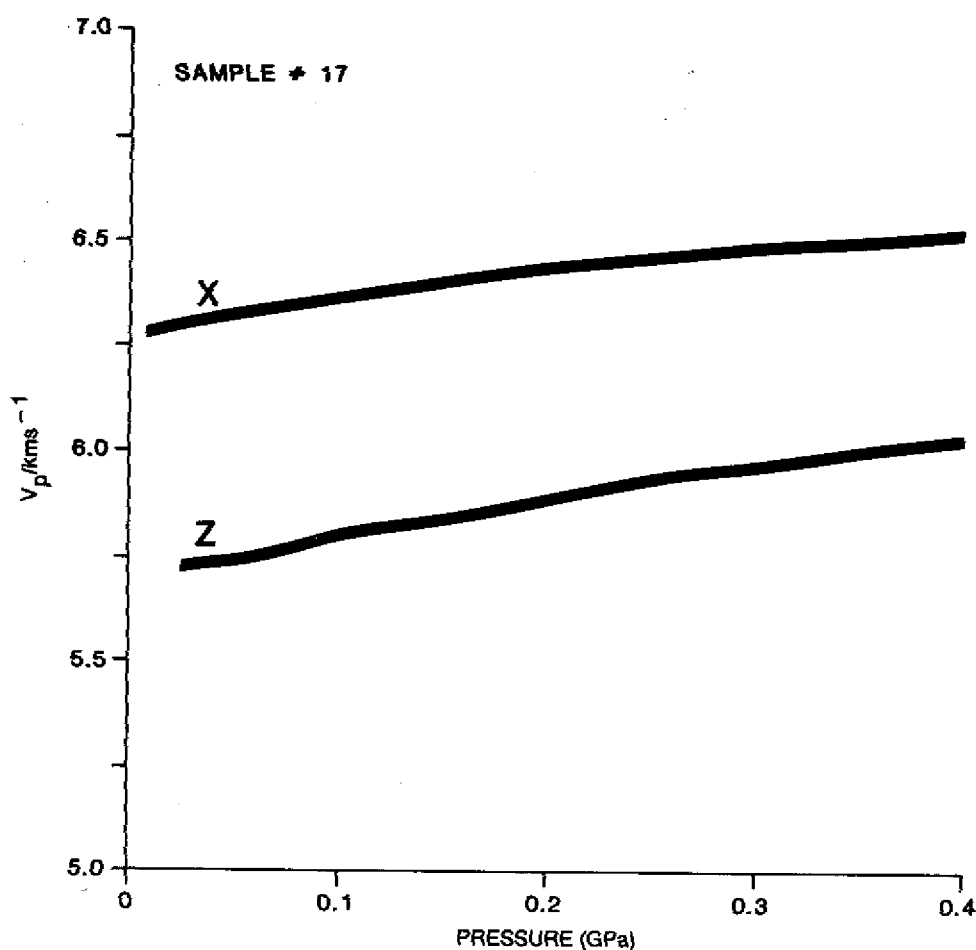


Fig. 19 — Maximum (X) and minimum (Z) velocities determined from the acoustic sounding of macroscopically homogenous mylonite rock; an example of an imposed acoustic structure (after Chroston and Max (1988)). X is along striping, Z is across. Attenuation is also higher in the Z direction, but this was not quantified. Variation of about 20% shows the existence of anisotropic acoustic structure where none would otherwise be expected from general geological descriptions.

anisotropy calculated by $(V_{\max} - V_{\min}/V_{\max}) \times 100$ shows that most values are about 5%, but some higher values of 8% to 10% were also found. These are minimum values, as the direction of the true V_{\max} and V_{\min} may not have lain precisely in the measured directions. Indeed, the samples that have been fully triaxially tested with three cores show significant differences in the velocities between the X and Z directions in these specimens, which otherwise appear identical. The magnitude of the observed acoustic anisotropy is comparable with that seen in many metamorphic rocks present on North Atlantic continental shelves (Christensen 1965; Chroston and Evans 1983; and Fountain et al. 1984). Seismic anisotropy is a pervasive and consistent feature of geological materials, and values from 5% to 10% should be regarded as minimum values for acoustic anisotropy.

The possibility that the change in velocity in the Chroston and Max (1988) sample set may have been due to density changes was investigated by comparing velocity differences with those that might be expected assuming Birch's Law with different mean atomic weights (Birch 1960, 1961). Typically

one might expect an increase in velocity of about 0.3 km s^{-1} for an increase in density of $0.1 \times 103 \text{ kg m}^{-3}$. For most samples tested, the differences in density were too small to account for the velocity increase; in four cases, the velocity increase corresponds anomalously to a significant density decrease. Although a few cases could have been attributable to a density-velocity relationship, it would appear that the presence of a significant anisotropic acoustic-structure in a macroscopically homogeneous rock or sediment can be imparted by lamellae on a subwavelength scale.

Figure 20 shows a parametric acoustic record from deep water in the Norwegian basin taken by the *R/V Meteor* (Gerlach et al. 1986; and Kassens, personal communication). Use of the Krupp-Atlas parametric sonar allows resolution of fine-scale reflectors at depths where other depth sounders and bottom profilers are ineffective. At one point on the track, a gravity core was obtained from pelagic sediments that are often regarded as having no strong geological layering. A detailed core examination was carried out. Comparison of the core analysis and the paracoustic record shows that there is a direct relationship between the many small acoustic events or reflections and small and impersistent variations in the shear sediment strength with depth. These thin zones showed no grain-size variation from bounding lower velocity zones; velocity contrasts were almost entirely caused by porosity contrasts. The presence of reflections shows that this deep-ocean sediment is capable of reflecting acoustic energy from units that are between 1.5- and 2-m thick for at least the upper 8 m of sediment that was tested. Because of the stable deposition mode in these pelagic sediments, this acoustic structure can be expected to be pervasive, at least in this region of the Norwegian Sea.

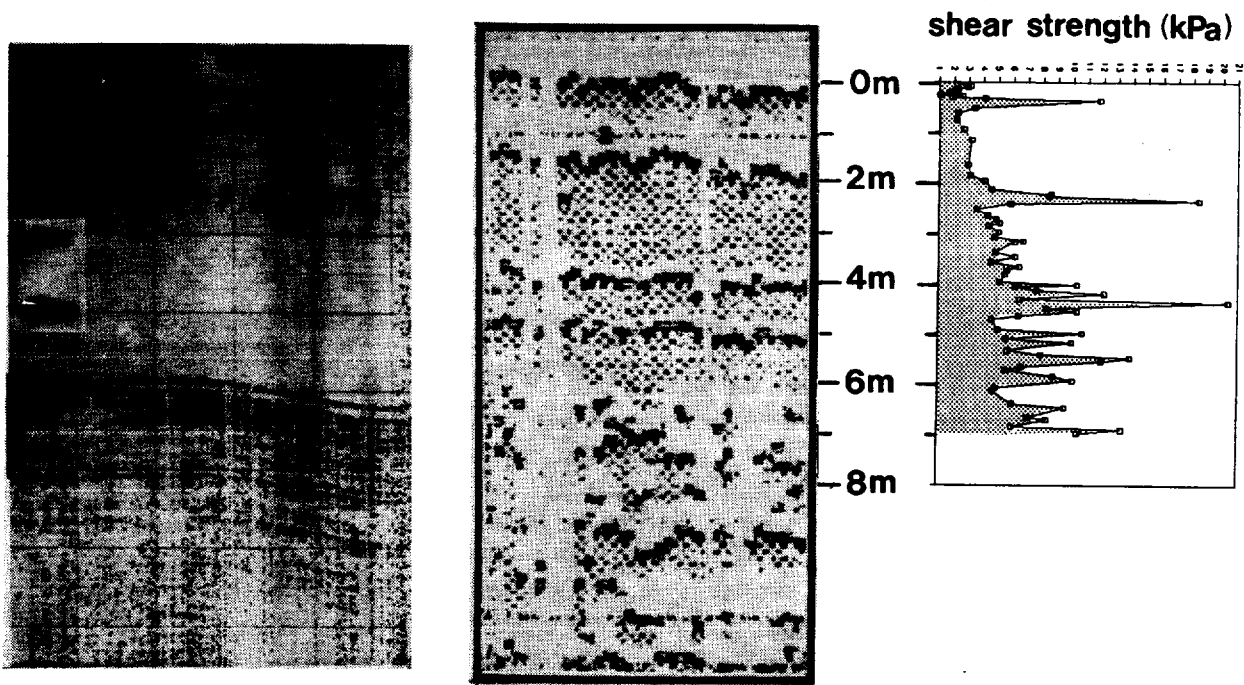


Fig. 20 — Shallow seismic structure and shear strength. Figure from advertising brochure for the Krupp-Atlas Hydrosweep-parametric sonar bottom imaging bathymetric and shallow bottom profiling system. Original was provided by H. Kassins of the University of Keele and is used here with grateful permission.

3.3 Naturally Occurring Frequency Dependence of Bottom Loss

The concept of many small and often discontinuous layers causing reflection or ducting can be applied to ocean-bottom sediment. Many small-scale reflectors, even of a limited lateral extent, can cause constructive reinforcement of wave fronts, with consequently enhanced reflection (Fig. 21(a)). Waveguided energy can also jump from one set of guides to another in subparallel sets because the propagating energy "sees" matrices of impedance contrasts, not specific surfaces (Fig. 21(b)). Where waveguides exist, reverberation is a common attribute of sound propagation. Relating the known existence of irregular sediment velocity or shear profiles with acoustic return has not commonly been carried out, however, especially in deep water where detail in surface sediment is difficult to resolve on the small scale.

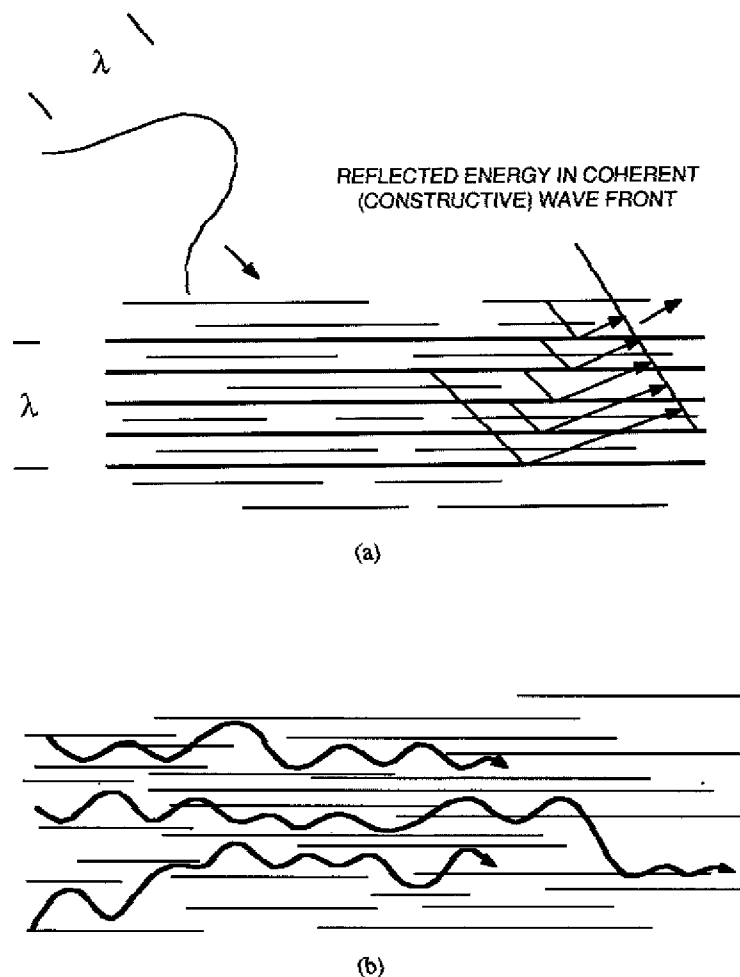


Fig. 21 — (a) Diagram showing the relationship between acoustic energy, at an arbitrary specific frequency, and stacked, subparallel impedance horizons, such as are commonly found in seabed sediments. Acoustic energy naturally "finds" suitably spaced reflectors at the one-quarter, one-half, and wavelength distance resulting in constructive reinforcement of reflected energy; (b) Acoustic energy jumping within a set of waveguides. Lateral propagation of the constrained acoustic energy is not confined to individual horizons.

Acoustical seafloor properties are primarily determined by the physical roughness, layering, and composition. Although reflectivity can be expressed by functions of bulk compressional and shear waves and density (Akal 1974), very low losses can result from a system of regular layering where the thickness of double layers equals half the acoustic wavelength (Hastrup 1969). This small-scale layering is common on continental shelves and in ocean sediments at virtually any depth.

It is well established that strong reflections can be generated from beds thinner than the wavelength (Widess 1973) and also by constructive interference from a zone of alternating high and low acoustic impedance (Kind 1976; Fountain et al. 1984; Jones and Nur 1982; and Kennett 1985). Synthetic modeling of various laminated structures was carried out by Jones and Nur (1982), but their units of acoustic impedance were 110-m thick, and the results may not be directly proportional to more thinly laminated materials. Constructive interference based on the individual acoustic impedances may be important where the individual lamina are not too thin in comparison with the normal reflection seismic wavelengths. Best constructive reinforcement takes place at $1/4$ wavelength spacing, but multiples such as $1/32$ and $1/64$ of wavelength will also introduce frequency/grazing angle-dependent relationships. Thus, units of rhythmically bedded strata have the potential to cause selective constructive reinforcement of incident acoustic energy. If the lateral extent of the anisotropic "units" is less than the fresnel zone, however, this would diminish the amplitude of the reflected wave.

Specific wavelength energy can be expected to be selectively enhanced because the formation of subparallel-impedance contrasts is a geological rather than a statistically random process. At a given frequency, a regular spacing of smaller-than-wavelength reflectors will form constructive reinforcement of incident energy; this is termed the "Bragg scattering effect" in X-ray diffraction spectrometry, where a rotating source of specific frequency radiation is used to resolve atomic spacing of crystallographic planes in mineral analysis. For instance, in a rhythmically laminated ocean-bottom sediment such as turbidite or many pelagic sediments, a specific range of distances between impedance-contrast horizons will naturally occur. The spacing will depend on the geological history of deposition; the acoustic impedance will be the sum of effects induced during both the primary and secondary geological histories.

There are important variations in frequency-dependent bottom-loss transmission curves. There are also important steps in the relative absorptions at specific frequencies (especially lower frequencies) suggesting that a physical parameter is related to a specific grazing angle/frequency relationship. In some experiments, low-frequency loss is consistently higher than high-frequency loss even though losses generally increase with increasing frequency. Zhou and Zhang (1987) suggest that nonlinearity in frequency-dependent absorption of sound may be a common occurrence that they attribute to some characteristic of the upper-sediment layer. Holthusen and Vidmar (1982) also note that reduction in bottom loss in an acoustically laminated bottom can be as great as 10 dB; they regard the decrease in bottom loss as a collective effect of the layered structure and that it is dependent upon constructive interference. It is likely that the naturally occurring spacing of impedance contrasts, which is dependent on the geological history, may be an important contributor to anomalously low-bottom loss at specific frequencies. Regular spacing will exert a selective effect upon incident broadband acoustic energy (Fig. 21(a)). As the geological history of sedimentation within a sedimentary terrane will have an internal coherence, expansion of the terrane concept to more deep-water areas where intensive bottom interaction does not take place except at very low frequencies and then only over long distances may be practical to characterize geoacoustic response.

It is probable that significant acoustic energy can be returned to water by reflection even from sediments that might appear, from a primary geological point of view, to be rather homogeneous. The secondary geological attribute of gas hydrate in sediment can alter, induce, or accentuate porosity laminations and has the potential to strongly alter the primary geological character of that part of the sediment column most relevant to bottom-acoustic interaction. For instance, when a unit of sediment is hydrating at a constant rate, the bands of minimum porosity will effectively solidify first, while the fluid in the more porous beds becomes more viscous with hydrate crystallization but still exhibits the acoustic character of a fluid. This selective tightening of alternating sedimentary bands will accentuate the acoustic character beginning within meters of the biological zone of the sediment surface. Theoretical and experimental work is necessary to constrain acoustic modeling and the implications of acoustically laminated sediments while assessing the potential differences between in situ and laboratory determinations of velocity structure.

4.0 NAVY GEOACOUSTIC BOTTOM-LOSS CHARACTERIZATION

4.1 Predicting Geoacoustic Response Through Modeling

Predicting acoustic transmission in ocean areas is vital to the Navy for both surveillance and engagement scenarios. In the water column, accurately predicting acoustic propagation can often be difficult, but where there is also interaction with the bottom as well as the water surface, prediction can be difficult indeed. The accuracy with which transmission-loss prediction can be made usually diminishes dramatically with the increasing complexity of the bottom environment.

Prediction of bottom loss is estimated by mathematically modeling propagation paths through the environment and calculating the results of acoustic transmission in the water and through geological materials and their interfaces, at and below the bottom, with respect to variable source and receiver. It is necessary to characterize or model or simplify the sea bottom, however, because widespread availability of detailed acoustic-transmission properties of all areas of interest are not, and are not likely to be, generally available. A geoacoustic model is defined (Hamilton 1980) as "a model of the real sea floor with emphasis on measured, extrapolated, and predicted values of those properties important in underwater acoustics and those aspects of geophysics involving sound transmission. Simple geometrical and material models for the bottom are usually assumed as general cases, with the aim of providing reasonable predictions in the absence of specific measurements."

Although synthetic models have been proposed for thickly sedimented areas that can be made to effectively model experimental geoacoustic response where it is known (Monet et al. 1983), they do not fulfill Hamilton's definition of a geoacoustic model because they often assign physical properties that do not exist in those areas to layers in the bottom. The bottom, especially in shallow water, is not commonly layered parallel with the bottom surface. Simplifications of synthetic models apparently offer corroboration of geoacoustic experiments that are as good or better than the most common current synthetic model (McCammon 1988). For Navy needs, it does not particularly matter whether a working transmission-loss prediction model is primarily geoacoustic or synthetic based; but for deducing bottom types from acoustic data, a geoacoustic model is necessary. One aim of this report is to demonstrate that when a broader range of geoacoustic properties are taken into account than were thought to be applicable, new geoacoustic models can yield results that approximate the results of a fully compensated synthetic model.

Where there is bottom interaction, two main problems to modeling detailed transmission need to be addressed if geoacoustic modeling and transmission-loss prediction are to advance. First, geoacoustic parameters of the bottom that are especially important at low frequencies have not been fully considered; this is the fault of inadequate data input. Existing high- and low-frequency data bases available to the Navy for a high percentage of the world's oceans, for instance (Naval Oceanographic Office 1988(a) and (b)), have not been assembled with reference to the existence of either enhanced acoustically laminated bottoms or the presence of gas hydrate, both of which are known, in principal, to strongly affect bottom-acoustic interaction. Until recently, characterization of the bottom in terms of specific materials and their disposition, as well as artifacts of disposition and morphology of surfaces that induce anisotropic behavior of acoustic propagation, have not been adequately considered. Second, models may not be able to mathematically encompass the geoacoustic variables that are now known to affect acoustic propagation. For instance, the common bottom-loss predictive models can take into account adequately laminated acoustic-impedance contrasts that are not parallel to the bathymetric bottom; as this condition is characteristic of important continental-shelf areas such as the southwest approaches to the British Isles, the value of both range dependent and independent low-frequency propagation modeling (< 500 Hz) must be called into question. In addition, azimuth variability of propagation through any particular point is difficult for any model if the cause is not a first-order variable.

4.2 Primary And Secondary Geological Attributes

Ocean-floor sediments can be described from a number of different viewpoints. To the geologist and geophysicist who are academically concerned with the formation of oceanic crust or the overlying sediments the primary geological attributes of the age, disposition, chemistry, and overall history of formation are the principal means by which a description of an ocean-bottom area is made. These primary characteristics and their descriptions form the bases for subsequent research and provide clues in unravelling the geological history of ancient oceans, whose remains can be found within one-time mountain belts (Williams and Max 1980).

Secondary geological attributes, however, can be of great importance to bottom-acoustic interaction. These attributes concern the modification or the development of characteristic geoacoustic properties such as attenuation and velocity, and the establishment of velocity profiles. The most widely recognized secondary geological attribute in deep-ocean sediments is compaction, which by altering the porosity and telescoping impedance contrasts, exerts the primary control over the development of velocity gradients and acoustic structure. Cementing and filling porous spaces through diagenetic processes can also be important in deep-ocean sediments.

Initially, gas hydrate crystallization will have the effect of expelling fluid from sediment as the individual crystals form. As hydration continues, interstitial spaces will fill by the formation of new crystals and by their joining together, which will have the result of forming a solid mesh of hydrate crystals. As saturation of hydrate progresses, the solid becomes more dense and of greater interest to bottom-acoustic interaction, introduces both much higher velocities and a proposed new velocity structure that should be applied to ocean-bottom sediments where gas hydrate has developed (Fig. 22). Where density, velocity, attenuation, and porosity have been previously considered as being regularly altering parameters that are dominantly controlled by compaction as a function of the sedimentary material and depth of burial, the presence of gas hydrate has the potential of strongly changing those parameters. The specific alteration of primary geoacoustic properties and the development of the proposed new geoacoustic-model profile is discussed in Section 5.

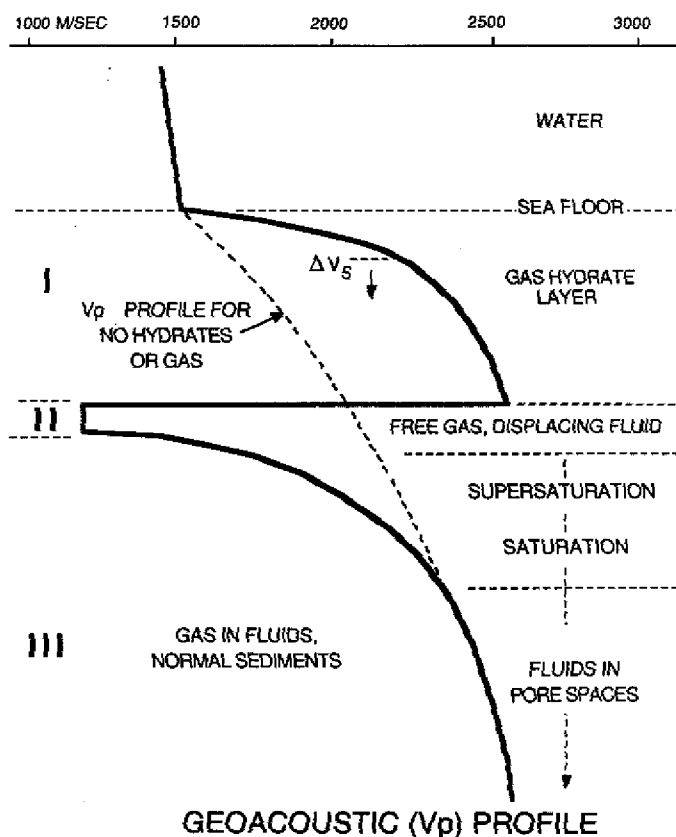


Fig. 22 — Proposed general-compressed-velocity profile for hydrated deep-sea sediment. No vertical scale is shown because the relationship of seawater and sediment depths will affect both the gradients and the thickness of the gas hydrate layer.

Because gas hydrate in seabed sediments is unstable at lower temperatures and pressures, it can rarely survive transport along with a core or dredge sample to the surface. The exceptions have been in rapidly surfaced dredges and in pressurized core barrels. Large-scale Navy programs have taken little notice of the gas hydrate presence and what its expected influence on bottom-acoustic interaction was to be. It is regarded as a rarity, because little was known until recently about its physical properties or its distribution.

Gas hydrate, and often free gas at depth, is now recognized as widely occurring in the world's oceans, and its presence should be regarded as the general, not the special case. Its presence, to some degree of development and saturation, should be ubiquitous.

4.3. Geoacoustic Physical Parameters and Their Representation as Physical Models

Because the bottom environment is complex, large-scale Navy sampling programs have been carried out in the oceans. These have a sedimentological or primary geological aim, however, and specific physical attributes and commonly measured on specimens at surface ambient pressures and temperatures (Baldwin et al. 1985). An unspoken assumption is that the specimens measured in the laboratory have an *in situ* analog; this assumption is unjustified in the case of gas hydrate. These

measurements are integrated with laboratory experiments that measure acoustic response to parameterize the specific response of sediments and rocks of particular densities, particle size, particle-size variation, and composition. Relating the traditional laboratory work with specific ocean-bottom response determined from acoustic experiments, however, often results in anomalous conclusions or important deviations of experimental results from the predicted geoacoustic response. Nonetheless, acoustic measurements and laboratory work continue in an attempt to identify the significant propagation-controlling aspects of ocean bottoms. Synthetic, rather than geoacoustic models, usually have the disadvantage of not being directly relatable with seabed geology of either primary or secondary nature (Monet et al. 1983; McCammon 1988).

Traditionally, bottom loss is concerned with scattering and attenuation effects of acoustic energy. At lower frequencies (below 1000 Hz), shear and body-wave energy conversion also become a primary extractors of acoustic energy from the water column (Akal et al. 1983). At low frequencies, all bottom materials that act to strongly enhance bottom-acoustic loss become increasingly important.

Acoustic velocities in bottom sediments and rocks in sedimentary basins that are often misnamed sediments are usually dealt with as a uniform material whose velocity gradationally increases with depth or with the initial velocity predicted at a place inferred from a measurement or estimate of the dominant sediment type, such as sand, fine sand, or clay. It is well known, however, that the bottoms and subbottoms, especially in shallow-water areas, rarely achieve this elemental simplicity. It is only logical, therefore, that acoustical prediction models should take into account the environment in a realistic manner to successfully predict the effects of interaction, which may include transmission enhancement through sound ducting, as well as loss.

The ability of a rock or sediment to cause reflection in preference to refraction is largely controlled by frequency and the angle of incident energy with respect to the impedance of contrast planes. Sediment particle size and the predicted degree of compaction, which are directly inferred as a depth function, are related to tables of laboratory-measured values determined from sediments. Sediment particle size, porosity, and provenance are given the highest status in inferring bottom-acoustic interaction (Urick 1975; and Hamilton 1980). Unfortunately, no significant allowance has yet been made in taking into account the presence of gas and gas hydrates in identifying realistic acoustic-velocity structures in bottom sediments. Along continental shelves, complex disposition of geoacoustic provinces have been defined (Lavoie 1985) based on sediment thickness and the type of subsediment basement, with apparently little regard to the nature of diagenetically induced acoustic anisotropies or the orientation of acoustic-impedance lamination.

Simple reverse-gradient zones (acoustic channels), which will inevitably accompany the presence of gas hydrate, have been considered by acoustic modelers only rarely (Vidmar and Lindberg 1987). Constructive interference from layered-impedance zones of primarily geological origin, however, has been quantified for bottom loss (Greene and Rubenstein 1985). These efforts, however, have not assessed the necessary range of realistic properties of a gas-hydrated seafloor. Daniels and Vidmar (1982), in calculating expected bottom loss, used a P-wave velocity of 2.7 km/s, which was close to the maximum gas hydrate water-saturated sediment velocity determined from experimentally produced gas hydrates (Stoll 1974). It is now known (Fig. 18) that V_p -wave measurements of naturally occurring gas hydrates from drill holes range up to 4.4 km/s (Collett 1983). It is also known that gas hydrates can form thick blankets, rather than being confined to the top few meters of sediment. Thus a new modeling of gas hydrates effects in deep sediments is necessary to gauge the overall effect on acoustic propagation where there is bottom interaction.

5.0 GEOPHYSICAL AND GEOACOUSTIC MODEL OF DEEP-OCEAN SEDIMENTS CONTAINING GAS HYDRATE

5.1. Purpose of Modeling

The purpose of erecting a geophysical model of the seismoacoustic properties of ocean floor sediments is to generalize those physical properties important to acoustic propagation so that relatively simple calculation of the matrix of effects can be made. Physical parameters such as V_p , V_s , attenuation, and density are of primary interest. Hamilton (1980, p. 1314) has noted that . . . "there is an almost infinite variety of geoacoustic models; consequently, the floor of the world's ocean cannot be defined by any single model or even a small number of models." His observation reflects the wide number of differing primary geological situations and, in the deep oceans, the wide variety of sediment types and thicknesses.

If the secondary geological attributes induced by the presence of widespread gas hydrate (\pm PBSR) are significant, however, then there should be a convergence of bottom-acoustic response that will be controlled by a combination of the primary and, increasingly important, secondary geological attributes. The new geoacoustic velocity profile (Fig. 22) and other geoacoustical parameters of deep-ocean sediments that can be expected to be dominated by the presence of gas hydrates may allow for exploration and survey in deep-ocean sediment.

Three general geoenvironmental situations involving sediment, gas hydrate (\pm PBSR), and acoustic basement/top-oceanic crust can exist in the deep ocean. They are:

- Unhydrated sediment. Although the distribution of gas hydrate is uncertain at this time, no investigation for their presence has shown them to exist. Given their thermodynamic stability and the known factor of widespread gas production, it is likely that they are ubiquitous. Nonetheless, because the acoustic community has treated sediments in the ocean bottom as unhydrated in the past, this condition is modeled to allow comparison between unhydrated and hydrated sediments. Table 2 shows how unhydrated sediments are used as a reference to existing modeling.
- Hydrated sediment where the base of the hydrate is in the sediment above acoustic basement. The case that is modeled to show the bottom-acoustic propagation deviations from the unhydrated sediment case in thickly sedimented areas. Tables 2 and 3 both show hydrate and hydrate plus PBSR considered separately, and the acoustic data represent a best estimate of the averaged properties, which can be expected to vary considerably on the small scale.
- Hydrated sediment where the base of the hydrate is below acoustic basement. This complex case might occur in thinly sedimented areas where the hydrate would be stable down into the subjacent rock. Because gas production in the rock is liable to be significantly lower than in sediment and the porosity in the rock is lower than sediment, less gas will be produced and once produced, will have difficulty migrating upward into the sediment. Petrogenic gas produced in the sediment will be minimal because of the low temperatures and light burial, and biogenic gas produced in the top of the sediment may largely migrate into the water column and gasify on ascent. In addition the nature of the rock may be critical, whereas gas hydrate is stable in virtually all deep-ocean sediment types. This, therefore, is a special case that may have many subsituations, and it has not been modeled.

Table 2 — Data for the Reflection Coefficient Calculations of the SAFARI Model for the Three Geoenvironmental Cases: (a) — Unhydrated Sediment; (b) — Hydrated Sediment; and (c) — Hydrated Sediment with PBSR. See Schmidt (1988) for details of calculation and plotting parameters. Column A, depth from top of sediment (water column is treated as an indefinite a half-space with the source field is equivalent to a plane wave incident at the lower water interface); b, Compressional wave velocity; c, Shear wave velocity; d, Compressional attenuation (dB/wavelength); e, Shear attenuation (dB/wavelength); f, Density (g/cm³)

(a) Unhydrated Sediments						(b) Hydrated sediments						(c) Hydrated sediments with BSR						
(a)	(b)	(c)	(d)	(e)	(f)	(a)	(b)	(c)	(d)	(e)	(f)	(a)	(b)	(c)	(d)	(e)	(f)	
0	1535	0	0	.0	1.043	0	1525	127	.30	.5	1.15	0	1535	0	.0	.0	1.043	
0	1525	127	.30	.5	1.15	5	1560	130	.37	.55	1.2	5	1525	127	.30	.5	1.15	
5	1535	130	.37	.55	1.2	20	1650	142	.35	.6	1.25	20	1650	130	.37	.55	1.2	
20	1545	142	.35	.6	1.25	30	1700	155	.25	.5	1.4	30	1650	142	.35	.6	1.25	
30	1545	155	.25	.5	1.4	50	1750	200	.23	.44	1.46	50	1700	155	.25	.5	1.4	
50	1562	190	.25	.45	1.42	60	1800	275	.19	.37	1.65	60	1750	200	.23	.44	1.46	
60	1575	210	.23	.4	1.55	70	1850	350	.16	.32	1.80	70	1800	275	.19	.37	1.65	
70	1590	250	.20	.4	1.75	80	1900	435	.15	.28	1.85	80	1850	350	.16	.32	1.80	
80	1600	300	.20	.39	1.8	90	1950	485	.14	.27	1.95	90	1900	435	.15	.28	1.85	
90	1610	345	.20	.38	1.85	100	1985	510	.13	.27	1.98	100	1950	485	.14	.27	1.95	
100	1649	390	.19	.35	1.68	150	2050	560	.12	.26	2.0	150	2050	560	.12	.26	2.0	
150	1705	420	.19	.35	1.73	200	2100	595	.11	.24	2.1	200	2100	595	.11	.24	2.1	
200	1780	448	.18	.34	1.81	250	2150	655	.11	.23	2.2	250	2150	655	.11	.23	2.2	
250	1800	480	.17	.33	1.87	300	2225	695	.11	.22	2.2	300	2225	695	.11	.22	2.2	
300	1864	507	.16	.32	1.93	350	2300	740	.11	.22	2.2	350	2300	740	.11	.22	2.2	
350	1896	543	.16	.32	1.98	400	2360	785	.10	.21	2.2	400	2360	785	.10	.21	2.2	
400	1960	570	.16	.31	2.03	450	2430	800	.10	.21	2.3	450	2430	800	.10	.21	2.3	
450	1996	605	.16	.31	2.07	500	2475	840	.10	.20	2.3	500	2475	840	.10	.20	2.3	
500	2048	636	.16	.30	2.11	550	2500	880	.10	.20	2.4	550	2500	880	.10	.20	2.4	
550	2085	680	.16	.30	2.13	600	2128	702	.16	.30	2.15	600	2475	840	.10	.20	2.3	
600	2128	702	.16	.30	2.15	650	2170	728	.16	.30	2.16	650	2500	880	.10	.20	2.4	
650	2170	728	.16	.30	2.16	700	2202	755	.15	.29	2.17	700	1200	100	.46	1.0	1.80	
700	2202	755	.15	.29	2.17	750	2233	776	.15	.28	2.18	750	1250	160	.45	1.0	1.80	
750	2232	776	.15	.28	2.18	800	2269	810	.15	.27	2.19	800	2202	755	.15	.29	2.17	
800	2269	810	.15	.27	2.19	850	2302	832	.14	.26	2.20	850	2233	776	.15	.28	2.18	
850	2302	832	.14	.26	2.20	900	2330	855	.14	.25	2.22	900	2269	810	.15	.27	2.19	
900	2330	855	.14	.25	2.22	950	2355	879	.13	.24	2.23	950	2302	832	.14	.26	2.20	
950	2355	879	.13	.24	2.23	1000	2385	900	.13	.24	2.24	1000	2330	855	.14	.25	2.22	
1000	2385	900	.13	.24	2.24							1000	2355	879	.13	.24	2.23	
													1000	2385	900	.13	.24	2.24

Table 3 — Data input for the reflection coefficient calculations of the SAFARI model for two geoenvironmental cases: (a) Thoroughly hydrated sediment of the same thickness as used for the undersaturated hydrate cases for Table 2; and (b) Thoroughly hydrated sediment with PBSR at a high level representing either a high heat flow or shallower water situation. Columns and references to Schmidt (1988) the same as for Table 2.

(a) Hydrate Layer						(b) Hydrate Layer with BSR					
(a)	(b)	(c)	(d)	(e)	(f)	(a)	(b)	(c)	(d)	(e)	(f)
0	1535	0	.0	.0	1.043	0	1535	0	.0	.0	1.043
0	1525	127	.30	.5	1.15	0	1525	127	.30	.5	1.15
5	1560	130	.37	.55	1.2	5	1560	130	.37	.55	1.2
20	1700	155	.25	.5	1.4	20	1700	155	.25	.5	1.4
30	1800	275	.19	.37	1.65	30	1800	275	.19	.37	1.65
40	1900	435	.15	.28	1.85	40	1900	435	.15	.28	1.85
50	2000	530	.13	.27	1.98	50	2000	530	.13	.27	1.98
60	2100	595	.11	.24	2.1	60	2100	595	.11	.24	2.1
70	2200	690	.11	.23	2.2	70	2200	690	.11	.23	2.2
80	2300	740	.11	.22	2.3	80	2300	740	.11	.22	2.3
90	2400	790	.10	.21	2.3	90	2400	790	.10	.21	2.3
100	2500	880	.10	.21	2.3	100	2500	880	.10	.21	2.3
110	2600	915	.10	.21	2.4	110	2600	915	.10	.21	2.4
120	2700	960	.10	.20	2.5	120	2700	960	.10	.20	2.5
600	2128	702	.16	.30	2.15	150	1200	100	.46	1.0	1.8
1000	2385	900	.13	.24	2.24	200	1750	442	.18	.34	1.9
						600	2128	702	.16	.30	2.15
						1000	2385	900	.13	.24	2.24

- Previous acoustic reflection-loss calculations and the more realistic nature of the current model. Daniels and Vidmar (1982) calculated bottom loss as a function of grazing angle for normal sediment bottom—bottom with soft (undersaturated and low porosity percentage) and hard (saturated and high percentage of porosity) gas hydrate layer. Their 100-m thick hydrate layer is thinner than would be expected in ocean basins and was modeled as having the same acoustic properties throughout. This homogeneous thin-layer model can now be regarded as an unrealistic representation of the hydrate layer. In addition, they did not include the presence of PBSR in modeling. They concluded that the ability of the gas hydrate to bear elastic waves and reduce attenuation were important facets of the geoacoustic-profile alteration of soft or undersaturated hydrate, and that the development of gas hydrate and the effect on bottom loss are not likely to be a purely linear relationship with depth. They concluded that hydrates have a potentially profound impact on underwater acoustics. While concurring with their general conclusions, modeling carried out here is done with new geological information about the presence of hydrates and their geoacoustic properties with respect to depth in the sediment that attempts to closely model the subbottom environment in deep-ocean sediments.

The thickness of the gas hydrate layer modeled here is ~600 m based on the known thickness in sediment at about 3-km water depth (Fig. 12). This water depth is convenient because ocean-basin sediments occur within 0.5 km of this depth, and thus the results of the modeling will have general applicability; it is also the approximate water and gas hydrate depth of the proven hydrate deposits at Blake Spur, off the southeast coast of the United States. The acoustic velocities modeled are a gradient to the seismic refraction analysis that yielded a gas hydrate/PBSR V_p four-layer solution; more saturated hydrate is regarded as forming the lower part of the gradient, while less saturated hydrate forms the upper part because of the manner in which gas is produced and hydrated. Possible impedance enhancement of layered structure in the upper part of the hydrate is not modeled because of uncertainty about the uniformity of widespread original layering, uncertainty as to both variation and degree of enhancement possible, and the chance that by introducing an extremely finely laminated structure and many more arbitrary layers in the model, that artifacts of the calculation could skew the result.

The gas hydrate bottom-following blanket introduces seismoacoustic character that varies considerably from that of unhydrated sediment as seen again in Tables 2 and 3.

5.2 Source of Velocity Profiles

5.2.1 Unhydrated Sediment as Reference

Because the presence of gas hydrate and gas in deep-sea sediment has not been systematically modeled, V_p and V_s values for unhydrated sediment, which are used here as the theoretical basis against which to compare the effects of seismoacoustic interaction in hydrated sediments, are taken from table values used by acousticians rather than from more modern geological information. The transmission-loss results are comparable with other bottom-loss modeling done within the acoustical community. In both cases, however, depth/velocity values are averages or best-fit curve pictures and variations from place to place are to be expected. Further work will be necessary to incorporate the new information gained from the Deep Sea Drilling Program and to reassess changes in acoustic properties incurred in sampling and recovering material from the deep-ocean floor to the surface. For this study, it is assumed that the slight differences that vary irregularly (usually by no more than 25 m/s) are not large enough to cause a significant variation. Surface-sediment velocities for surface and 100-m depth intervals to 1000 m are taken from Hamilton (1979; 1980 Table VI(a)) and for surface and 10-m depths, from Daniels and Vidmar (1982). Intermediate velocities for layer boundary depths are extrapolated linearly, except for V_s from the surface to 30-m depth, where extrapolations fit a synthetic curve.

Values for attenuation of unhydrated sediments have been derived from Kuperman et al. (1985) and Schmidt (1988) and from personal communication with members of the Shallow Water Acoustics Branch (5160) of the Naval Research Laboratory (NRL) who are familiar with the (SAFARI) seismoacoustic model that has been used in this study. Again, different numbers are considered more appropriate by some, but variation is probably not great. Deviation from other attenuation curves for similar sediments (Hamilton 1980; and Daniels and Vidar 1982) are considered insignificant, but one case with a differing profile (Table 2) has been modeled for comparison as an example.

5.2.2 Hydrated Sediments

Sound-speed profile in a gas hydrate and PBSR sea bottom

Gas hydrate has the potential of transforming what has been commonly assumed to be the sound-speed profile in unhydrated sediments (Fig. 22; Tables 2(a), 3(a)) where there is a regularly increasing sound-speed velocity with depth. Velocities and gradients have been uniformly treated as reflecting the primary geological attributes of the nature of the material and its physical properties, and the porosity, which is treated as a depth-dependent function. When hydrates are present, however, not only can higher acoustic velocities be expected, but the sound-speed profile can be expected to depart radically from that of the normal profile used for unhydrated sediment (Fig. 22). Three main zones are present; they are the gas hydrate layer, the free-gas zone (only developed in PBSR areas), and the normal-sediment zone.

Because the base of the hydrate is continually moving upward at the same rate as sedimentation, the lower part of the hydrate will be more rigid and solid than the upper part because it has been hydrating longer and is first exposed to rising gas. In this relationship, the P-wave velocity curve can be expected to show a strong gradient in the topmost part that turns to a more slowly increasing velocity profile with depth. Velocity reversals reflecting either acoustically laminated materials or accentuation of laminated impedance contrasts caused by the presence of gas hydrate are not part of this suggested model. Allowance for their presence in future modeling may have to be made if the upper part of the gas hydrate profile is found to be significantly acoustically laminated with respect to the velocity profile induced overall. Thus the velocity profile for a gas hydrate horizon is strongly upward-refracting; reflections attributable to acoustic-impedance lamination might enhance the tendency to lower bottom loss. Sediment below the hydrate layer once had hydrates in it, but assigning specific properties to these sediments that would differ in any significant way from a simply unhydrated section has not been speculated on for this modeling.

At the base of the hydrate layer, the velocity will decrease to near that expected in unhydrated sediment where there is no free gas layer and thus no PBSR. Where there is a PBSR, however, the velocity suddenly decreases to less than the velocity of sound in water, and a strong negative impedance contrast is formed. In PBSR regions, the free-gas layer gives way to first gas in supersaturation and then gas in saturation. Much is known about the acoustic effect of gas in fluids from diving medicine (Flemming and Max 1988), but their effect on propagation is probably not important to acoustic propagation because of the depth in sediment where their effects exist, and their presence only below the hydrate. A slight sound-velocity gradient is assumed for the gas layer below the PBSR because heavier gas and distillate fractions will probably be found in greater abundance in the lower part. Where the normal fluid in sediment-pore spaces is encountered, the gas hydrate/PBSR transition

in the primitive hydrates will not maintain a proportional increase, however, because the early formed particles in the uncompacted sediment in the upper 20 to 30 m of a normal abyssal bottom (DSDP-series publications) continue to be fluid-supported particles. Although this $V_p - V_s$ relationship may be somewhat contentious and needs widespread verification, it is likely that this upper sediment mass will have a higher density and will respond as a more viscous fluid but will not be capable of maintaining proportionally higher shear-wave velocities. The nonlinear $V_p - V_s$ relationship in the unhydrated sediment (Tables 2 and 3) is reflected by the velocity figures for the surface and 10-m depth used by Daniels and Vidmar (1982, Table 1) and for 100 to 1000 m by Hamilton (1980, Table VIa) and models sediment rigidity (Vidmar, 1979). The velocity profiles for the transmission-loss modeling show this relationship in the upper sediment column, where it has been applied to the presence of unbonded and bonded hydrate. Figure 23 diagrammatically shows the anticipated relationship in the uppermost sediment, given that disseminated rather than banded gas hydrates are forming. Undersaturated clathrate decreases porosity without increasing density. Banded hydrates may be more difficult to model and will be dealt with subsequently.

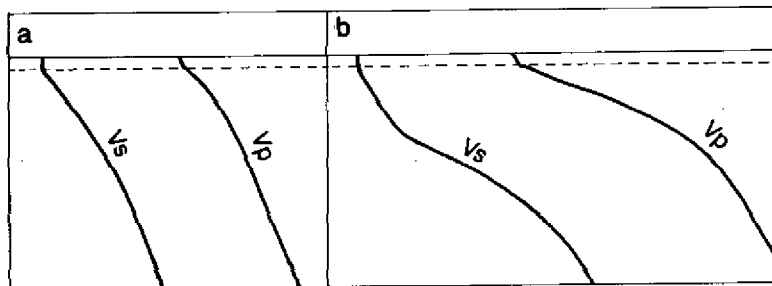


Fig. 23 — Proposed relationship between V_p and V_s in uppermost zone of disseminated hydrate. Velocity increases to right; depth increases downward. Uppermost zone of highly fluid sediment without hydrate. (a) Without hydrate, velocities tend to have similar profiles. (b) With disseminated clathrate, initial increase in V_p greater than V_s , until sediment-hydrate becomes grain-boundary supported.

Attenuation

Attenuation in gas hydrate at different levels of saturation is little known, but some general physical relationships should hold; these have been applied in constructing the attenuation values in Tables 2 and 3 that have been used in modeling acoustic response. As hydrate forms, it displaces fluid from the sediment or bonds water in a crystalline matrix. This phenomenon should have the effect of reducing attenuation, because there should be an increased number of solid-solid contacts along with a lower porosity for fluid and gas-fluid mixtures. As the sediment hydrates, its rigidity increases. With increased saturation of the hydrate crystals, their density increases, their acoustic velocity increases, and further nucleation takes place in the still-porous spaces. At some stage, the hydrate crystals begin to bond with each other and the sediment particles, and from this point through further hydration, the sediment increasingly behaves acoustically as a solid with decrease of attenuation to about that of a well-crystallized rock.

Attenuation in the upper part of the hydrate is a little different from that of unhydrated sediment, but about the point on the velocity profile that there is a marked change in the ability of the sediment-pore fluid-hydrate to bear significant elastic-wave energy (Fig. 22), attenuation should begin to decrease steadily toward some minimum for the significantly hydrated lower part of the hydrate layer. The attenuation profiles (Tables 2 and 3) reflect the best estimates of this phenomenon of hydrate's ability to lower attenuation in the sediment.

Attenuation in the gas layer below a PBSR (which may not be developed everywhere) is likely to be greatly increased over that in the base of the hydrate, but this may have little effect on acoustic propagation at very low frequencies because much of the acoustic energy that can penetrate to the base of the hydrate layer will be reflected at the PBSR impedance barrier. At very low frequencies, however, acoustic energy might refract into the gas layer and below. Very low-frequency acoustics are not considered in this report, however, and this topic should be considered separately.

Density

The density of methane hydrate varies from 0.8 in the first-formed and undersaturated form to 1.2 g/cm³ in the most saturated examples examined. Undersaturated hydrate, therefore, has positive buoyancy and will rise into and upward in the water column, where it will evolve to gas when it passes out of the high-pressure stability field unless it is either saturated rapidly to sufficiently high density or is held down in the sediment. The least-dense hydrate will be found in the upper part of the hydrate layer and the most dense in the bottom.

Hydration has two main effects on the density of sea-floor sediment volume. First, the upper part of the sediment may be both loosely bound and more rigid while, as a mass, it becomes slightly less dense owing to the replacement of saline, cold water by less dense hydrate. It is not possible to estimate the exact relationship between hydration, hydration and saturation rates, and density, but with increased hydration, the sediment should again become more dense. Second, the hydrate will hold open once porous space from the effects of compaction because it is a solid; the normal relationships between sediment depth and density may be different in a hydrated sediment on the ocean bottom from those observed in cores recovered from deep-ocean sediment in which no attempt to preserve the hydrate and the deep-ocean acoustic character has been made. The in situ variation in density with depth is again an issue in need of resolution to establish an accurate acoustic structure for hydrated sediments. The overall effect of hydrate presence will be to reduce density at virtually all depths from that which would be predicted in the absence of hydrate.

6.0 TRANSMISSION LOSS CAUSED BY THE PRESENCE OF GAS HYDRATE AND PBSR

6.1 Geoacoustic Modeling and Predicting of Bottom Loss

Because gas hydrate and gas hydrate/PBSR geoacoustic profiles in ocean-bottom sediments have not been widely modeled as to variation in bottom-interaction response from unhydrated profiles, preliminary modeling has been carried out here to assess first-order effects. The results of this modeling

appear to support the contention that the presence of gas hydrate and gas hydrate/PBSR introduces a significant bottom-acoustic interaction effect. The modeling is not intended to examine exhaustively a full range of frequencies but to allow a general comparison of the frequency/interaction variation.

The range independent seismoacoustic fast-field algorithm SAFARI in FIPR mode, which calculates the plane-wave reflection coefficients for an arbitrarily stratified fluid/solid halfspace matrix (Schmidt 1988) was used. The model theoretically yields an exact solution to the wave equation in a horizontally stratified fluid/solid environment. Because gas hydrate is stable within a layer whose thickness is related to depth from the surface of ocean-floor sediment and variation within the layer can also be expected to vary according to sediment depth assuming only gradual variations in gas availability and hydration rate, it is particularly well suited to be modeled in this manner.

The data tables used to calculate transmission loss vs grazing angle for a preliminary investigation of the bottom-interaction effect of hydrate and hydrate with an underlying free-gas layer have been constructed with reference to the induced changes in sound speed, attenuation, and density that have been discussed in Section 5. These values (Tables 2 and 3) are subject to change but represent the best estimates for the geoacoustic parameters that can be made at this time. The choice of layer thickness is arbitrary; the layers have been chosen to most conveniently approximate the sound velocity profile (Fig. 22) that is considered appropriate for gas hydrate-gas layers and the attendant geoacoustic parameters.

Three general cases have been modeled: unhydrated sediment, hydrated sediment, and hydrated sediment with PBSR (subjacent free-gas layer). Each has been modeled at 10 Hz, a convenient VLF (Fig. 24), and 50 Hz (Fig. 25), which are commonly used modeling and experimental frequencies; and 1000 Hz (Fig. 26), which marks the frequency at which some geological materials with widely differing low-frequency seismoacoustic responses have been found to lose their seismoacoustic distinctiveness. In addition, a relatively thin-layer gas hydrate/PBSR has been modeled (Fig. 27) for comparison.

A simple-hydrate steep-sound velocity gradient followed by a less-steep gradient is used; this constitutes the simplest approximation for sound velocity vs depth values for the hydrate layer. Calculations for a more complex conjectural sound-velocity model that involves greater depth to the base of the hydrate layer, and consequently somewhat higher velocities because of greater hydrate saturation, have been made for 50 Hz, but the results are not significantly different from the simple hydrate model runs.

6.2 Results of the Model Predictions for Transmission Loss

6.2.1 Environmental Situation I—Generalized Hydrate Layer

This environmental model is the closest approximation to the generalized hydrate and hydrate-PBSR velocity profile and accompanying geoacoustic parameter set. It represents the best attempt to fit model input parameters to real thickness of proven hydrate and PBSR lying in a specific water depth for which a generalized velocity profile has been calculated from seismic refraction data.

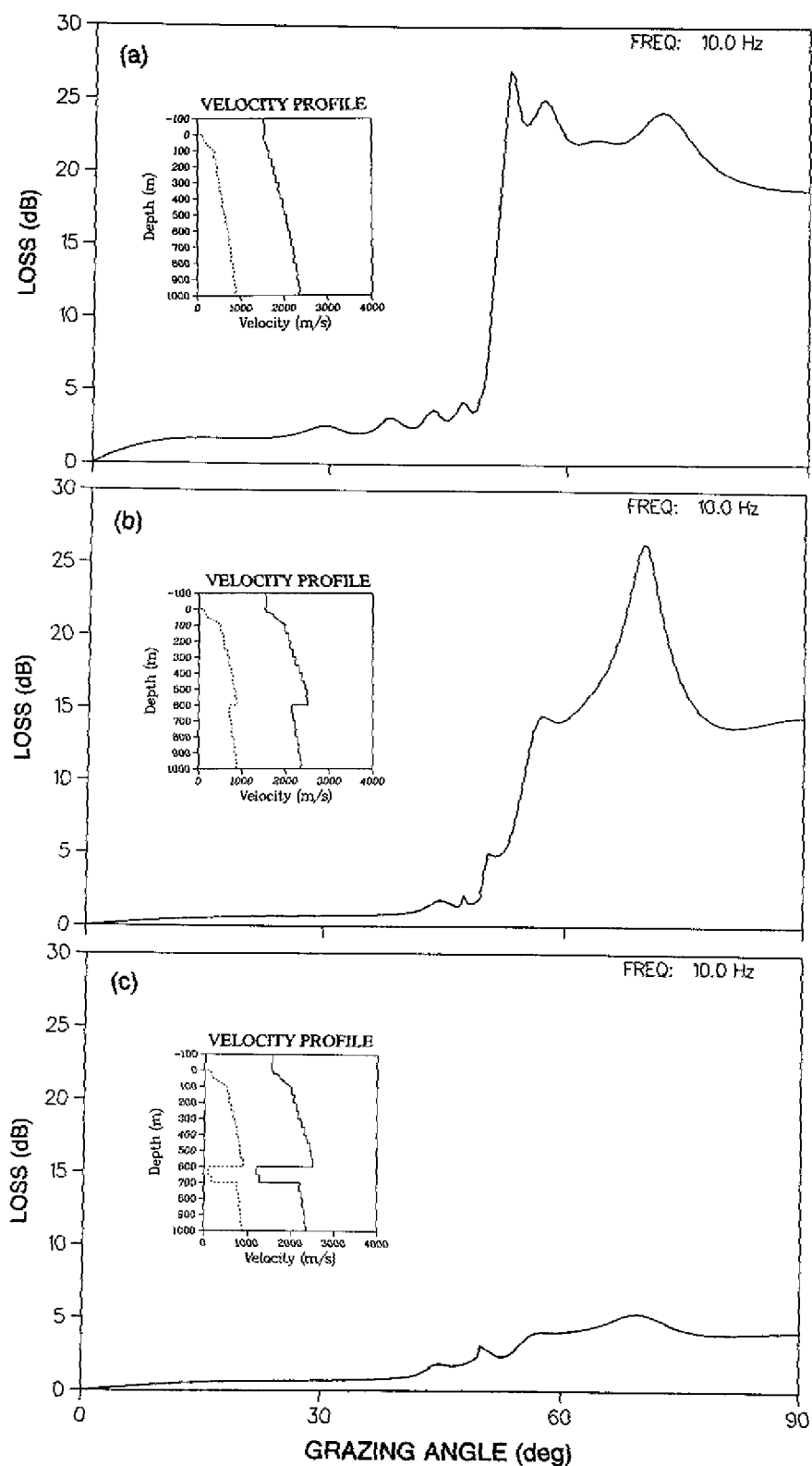


Fig. 24 — Reflection coefficients—10 Hz; (a) unhydrated sediment; (b) hydrated sediment; and (c) hydrated sediment with BSR

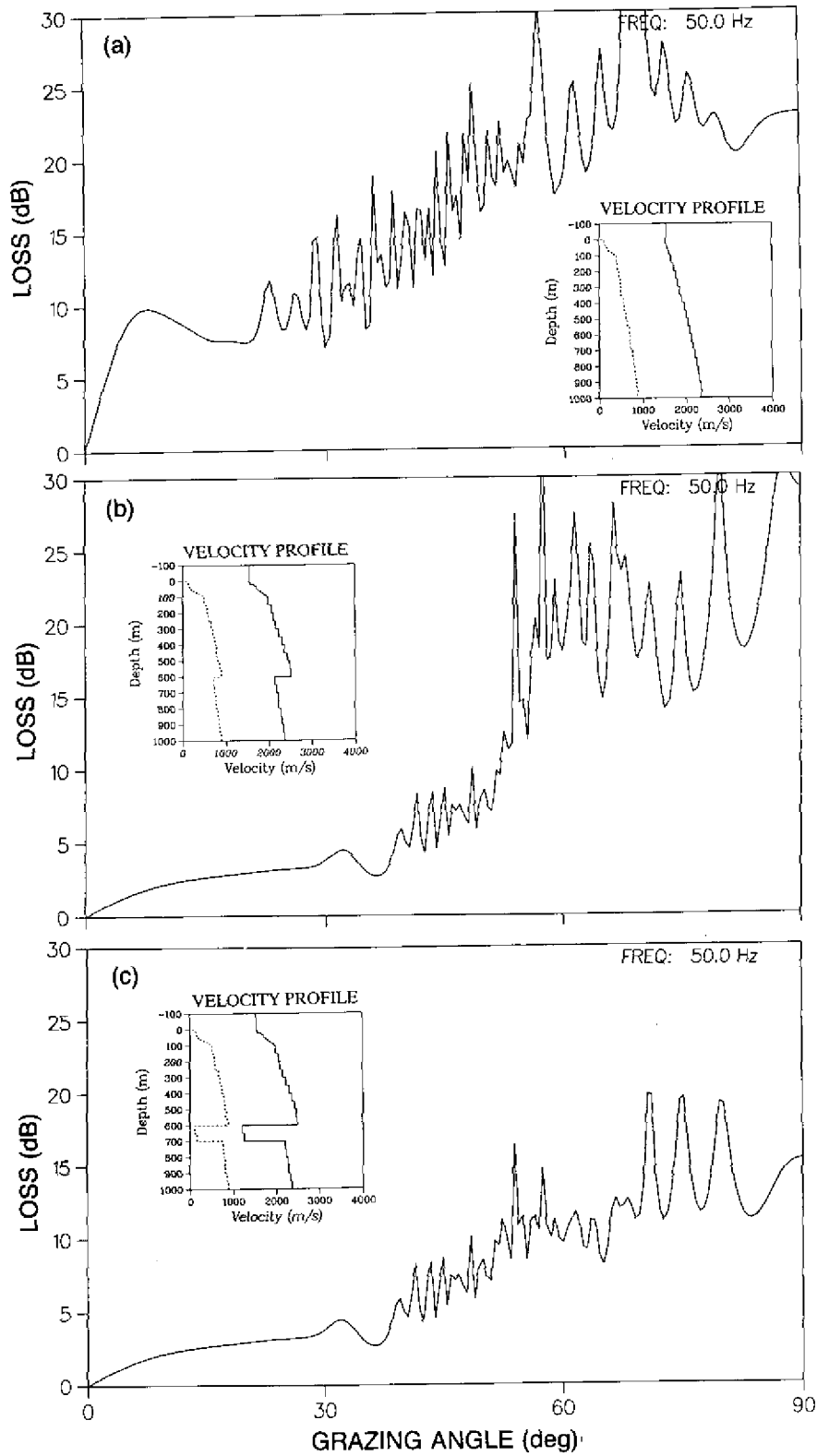


Fig. 25 — Reflection coefficients at 50 Hz; (a) unhydrated sediment; (b) hydrated sediment; and (c) hydrated sediment with BSR

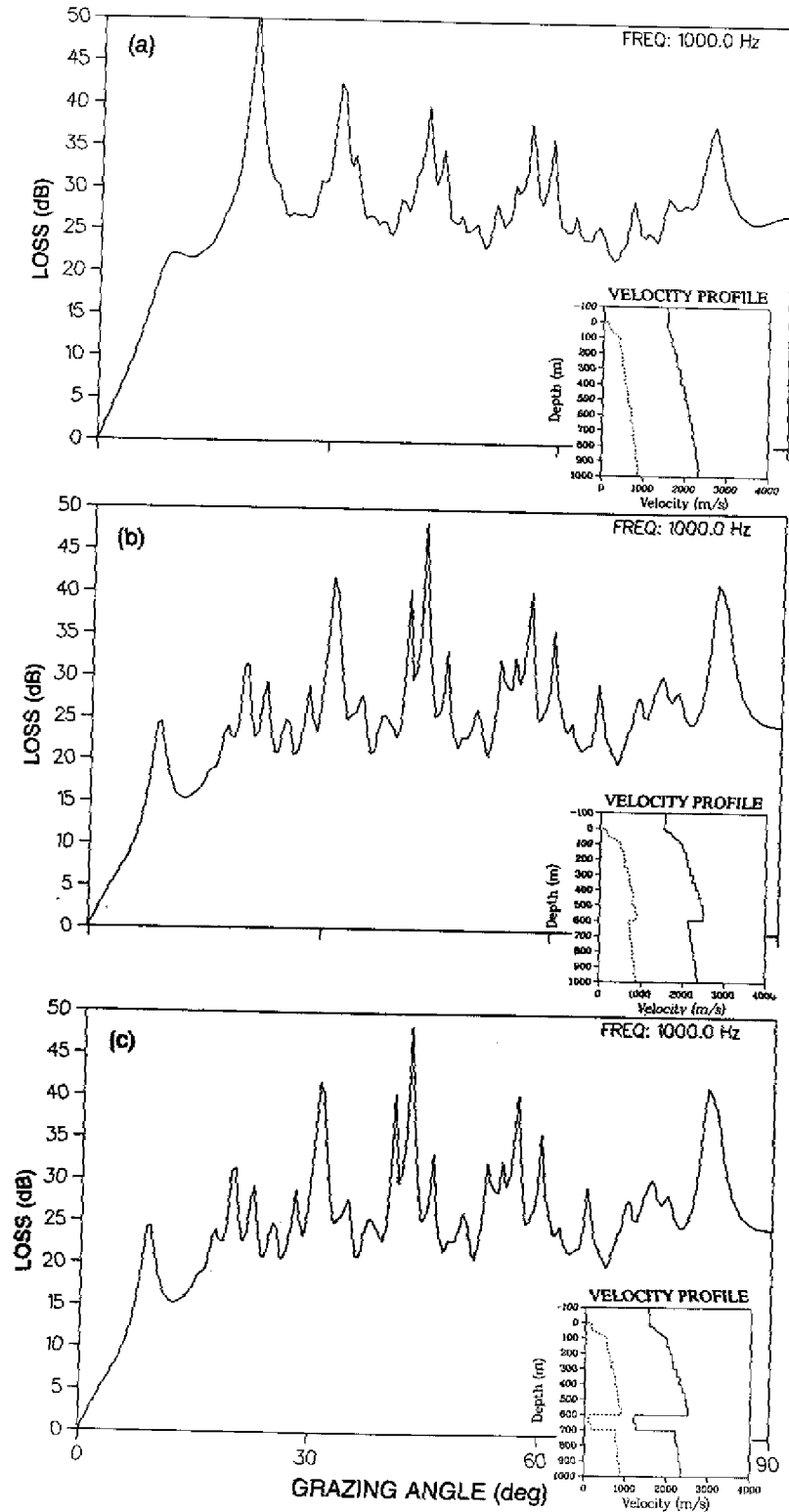


Fig. 26 — Reflection coefficients at 1 kHz; (a) unhydrated sediment, (b) hydrated sediment; and (c) hydrated sediment with BSR

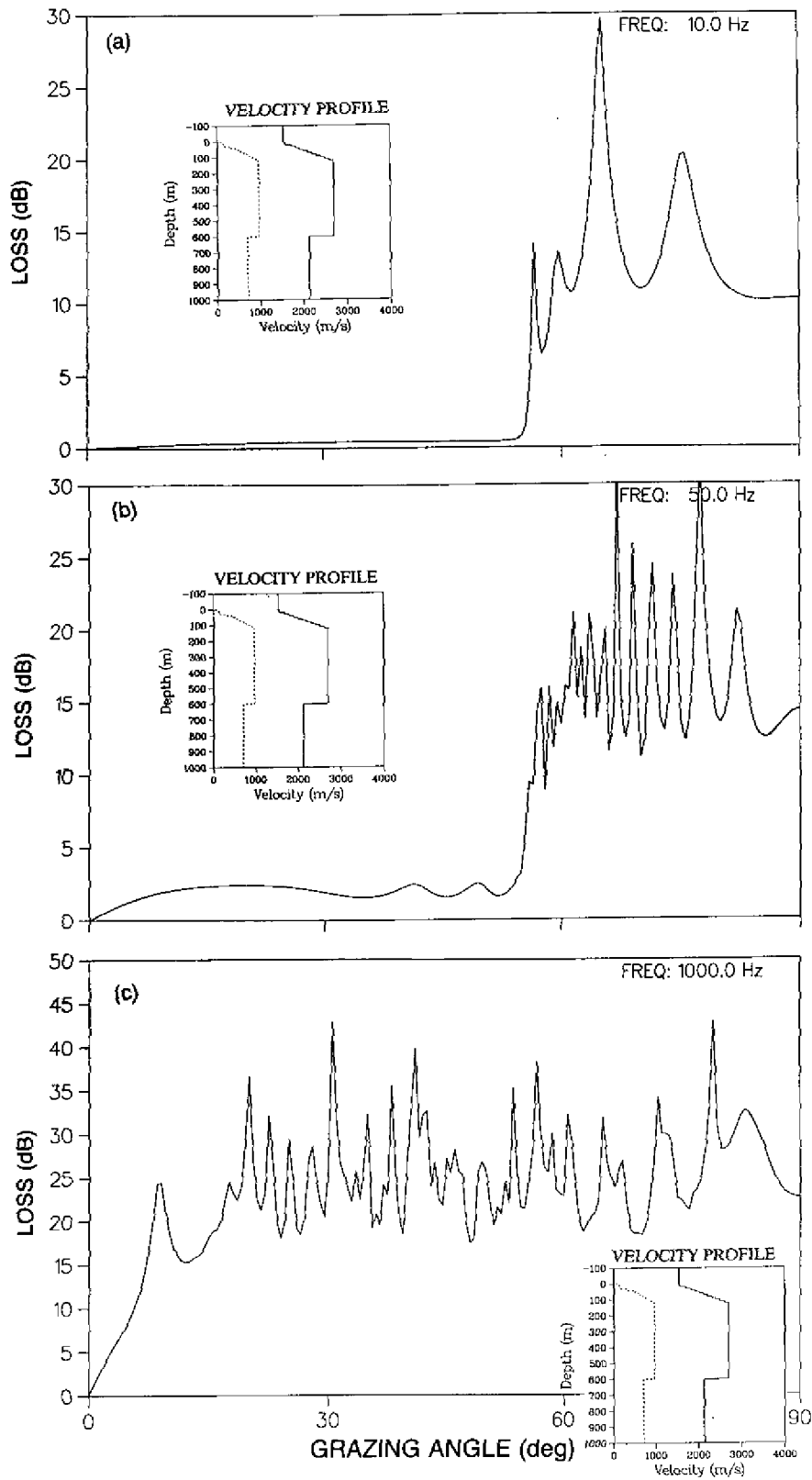


Fig. 27 — Reflection coefficients of the hydrate layer at (a) 10 Hz; (b) 50 Hz; and (c) 1 kHz

Figure 24 compares bottom loss at 10 Hz for the three cases. Loss in unhydrated sediment (Fig. 24(a)) used as a reference case shows low-grazing-angle loss up to $\sim 50^\circ$, which is probably the critical angle. Loss then rises abruptly to ~ 25 dB and then diminishes slightly approaching 90° . The loss curve is relatively smooth indicating simple wave-interaction effects except for a slight increase in complexity in the vicinity of the critical angle. At low-grazing angles in hydrated sediment (Fig. 24(b)), loss diminishes to about half of that in unhydrated sediment; at higher grazing angles, loss diminishes substantially with the exception of a maximum-loss peak slightly over 25 dB at $\sim 70^\circ$. In hydrated sediment with PBSR (Fig. 24(c)), low-grazing-angle loss is almost the same as in the hydrated case, which possibly indicates that at low-grazing angles, there is virtually complete wave turning and refraction back into the water column above the 600-m PBSR depth; at higher grazing angles, bottom loss diminishes dramatically.

For acoustic energy at 10 Hz, therefore, the presence of first a hydrate layer and then a hydrate layer underlain by gas-charged sediments acts strongly to diminish bottom loss where there is significant bottom interaction. At low-grazing angles, an already low loss is further diminished by about one half and high-angle loss is diminished by a factor of about four in the extreme cases.

Figure 25 compares bottom losses at 50 Hz for the three cases. Loss in unhydrated sediment (Fig. 25(a)) shows moderate low-grazing angle loss that becomes more complex above 20° . At about 50° the character of the loss changes to a broad response that is highly variable. In the hydrated sediment (Fig. 25(b)), loss below 40° is dramatically reduced and appears to be less complex; from 40° to $\sim 50^\circ$, loss is more complex than at lower grazing angles, but is also significantly lower than for unhydrated sediment. Loss above 50° is highly complex except immediately approaching 90° loss where it is somewhat lower than unhydrated sediment. In hydrated sediment with PBSR (Fig. 25(c)), low-grazing angle loss is virtually identical with loss in unhydrated sediment, but the higher grazing angles show a dramatically reduced loss with a hint of periodicity that could reflect the effects of constructive reinforcement.

For acoustic energy at 50 Hz, therefore, the presence of first a hydrate layer and then a hydrate layer underlain by gas-charged sediments acts strongly to diminish bottom loss where there is significant bottom interaction. Low-grazing angles show a decrease in dB loss to about one half of the unhydrated example. Because the response is virtually unchanged with the addition of a PBSR, low-grazing angle energy is probably not penetrating to the 600-m depth of the PBSR. At high-grazing angles, however, averaged variation between unhydrated and hydrated sediment is minor and is a matter of detail only. When the PBSR is present, however, high grazing-angle energy-transmission loss is diminished considerably; this is probably a result of reflection at the strong impedance contrast that is the PBSR.

Figure 26 compares bottom losses at 1 kHz for the three cases. Loss in unhydrated sediment (Fig. 26(a)) shows high losses of ~ 25 dB average, with a periodic structure that could be explained by constructive reinforcement of wave fronts in the highly layered medium. In the hydrated sediment (Fig. 26(b)), loss diminishes slightly and the periodic structure is less apparent, but only at grazing angles below $\sim 50^\circ$. In hydrated sediment with PBSR (Fig. 26(c)), loss is virtually identical to that in hydrated sediment, with only very minor variation at the highest grazing angles.

For acoustic energy at 1 kHz, therefore, the presence of first a hydrate layer and then a hydrate layer underlain by gas-charged sediments does not act strongly to diminish bottom loss where there is significant bottom interaction. At frequencies above 1 kHz, it is likely that the effect of hydrate and

hydrate PBSR will have little effect on bottom loss as even less energy will penetrate significantly into the bottom at higher frequencies.

6.2.2 Environmental Situation 2—Thoroughly Saturated Layer and Shallow PBSR

These modeling runs investigate bottom loss for a generalized gas hydrate layer of similar thickness to that used in Section 6.2.1, but here the hydrate is more saturated and has a steeper upper gradient and an averaged higher velocity; other geoacoustic parameters also have been modified (Table 3(a)). Figure 27 compares bottom losses in the hydrate layer. At 10 Hz (Fig. 27(a)), 50 Hz (Fig. 27(b)), and 1 kHz (Fig. 27(c)), the relationships between bottom loss and grazing angle is very similar to those for the hydrated layer in Section 6.2.1. Losses here, however, are substantially lower at the lower frequencies but only insignificantly lower at 1 kHz.

Figure 28 compares bottom loss in the hydrate layer having a shallow PBSR. At 10 Hz (Fig. 28(a)), only the higher grazing angles show a lower loss accompanying a substantially different return structure. Higher grazing-angle loss at 50 Hz (Fig. 28(b)) is substantially lowered, but lower angle loss is also little altered. At 1 kHz (Fig. 28(c)), there is little variation between shallow hydrate with a PBSR and a thicker horizon with no PBSR and with the hydrate and hydrate PBSR predictions from Section 6.2.1. All of the hydrate profile runs involve somewhat lower transmission loss than those for the unhydrated sediment (Fig. 24).

6.3 Gas Hydrate and PBSR Bottom Loss Effect: Conclusions

From this modeling data these conclusions can be drawn:

- The presence of gas hydrate results in lower bottom loss than is found for an unhydrated bottom,
- The effect of gas hydrate on diminishing bottom loss is more important at lower frequencies,
- At lower frequencies, a hydrate layer without PBSR primarily affects grazing angles up to 45° to 50°, and
- At lower frequencies, the addition of a gas layer (PBSR) is associated with significant lowering of bottom loss at higher grazing angles.

6.4 Frequency Dependence of Low Grazing Angle Loss

Because there is a general decrease in bottom loss and an increased effect on bottom loss at lower frequencies (at least at the 10, 50, and 1000 Hz frequencies modeled for the three environmental cases), a number of model runs have been carried out to determine the frequencies at which a hydrated bottom exerts a significant control over calculated reflection coefficient loss. This set of runs tests the hypothesis that there may be a critical frequency that separates significant bottom loss in the lower frequency range from less significant loss variation above. Alternatively, the effect could be gradual with increasing frequency.

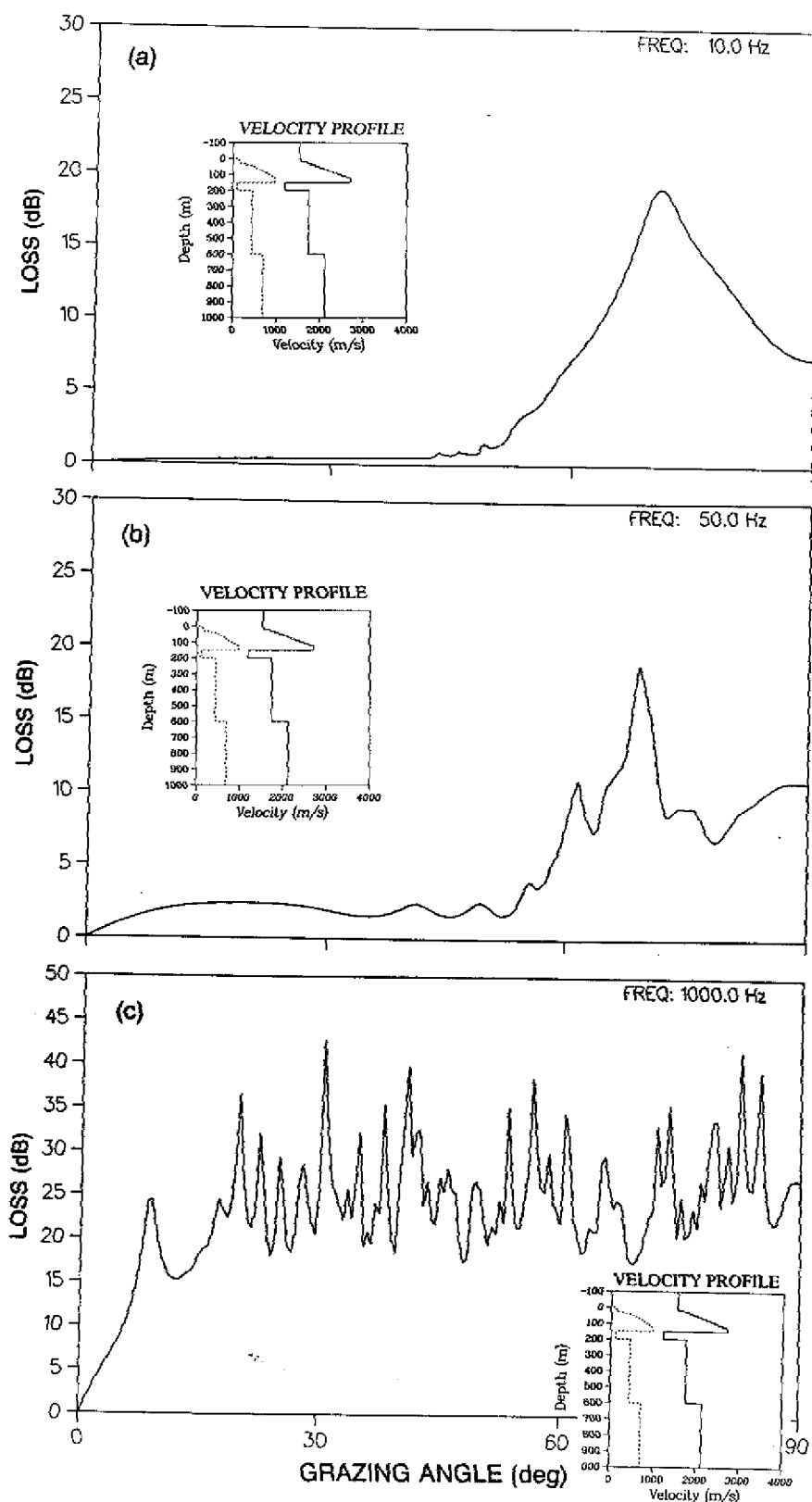


Fig. 28 — Reflection coefficients of the hydrate layer with BSR at (a) 10 Hz; (b) 50 Hz; and (c) 1 kHz

Frequencies at 10 and 50 Hz upward at 50 Hz intervals to 500 Hz and upward from 500 Hz to 1 kHz at 100 Hz intervals have been run for hydrated sediment-reflection loss coefficients (Table 2(b)) by use of the SAFARI-FIPR fast-field algorithm. These results are directly comparable with the SAFARI runs in Section 6. Here, however, the individual transmission-loss curves have been averaged so that their individual complexity does not obscure their general relationships. Averaging has been carried out manually by using linear interpolation over 15° (grazing angle) segments with a 5° overlap and bounding segments for each frequency.

These curves approximate the more irregular acoustic-loss structures. They are plotted on Figure 29 for comparison only to $\sim 60^\circ$ grazing angle, because lower grazing angles are of concern for longer range propagation. The relationships between the curves of individual frequencies are most clear between 0° and 45° ; above that, the variation could be an artifact caused by the averaging process because of the development of longer period loss variation; discussion of averaged loss relationships here, therefore, are for grazing angles between 0° and 45° .

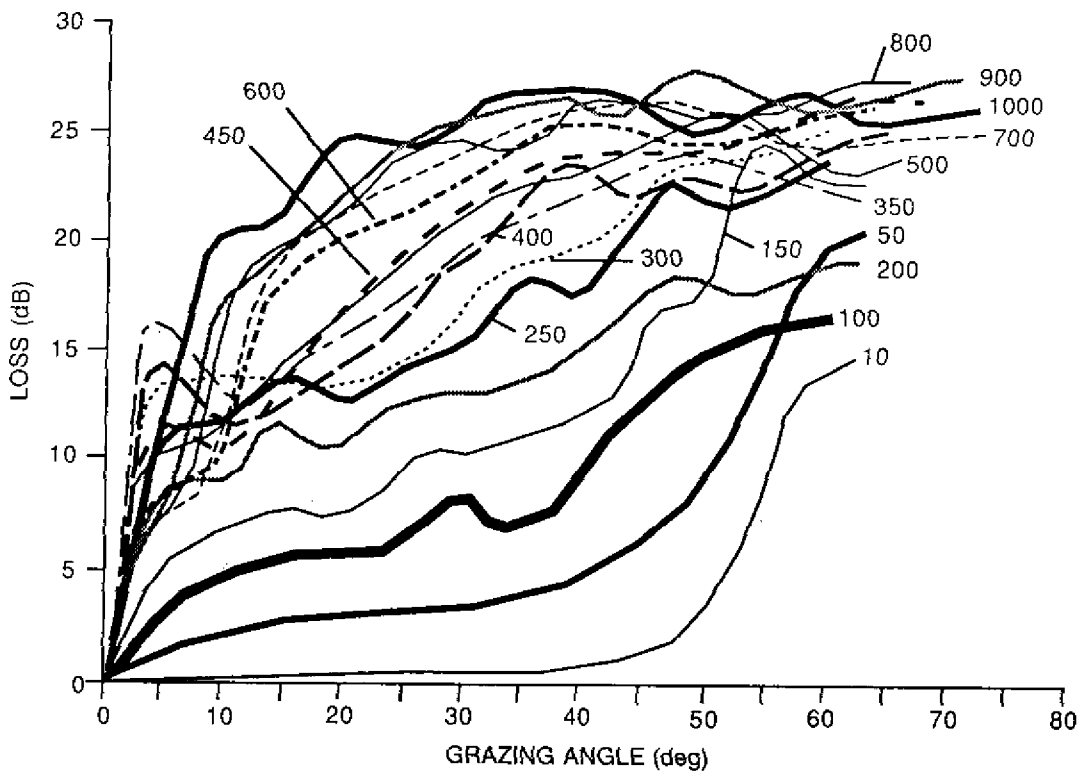


Fig. 29 — Averaged reflection coefficients for hydrated segments

Loss rises uniformly by about 2.5 dB from 10 to 200 Hz, and from 250 to 350 Hz, loss continues to rise similarly with the development of a high-loss anomaly between 0° and 12° from otherwise gradually ascending curves with increased grazing angle (Fig. 29). The 400 Hz loss curve lies below the 350 Hz curve for much of its length, and the curves for this and the higher frequencies lie more tightly clustered and in more complex spatial relationships.

Three main groupings of the averaged transmission-loss curves occur. At the lower frequencies, between 10 and 350 Hz, there is a direct frequency dependence between increased bottom loss and increased frequency. The mid-frequency range, from 400 to 600 Hz, clusters; the cluster includes the 350 Hz general-loss curve. Loss from 600 Hz to 1 kHz also clusters closely, with overlap in the complex 0 to 12 Hz range and above the 45° grazing angle. Complexity in the 0° to 12° range is probably the result of an artifact of the algorithm calculating for the arbitrary layer structure chosen to most closely approximate the sound-speed profile; the maximum loss at 350 Hz in the 5° range is highly anomalous. Runs with different arbitrary-layer structures show similar averaged curves, but the details of loss variation can be quite different.

The range 350 ± 50 Hz constitutes a critical area between frequency independent and dependent loss regions. In the lower range of frequencies, higher frequencies are associated with average higher loss, at least in the 0° to 45° grazing-angle range. At higher frequencies, loss curves of the frequencies cluster, and although there remains a general relationship of higher loss with higher frequency, the raw and averaged curves often cross and invert this relationship.

It may prove to be an interesting phenomenon that the 350 ± 50 Hz frequency appears to separate two major frequency regimes of bottom-acoustic response in a typically (deep-water) hydrated bottom, which is similar to the best transmission frequency in shallow water (Jensen and Kuperman 1983; and Gershfield and Eller 1985). These authors have suggested that from experimental shallow-water acoustical experimental data a frequency in the 350 ± 50 Hz range separates a regime dominated by volume loss mainly through attenuation at the higher frequencies from elastic waves and other conversion losses within the bottom at lower frequencies. It may be that this critical frequency may apply in both deep (at least in the presence of hydrated sediment) and shallow water.

6.5 Modeling of the Bottom-Interaction Effects Caused by the Presence of the Gas Hydrate Layer

Work is in progress that involves further modeling using SAFARI and other wave-solution models and modal analyses, which will alleviate the problem of approximating a layered structure and allow direct examination of various velocity and attenuation gradients. Transmission-loss modeling is also necessary to characterize the effect of the presence of gas hydrate presence.

The V_p profile (Fig. 22) is a generalized physical model that carries with it consequent physical properties such as density V_s and attenuation. This model serves to demonstrate the nature of variation from a profile for unhydrated ocean floor sediment that can be expected where an idealized section of fully hydrated sediment occurs, but it is not intended that this model should be regarded as the only profile that depicts sound speed gradients and physical properties of hydrated sediment. There are a number of issues that remain to be investigated before a fully representative set of profiles can be established.

In the upper part of the hydrate stability zone, an acoustically laminated structure can be expected. This was not considered in detail here because little information about the degree of layering or the spacing of the hydrate-saturated sediment exists for deep water areas. The rapid increase in V_p used in Fig. 22, however, may adequately model the combined reflection-refraction character of the upper part of a hydrate layer; modeling of a variety of layer structures is necessary to estimate variation. Models of layered structure should be derived from drilling logs and seismic reflection data rather than being based on theoretical considerations.

Hydrate occurs in solid mats, nodules, and irregularly shaped volumes, as well as in varying amounts of scattered and amalgamated crystals in the pore spaces in sediment. No attempt has yet been made to model the horizontal variability of hydrate within the hydrate stability zone because not enough is yet known about hydrate natural occurrences. The current model and the modeling carried out for this study are for a range-independent case; in the real oceans, range-dependent cases can also be expected.

7.0 DETERMINING THE SEISMOACOUSTIC CHARACTER OF THE GAS HYDRATE LAYER AND THE NEED FOR IN SITU MEASUREMENT

The reflection-loss coefficient modeling carried out in Section 6 of this report shows the salient properties of the gas hydrate layer insofar as they could be deduced by knowing the physical properties and the mechanisms of formations and concentrations. Even though the hydrate layer is widespread, very little is known about its actual acoustic structure or its variability both locally and from area to area. Because of the cost and the ephemeral nature of hydrates, it is unlikely that the problem can be resolved entirely through physical sampling and laboratory measurements. In situ acoustic-structure verification and its variation both within and between sedimentary provinces is necessary before acoustic transmission loss and reflection-loss character can be modeled in a predictive manner for operational Navy purposes.

Seismic-reflection analysis will not be adequate to establish an acoustic structure that will allow for fine-scale modeling of the hydrate layer because of the normal vertical compression of the individual data stacks on reflection records. Examining the fine-scale acoustic character of the hydrate layer and the subjacent sediments in at least one example, however, does reveal an acoustic structure similar to that modeled. The upper part of the hydrate layer has many narrow and sharp impedance contrasts, while the lower part of the layer shows the predicted weak response (Fig. 30). Below the strong negative-impedance contrast at the base of the layer, there exists a local strongly alternating-impedance character that gives way downward to a normal acoustic response for interbedded sandy, silty sediment.

The acoustic records are a sum of the sediment plus gas hydrate effects; it is difficult to separate the effects of original sediment from those induced by the hydrate layer. For instance, the spiky nature of the impedance contrasts in the upper part of the hydrate might be due largely to the presence of hydrate, but there may also be a highly bed-differentiated sediment present that was more important in establishing the acoustic character. The weak differentiation in the lower part of the hydrate layer conforms extremely well with the theory about what the acoustic character *should be*, but it is not possible to say from the seismic-reflection records alone that the "acoustic damping" is entirely caused by the presence of hydrate. The base of the hydrate might also be coincident with a thick, acoustically transparent primary geological-sedimentary unit. Although the acoustic structure of these profiles (Fig. 30) is similar to that expected in a hydrate layer, the degree of hydrate variation is important in establishing the bottom-loss character.

A combination of seismic-reflection and seismic-refraction data is necessary to characterize the acoustic structure of the gas hydrate layers for Navy needs. Reflection seismics establish the overall character of the hydrate zone and clearly define the base depth of the hydrate where there is a well-defined BSR. Seismic reflection records can confirm the presence of a hydrate layer. Reflection-seismic data incorporated in a hard-copy record exists in digital form and can be retrieved and reprocessed for the detailed examination necessary to establish the acoustic structure of the hydrate zone.

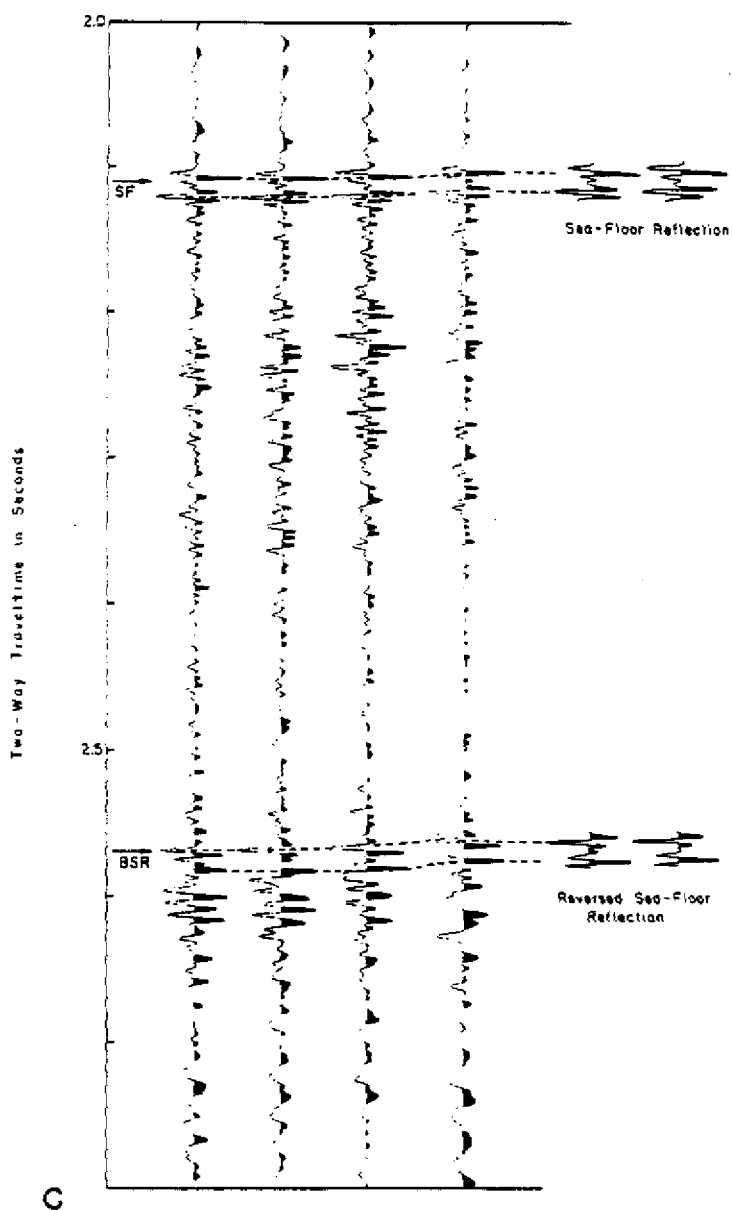


Fig. 30 — Watergum seismic traces from the upper Amazon deltaic cone where the presence of gas hydrate has been identified from the presence of PBSR on seismic reflection records. BSR phase-reversal at 2.57-s subbottom (from Manley and Flood (1988)).

This examination of seismic data would require a significant effort because of the information available. Seismic-refraction experiments can then be modeled to the velocity/depth inversion in any area so that the acoustic structure of the hydrate itself can be more accurately-calculated as a many-layered zone.

8.0 SIGNIFICANCE OF IN SITU GAS AND GAS HYDRATES AND THEIR GEOACOUSTIC-ENVIRONMENTAL IMPLICATIONS: CONCLUSIONS

The conclusions reached are these:

- gas hydrates and gas-enhanced, acoustically stratified bottoms cause important bottom-acoustic interaction anomalies;
- gas and gas hydrate significantly alter the acoustic structures and sediment velocities to return more incident-acoustic energy to the water column than would otherwise be predicted;
- these geoacoustic anomalies are secondary or diagenetic in origin and develop in the bottom sediments following sedimentation;
- first-order geological attributes (such as grain size, initial porosity, and porosity-depth relationships) may be significantly less important to geoacoustic interaction than secondary attributes that may completely alter the primary geoacoustic character;
- secondary alteration of bottom sediments is transitory in nature because the induced geoacoustic properties only exist under the bottom-pressure-temperature regime;
- inferring geoacoustic response from laboratory sediment testing under atmospheric conditions may be valid for some shallow-water sediments, but almost certainly not for deep-ocean sediments;
- geological bottom-sediment sampling that does not preserve the bottom-thermodynamic conditions are unlikely to reveal the in situ geoacoustic character during laboratory analysis. During recovery of deep sea specimens to atmospheric conditions, the diagenetic attributes disappear;
- testing the geoacoustic character of bottom sediments should be carried out in situ;
- modeling geoacoustic response must include a realistic combination of both primary and secondary geological attributes of the in situ bottom sediments;
- more work is needed to quantify the gas hydrate relationship and its geoacoustic effect as well as identifying areas where gas hydrate/BRS are significant developed so that proper areally descriptive geoacoustic areas can be delineated, and
- acoustic experimental data involving bottom interaction from differing sediment provinces should be studied to assess why primary-geological attributes alone are insufficient to explain variations from bottom interaction predictions. For instance, if it can be shown that

acoustic response from widely differing materials (such as pelagic sediments and turbidites) converged, the presence of a secondary geological attribute (such as gas hydrate) could be identified as a reasonable explanation.

9.0 ACKNOWLEDGMENTS

Thanks to A. Solheim of the Norsk Polarinstutt for bringing gas hydrates to my attention, for sharing his data, and for our discussions. Thanks also to H. Kassens, University of Kiel (FRG), for discussions about acoustically laminated sediments in the Norwegian-Greenland Sea, and for making available her unpublished data. P. Vidmar has contributed substantially in published literature and has provided information in discussion to make this report possible.

Thanks also to Dr. T. Edgar, now of the United States Geological Survey, Reston, Virginia, for making available his collected notes on gas hydrates, for discussions concerning drilling, and sampling hydrates while he was with the Deep Sea Drilling Project, for reading the penultimate version of this paper, and for making helpful suggestions. G. Markle, now of the Naval Oceanographic Office, and S. McDonell, of the Naval Ocean Research and Development Activity at Stennis Space Center, Mississippi, provided further insights. G. Bryan of Lamont-Dougherty Geological Observatory commented on the early work focusing on physical properties of gas hydrate, J. Ewing, of Woods Hole Oceanographic Institution, also made invaluable comments about the field and laboratory investigations.

W.A. Kuperman made it possible to carry out the acoustic modeling and made himself freely available for consultation; my thanks to him and to John Perkins and other Code 5160 personnel at NRL for the use of their computer system. John Glattetre commented on portions of the text. Irene Jewett produced many of the computer figures. This work was funded by the AEAS Program of the Office of Naval Research.

10.0 REFERENCES

- Akal, T. (1974), "Acoustical Characteristics of the Sea Floor: Experimental Techniques and Some Examples from the Mediterranean Sea," *Marine Science* 1, 447-480.
- Aoki, Y., T. Tamano, and S. Kato (1982), "Detailed Structure of the Nankai Trough from Migrated Seismic Sections," J.S. Watkins and C.L. Drake (eds) in *Studies in Continental Margin Geology. Am. Assoc. Petroleum Geolo., Memoir* 34, 309-322.
- Baldwin, K.D., L.R. LeBlanc, and A.J. Silva (1985), "An Analysis of 3.5 kHz Acoustic Reflections and Sediment Physical Properties," *Ocean Eng.* 6, 475-492.
- Barkan, E.S. and A.N. Voronov (1982), "Zony Vozmozhnogo Gidatoobrazovaniia na territorii SSSR (Zones of Possible Hydrate Formation in the USSR)," *Sovetskaiia Geologiia* 7, 37-41.
- Barkan, E.S. and A.N. Voronov (1983), "Zones of Possible Hydrate Formation in the USSR," *Int. Geol. Rev.* 25, 1272-1275.
- Baturin, G.N. (1988), in *The Geochemistry of Manganese and Manganese Nodules in the Ocean*, D. Reidel Publishing Co., Boston.
- Bernstein, B.L., E.A. Silver, D.L. Reed, and K.S. Kirchoff-Stein (1988), Poster: Basement Duplexes within an Accretionary Wedge, Western Solomon Sea (Abstract), *Eos* 69, 1443.
- Bennett, R. (1988), U.S. Department of Energy Report, "Gas Hydrate Research in the Gulf of Mexico," DOE/MC/23145-2616 (DE88010279).

- Barrer, R.M. and W.I. Stuart (1957), "Non-Stoichiometric Clathrate Compounds of Water," *Proceedings of the Royal Society, London, Series A* 243, pp. 172-189.
- Bily, C. and J.W.L. Dick (1974), "Naturally Occurring Gas Hydrates in the Mackenzie Delta," *N.W.T. Bull. Can. Petroleum Geol.* 22, 320-352.
- Birch, F. (1960), "The Velocity of Compressional Waves in Rocks to 10 Kilobars, Part 1," *J. Geophys. Res.* 65, 1083-1102.
- Birch, F. (1961), "The Velocity of Compressional Waves in Rocks to 10 Kilobars, Part 2," *J. Geophys. Res.* 66, 2199-2224.
- Brooks, J.M. and W.R. Bryant (1985), U.S. Department of Energy DOE/MC/21088-1964 (DE86001011), "Geological and Geochemical Implications of Gas Hydrates in the Gulf of Mexico."
- Brooks, J.M., H.B. Cox, W.R. Bryant, M.C. Kennicutt II, R.G. Mann, and T.J. McDonald, "Association of Gas Hydrates and Oil Seepage in the Gulf of Mexico," *Organic Geochemistry* (in press).
- Brown, J.F., Jr. (1962), "Inclusion Compounds," *Sci. Am.* 207, 82-92.
- Bryan, G.M. and R.G. Markl (1966), Columbia University, Lamont Geological Observatory Technical Report No. 8 (CU-8-66-NOPBSR 85077), "Microtopography of the Blake-Bahama Region."
- Bugge, T. (1983), "Submarine Slides on the Norwegian Continental Margin with Special Emphasis on the Storegga Area, Continental Shelf Norway." IKU, Trondheim, Norway, Publication 10.
- Carlson, P.R., M. Golan-Bac, H.A. Karl, and K.A. Kenvolden (1985), "Seismic and Geochemical Evidence for Shallow Gas in Sediment on Navarin Continental Margin, Bering Sea." *Am. Assn. Petroleum Geol. Bull.* 69, 422-436.
- Carlson P.R., M.S. Marlow, L.M. Prson, and M.L. Somers (1987), U.S. Geological Survey Open-File Report 87-72, "Gloria Investigation of the Exclusive Economic Zone in the Deep Bering Sea."
- Carson, D.B. and D.L. Katz (1942), "Natural Gas Hydrates," *Petroleum Trans. Am. Inst. Mining Eng.* 146, 150-158.
- Cherski, N.V., V.P. Tsarev, and S.P. Nikitin (1983), "Issledovanie I Prognozirovanie Uslovii Nakopleniia Resursov Gaza v Gasogidratnykh Zalezhaka (Study and Prediction Conditions of Gas Accumulation in Gas Hydrate Deposits)," *Yakutskii Filial So An SSSR.*
- Christensen, N.I. (1965), "Compressional Wave Velocities in Metamorphic Rocks at Pressures to 10 Kilobars," *J. Geophys. Res.* 70, 6147-6164.
- Chroston, P.N. (1986), Geological Survey of Ireland, Open File Report, "Compressional Wave Velocities of Samples from the Delaney Dome Drill Hole and from Basement Rocks in Ireland."
- Chroston, P.N. and D.J. Evans (1983), "Seismic Velocities of Granulites from the Seiland Petrographic Province, N. Norway: Implications for Scandinavian Lower Continental Crust," *J. Geophys. Res.* 51, 14-21.
- Chroston, P.N. and M.D. Max (1988), "Seismic Anisotropy in Mylonites: an Example from the Mannin Thrust Zone, Southwest Connemara, Ireland," *Tectonophysics* 148, 29-39.
- Ciesnik, M.S. and J. Krason (1987), U.S. Department of Energy, Morgantown, DOE/MC/21181-1959 (DE88001052), "Geological Evolution and Analysis of Confirmed or Suspected Gas Hydrate Localities. V. 11. Basin Analysis, Formation and Stability of Gas Hydrates in the Black Sea."
- Collett, T.S. (1983), "Detection and Evaluation of Natural Gas Hydrates from Well Logs, Prudhoe Bay, Alaska," *Proceedings of the Fourth International Permafrost Conference, Fairbanks, Alaska*, 169-174.
- Cooper, A.K., D.W. Scholl, and M.S. Marlow (1986), "Structural Framework, Sedimentary Sequences, and the Hydrocarbon Potential of the Alutian and Bowers Basins, Bering Sea." in

MICHAEL D. MAX

- Geology and Resource Potential of the Continental Margin of Western North America and Adjacent Ocean Basins—Beaufort Sea to Baja California*, D.W. Scholl, A. Grantz, and J.G. Vedder (eds), Vol. 6, 473-502.
- Couper, A. (1983), *The Times Atlas of the Oceans* (Van Nostrand Reinhold Co., New York),
- Daniels, J.M. and P.J. Vidmar (1982), "Occurrence and Acoustical Significance of Natural Gas Hydrates in Marine Sediments," *J. Acoustical Soc. Am.* **72**, 1564-1573.
- Davidson, D.W. (1973), "Clathrate Hydrates," in *A Comprehensive Treatise*, Vol. 2, F. Franks (ed.) (Plenum Press, New York), pp. 115-234.
- Davidson, D.W., M.K. El-Defrawy, M.O. Fuglem, and A.S. Judge (1978), "Natural Gas Hydrates in Northern Canada," Proceedings, 3rd International Conference on Permafrost **1**, 937-943.
- Dean, J.A. (1974), *Lang's Handbook of Chemistry* (McGraw-Hill Book Company, New York).
- Dietrich, G. (1969), *Atlas of the Hydrography of the Northern Atlantic Ocean Based on the Polar Front Survey of the International Geophysical Year, Winter and Summer 1958*, International Council for the Exploration of the Sea (Hydrographic Service, Copenhagen).
- Dillon, W.P. and Paul C.K. (1983), "Marine Gas Hydrates-II; Geophysical Evidence," in *Natural Gas Hydrates: Properties, Occurrences, Recovery*, J.L. Cox, ed. (Butterworth, Boston), pp. 73-90.
- Dillon, W. and P. Popenoe (1988), "The Blake Plateau Basin and Carolina Trough," in *The Atlantic Continental Margin*, R.E. Sheridan and J.A. Grow (eds), U.S. Geological Survey of America, *The Geology of North America*, **1-2**, 291-328.
- Dillon, W.P., P. Popenoe, J.A. Grow, K.D. Klitgord, B.A. Swift, C.K. Paul, and K.V. Cashman (1982), "Growth Faulting and Salt Diapirism: Their Relationship and Control in the Carolina Trough, Eastern North America," in *Studies in Continental Margin Geology*, J.S. Watkins and C.L. Drake (eds), Am. Assoc. of Petroleum Geolo. Memoir **34**, 21-46.
- DOE (1987), U.S. Department of Energy DOE/METC-87/0246 (DE8700127), "Gas Hydrates Technology Status Report."

- Fountain, D.M., C.A. Hurich, and S.B. Smithson (1984), "Seismic Reflectivity of Mylonite Zones in the Crust," *Geology* 12, 195-198.
- Fowler, S.R., R.S. White, and K.E. Loudon (1985), "Sediment Dewatering in the Makran Accretionary Prism," *Earth and Planetary Sci. Lett.* 75, 427-438.
- Galate, J.W. and M.A. Goodman (1982), "Review and Evaluation of Evidence of In situ Gas Hydrates in the National Petroleum Reserve of Alaska," U.S. Geological Survey Report, Menlo Park, CA.
- Gerlach, S.A., J. Thiede, G. Graf, and F. Werner (1986), "Sedimentation im Europäischen Nordmeer," Christian-Albrechts Universität zu Kiel.
- Gerlach, S.A., J. Thiede, G. Graf and F. Werner (1986), Forschungsschiff Meteor, Riese 2 vom 19. Juni bis 16. Juli, 1986; Forschungsschiff Poseidon, Riese 128 vom 7. Mai bis 8. Juni 1986. Berichte aus dem Sonderforschungsbereich 313 "Sedimentation im Europäischen Nordmeer," Christian-Albrechts Universität zu Kiel.
- Gershfeld, D.A. and A.I. Eller (1985), "Geometric Considerations in Determining the Optimum Frequency of Acoustic Propagation in a Shallow Water Waveguide," *J. of the Acoustical Soc. Am.* 78, 632-641.
- Godbole, S.P. and V.A. Kamath (1987), "Section II. Review of Gas Hydrate Literature, Current Research and State-of-the-art Technology," G.D. Sharma, V.A. Kamath, S.P. Godbole, S.L. Patil, S.G. Paranjpe, P.N. Mutalik, and N. Nadem, *Development of Alaskan Gas Hydrate Resources*, Annual Report, October 1986-September 1987, U.S. Department of Energy DOE/FE/61114-2608 (DE88010270),
- Grantz, A., G.W. Boucher, and O.T. Whitney (1976), "Possible Solid Gas Hydrate and Natural Gas Deposits Beneath the Continental Slope of the Beaufort Sea." U.S. Geol. Survey Cir. 733, p. 17.
- Grantz, A. and S.D. May (1982), "Rifting History and Structural Development of the Continental Margin North of Alaska," in *Studies in Continental Margin Geology*, Am. Asso. of Petroleum Geol. Memoir 34, J.S. Watkins, and C.L. Drake (eds), pp. 77-100.
- Greene, R.R. and D.M. Rubenstein (1985), Science Applications International Corporation, SAIC-85/1036, "A Random Layer Model for Reflection from Ocean Bottom Sediments."
- Grow, J.A., W.P. Dillon, P. Popenoe and R.E. Sheridan (1979), "Diapirs Along the Continental Slope Southeast of Cape Hatteras" (abs), *Geol. Soc. of Am.* 28th annual meeting.
- Hamilton, E.L. (1974), "Geoacoustic Models of the Seafloor," in *Physics of Sound in Marine Sediments*, L.D. Hampden (ed.), (Plenum, New York).
- Hamilton, E.L. (1979), "Sound Velocity Gradients, in Marine Sediments," *J. Acoustical Soc. Am.* 65, 909-922.
- Hamilton, E.L. (1980), "Geoacoustic Modeling of the Sea Floor," *J. Acoustical Soc. Am.* 68, 1313-1340.
- Hand, J.H., D.L. Katz and V.K. Verma (1974), "Review of Gas Hydrates with Implications for Ocean Sediments," in *Natural Gases in Marine Sediments*, L.R. Kaplan (ed.) (Plenum, New York), pp. 197-194.
- Harrison, W.E. and J.A. Curiale (1982), Gas Hydrates in Sediments of Holes 497 and 498A, Deep Sea Drilling Project Leg 67," in *Initial Reports of the Deep Sea Drilling Project 67*, U.S. Government Printing Office, Washington, DC, 591-594.
- Hastrup, O.F. (1969), "The Effect of Periodic Bottom Layering on Acoustic Reflectivity," SACLANT ASW Research Center, Technical Report 149, La Spezia, Italy. (AD 856029),
- Hitchon, B. (1974), "Occurrence of Natural Gas Hydrates in Sedimentary Basins," in *Natural Gases in Marine Sediments*, I.R. Kaplan (ed.), (Plenum Press, New York), pp. 195-225.

- Holder, G.D., R.D. Malone, and W.F. Lawson (1987), "Effects of Gas Composition and Geothermal Properties on the Thickness and Depth of Natural-Gas-Hydrate Zones," *J. Petroleum Tech.*, 1147-1152.
- Holthusen, H. and P.J. Vidmar (1982), "The Effect of Near-Surface Layering on the Reflectivity of the Ocean Bottom," *J. Acoustical Soc. Am.* **72**, 226-234.
- Hovland, M. (1982), "Pockmarks and the Recent Geology of the Central Section of the Norwegian Trench," *Marine Geolo* **47**, 283-301.
- Hovland, M. and A.G. Judd (1988), *Seabed Pockmarks and Seepages. Impact on Geology, Biology and the Marine Environment* (Graham and Trotman, London).
- Hurdle, B.G. (1986), Chapt. 6, "The Sound-Speed Structure," in *The Nordic Seas*, B.G. Hurdle (ed.) (Springer, New York), pp. 155-181.
- IARPC (1987), *United States Arctic Research Plan*, Interagency Arctic Research Policy Committee, Washington, DC.
- Jeffrey, G.A. (1969), "Water Structure in Organic Hydrates," *Acc. Chem. Res.* **2**, 344-352.
- Jensen, F.B. and W.A. Kuperman (1983), "Optimum Frequency of Propagation in Shallow Water Environments," *J. Acoustical Soc. Am.* **73**, 813-819.
- Jhaveri, J. and D.B. Robinson (1965), "Hydrates in the Methane-nitrogen System," *Can. J. Chem. Eng.* **43**, 75-78.
- Johannessen, O.M. (1986), "Brief Overview of the Physical Oceanography," *The Nordic Seas*, B.G. Hurdle (ed.), (Springer, New York), pp. 102-127.
- Jones, T. and A. Nur (1982), "Seismic Velocity and Anisotropy in Mylonites and the Reflectivity of Deep Crustal Faults," *Geology* **10**, 260-263.
- Judge, A. (1982), "Natural Gas Hydrates in Canada," Proceedings, Fairbanks, Alaska, 4th Canadian Permafrost Conference, pp. 320-328.
- Kamath, A., S.P. Godbole, R.D. Ostermann, and R.D. Collett (1987), "Evaluation of the Stability of Gas Hydrates in Northern Alaska," *Cold Regions Sci. and Tech.* **4**, 107-119.
- Kassens, H., discussion at Naval Research Laboratory, March 1988, private communication.
- Katz, D.L., D. Cornell, R. Kobayashi, F.H. Poettmann, J.A. Vary, J.R. Elenbass, and C.F. Weinaug (1959), *Handbook of Natural Gas Engineering* (McGraw-Hill, New York).
- Kennett, B.L.N. (1985), *Seismic Wave Propagation in Stratified Media* (Cambridge University Press, Cambridge, England).
- Kieffe, H., M.J. Clouter and R.E. Gagnon (1986), "Determination of Acoustic Velocities of Clathrate Hydrates by Brillouin Spectroscopy," *J. Phys. Chem.* **89**, 3103-3108.
- Kind, R. (1976), "Computation of Reflection Coefficients for Layer Media," *J. of Geophys. Res.* **42**, 191-200.
- Komar, C.A. (ed.) (1986), U.S. Department of Energy, Morgantown, West Virginia, Gas Hydrates, Arctic/Offshore Research, and Deep Source Gas Contractors Reveiw Meeting.
- Krason, J. and M.S. Ciesnik (1986), U.S. Department of Energy DOE/MC/21181-1950 (DE87001078), "Geological Evolution and Analysis of Confirmed or Suspected Gas Hydrate Localities. V. 8. Basin Analysis, Formation and Stability of Gas Hydrates in the Northern California Offshore."
- Krason, J. and M.S. Ciesnik (1987), U.S. Department of Energy DOE/MC/21181-1950 (DE88001008), "Geological Evolution and Analysis of Confirmed or Suspected Gas Hydrate Localities. V. 10. Basin Analysis, Formation and Stability of Gas Hydrates of the Aleutian Trench and the Bering Sea."
- Kuperman, W.A., M.F. Werby, K.E. Gilbert, and G. Tango (1985), "Beam Forming on Bottom-interacting Tow-ship Noise," *IEEE J. Oceanic Eng.* **OE-10**, 290-298.
- Kvenvolden, K.A. (1988), "Methane Hydrates and Global Climate," *Global Biogeochemical Cycles* **2**, 221-229.

- Kvenvolden, K.A. and L.A. Barnard (1982), "Hydrates of Natural Gas in Continental Margins," *American Association of Petroleum Geologists Memoir* **34**, 631-64.
- Kvenvolden, K.A., L.A. Barnard, and D.H. Cameron (1982), "Pressure Compensated Core Sampling of Gas Hydrates, DSDP Site 533, Leg 74. in *Initial Reports of the Deep Sea Drilling Project 76* (draft).
- Kvenvolden, K.A. and A.K. Cooper (1987), "Natural Gas Hydrates of the Offshore Circum-Pacific Margin—A Future Energy Resource?" in *Transactions of the Circum-Pacific Energy and Mineral Resources Conference*, E. K. Horn (ed.), Circum-Pacific Council for Energy and Mineral Resources, 285-301.
- Kvenvolden, K.A. and T.J. McDonald (1982), "Gas Hydrates in the Middle America Trench, DSDP Leg 84," *Eos, Transactions of the Am. Geophys. Union* **63**, 101.
- Kvenvolden, K.A. and M.A. McMennamin (1980), "Hydrates Of Natural Gas: A Review of Their Geologic Occurrence." U.S. Geological Survey Circular 825.
- Lachenbruch, A.H., P.S. Galanis, and T.H. Moses (1988), "A Thermal Cross Section for the Permafrost and Hydrate Stability Zone in the Kuparuk and Prudhoe Bay Oil Fields," in U.S. Geological Circular 1016, *Geologic Studies in Alaska*, J.P. Galloway and T.D. Hamilton (eds), 47-51.
- Lancelot, Y. and J.I. Ewing (1973), in *Initial Reports on Deep Sea Drilling Project*, C.D. Hollister, J.I. Ewing, et al. (eds), U.S. Government Printing Office, Washington, DC, pp. 791-799.
- Lavoie, D. (1985), "Geoacoustic Models: Washington State Continental Margin," NORDA Report 85.
- Lawson, W.F., Reddy, S.M., Gregoire, C.E. and Vassallo, K.L. (1984) "Acoustic Velocity and Electrical Property Measurements in the DSDP Methane Hydrate Core," Internal Paper prepared for presentation. U.S. Department of Energy, Morgantown Technology Center.
- Makogon, Yu.F. (1981), in *Hydrates of Natural Gas* (Penn Well Publishing Company, Tulsa, OK).
- Makogon, Yu.F. (1988), "Gas-hydrate Accumulations and Permafrost Development," *Proceedings Fifth International Conference*, K. Senneset (ed.), 95-101.
- Malone, R.D. (1983), "Interdisciplinary Gas Hydrate Literature Bibliography," U.S. Department of Energy DOE/METC-83-65 (DE83013785).
- Manley, P.L. and R.D. Flood (1988), "Cyclic Sediment Deposition within Amazon Deep-sea Fan," *Am. Assoc. Petroleum Geologists* **72**, 912-925.
- Manley, P.L. and R.D. Flood, "Anomalous Sound Velocities in Near-surface, Organic-rich Gassy Sediments: Central Argentine Basin," *Deep-Sea Research* **36**, 611-623.
- Markle, R.G., discussions at NAVOCEANO, Stennis Space Center, July, 1989 (private communication).
- Markl, R.G. and G.M. Bryan (1983), "Stratigraphic Evolution of Blake Outer Ridge," *Am. Assoc. Petroleum Geol. Bull.* **67**, 666-683.
- Markl, R.G., G.M. Bryan, and J.I. Ewing (1970), "Structure of the Blake-Bahama Outer Ridge," *J. Geological Res.* **75**, 4539-4555.
- Matthews, J., discussions at NORDA, April, 1989 (private communication).
- Max, M.D. (1978), "Tectonic Control of Offshore Sedimentary Basins to the North and West of Ireland," *J. Petroleum Geology* **1**, 103-110.
- Max, M.D., "Acoustic and Navy Significance of Subsea Permafrost and Gas Hydrates in Arctic Continental Shelves," in preparation.
- McCammon, D.F. (1988), "Fundamental Relationships Between Geoacoustic Parameters and Predicted Bottom Loss Using a Thin Layer Model," *J. Geophys. Res.* **93**, 2363-2369.
- McCartney, B.S. and B. McK. Bary (1965), "Echo-sounding on Probable Gas Bubbles from the Bottom of Saanich Inlet, British Columbia," *Deep-Sea Res.* **12**, 285-294.

- Monet, W.F., R.R. Greene, and C.W. Spofford (1983), "Development of Geoacoustic Areas for the Bottom-Loss Upgrade (BLUG)," SAI-83-976-WA, Science Applications, Inc., McLean, VA.
- Naval Oceanographic Office (1988(a)), "Data Base Description for Low-Frequency Bottom Loss (LFBL)," Report OAML-DBD-12A.
- Naval Oceanographic Office (1988(b)), "Data Base Description for High-Frequency Bottom Loss (HFBL)," Report OAML-DBD-11A.
- Nelson, C.H., D.R. Thor, M.W. Sanstrom and K.A. Kvenvolden (1979). "Modern Biogenic Gas-generated Craters (Sea Floor "Pockmarks") on the Bering Shelf, Alaska," *Geol. Soc. Am. Bull.* **90**, 1144-1152.
- Oberhänsli, R. and P. Stoffers (eds) (1988), "Hydrothermal Activity and Metalliferous Sediments on the Ocean Floor," *Marine Geol.* **84**.
- Paull, C.K. and W.P. Dillon (1981), "The Appearance and Distribution of the Gas Hydrate Reflector off the Southeastern United States," US Geological Survey Open File Report 80-88.
- Paull, C.K., E.A. Schmuck, and J. Chanton (1989), "Carolina Trough Diapirs: Salt or Shale?" *Eos* **70**, 370, abstract.
- Pearson, C.F., P.M. Halleck, P.L. McGuire, R. Hermes, and M. Mathews (1983), "Natural Gas Hydrate Deposits: A Review of In Situ Properties," *J. Phys. Chem.* **87**, 4180-4185.
- Pfeifer, H.-R., H. Oberhänsli, and W. Epprecht (1988), "Geochemical Evidence for a Synsedimentary Hydrothermal Origin of Jurassic Iron-manganese Deposits at Gonzen (Sargans, Helvetic Alps, Switzerland)," in *Hydrothermal Activity and Metalliferous Sediments on the Ocean Floor*, R. Oberhänsli, and P. Stoffers (eds.), *Marine Geol.* **84**, Special Issue, 257-272.
- Pinet, P.R., P. Popenoe, M.L. Otter, and S.M. McCarthy (1981), Chapt. 8, "An Assessment of Potential Geologic Hazards of the Northern and Central Blake Plateau," in *Environmental Geologic Studies on the Southeastern Atlantic Outer Continental Shelf (1977-1978)*, P. Popenoe (ed.), U. S. Geological Survey Open-File Report 81-582-A, 8-1, pp. 8-48.
- Premuzic, E.T. (1980), "Organic Carbon and Nitrogen in the Surface Sediments of World Oceans and Seas: Distribution and Relationship To Bottom Topography." BNL 51084, Brookhaven National Laboratory, New York.
- Prior, D.B., E.H. Doyle, and M.J. Kaluza (1989), "Evidence for Sediment Eruption on Deep Sea Floor, Gulf of Mexico," *Science* **243**, 517-519.
- Rokeongen, K. and A. Tegdan (1983), Kartlegging av Grunn Gass. Erfaring med Offshore Instrumentering, Konferanse p Geilo.
- Romankevich, E.A. (1984), *Geochemistry of Organic Matter in the Ocean* (Springer, New York).
- Rutherford, R.S. and K.E. Hawker (1978), "Effects of Density Gradients on Bottom Reflection Loss for a Class of Marine Sediments," *J. Acoust. Soc. Am.* **63**, 750-757.
- Scholl, D.W. and J.S. Creager (1973), "Geologic Synthesis of Leg 19 (DSDP) Results: Far North Pacific, Aleutian Ridge, and Bering Sea," in *Initial Reports of the Deep Sea Drilling Project*, J.S. Creager, et al. (eds.), Vol. 19, pp. 897-913.
- Schmidt, H. (1988), "SAFARI Seismo-Acoustic Fast Field Algorithm for Range-Independent Environments," SACLANCEN Underwater Research Centre, La Spezia, Italy, Report SR-113.
- Schramm, M.W., Jr., E.J. Dedman, and J.P. Lindsey (1977), "Practical Stratigraphic Modeling and Interpretation," in *Seismic Stratigraphy—Applications to Hydrocarbon Exploration*, C.E. Payton (ed.), *Am. Assoc. Petroleum Geolo.*, Tulsa, OK, pp. 477-502.
- Sergiyenko, S.I. and V.I. Maydak (1983), "Formation Conditions for Heavy Oil Pools and Possible Hydrate Formation in the Northeastern Part of the Timan-Pechora Province," *Int. Geology Rev.* **25**, 1390-1392.
- Sheridan, R. E. et al. (1982), "Early History of the Atlantic Ocean and Gas Hydrates on the Blake Outer Ridge—Results of the Deep Sea Drilling Project Leg 76," *Geol. Soc. Am. Bull.* **93**, 876-885.

- Shipley, T.H. and B.M. Didyk (1982), "Occurrence of Methane Hydrates Offshore Southern Mexico," in *Initial Reports of the Deep Sea Drilling Project 66*, J.S. Watkins, et al. (eds.), Government Printing Office, Washington, DC.
- Shipley, T.H., M.H. Houston, R.T. Buffler, F.J. Shaub, K.J. McMillen, J.W. Ladd, and J. L. Worzel (1979), "Seismic Reflection Evidence for the Widespread Occurrence of Possible Gas-hydrate Horizons on Continental Slopes and Rises," *Am. Assoc. Petroleum Geol. Bull.* **63**, 2204-2213.
- Solheim, A. and F.R. Larsson (1987), "Seismic Indications of Shallow Gas in the Northern Barents Sea," Norsk Polarinstitutt Rapportserie Nr. 36, Map.
- Stoll, R.D. (1974), "Effects of Gas Hydrates in Sediments," in *Natural Gases in Marine Sediments*, I.R. Kaplan (ed.) (Plenum, New York), pp. 235-248.
- Stoll, R.D. and G.M. Bryan (1979), "Physical Properties of Sediments Containing Gas Hydrates," *J. Geophys. Res.* **84**, 1629-1634.
- Stoll, R.D., J. Ewing, and G.M. Bryan (1971), "Anomalous Wave Velocities in Sediments Containing Gas Hydrates," *J. Geophys. Res.* **76**, 2090.
- Sverdrup, H.U., M.W. Johnson, and R.H. Fleming (1961), in *The Oceans. Their Physics, Chemistry, and General Biology* (Prentice-Hall, Inc., Englewood Cliffs, NJ).
- Swift, J.H. (1986), "The Arctic Waters," in *The Nordic Sea*, B.G. Hurdle (ed.) (Springer, New York), pp. 128-153.
- Trevorrow, M., T. Yamamoto, A. Turgut, C. Abbott, M. Badiy, D. Goodman, and K. Ando (1988), "High Resolution Bottom Shear Modulus Profiler Experiments on the New Jersey Shelf, Summer, 1987," Geo-Acoustics Laboratory, University of Miami, Rosentiel School of Marine and Atmospheric Science, Report 1006.
- Trofimuk, A.A., Yu. F. Makogon, and V.S. Ykushev (1986), "Dynamics of the Zone of Hydrate Formation and its Effect on The Temperature Regime of the Cryolithozone," *Sov. Geol. and Geophys.* **27**, 1-7.
- Tucholke, B.E., G.M. Bryan, and J.I. Ewing (1977), "Gas-hydrate Horizons Detected in Seismic-profiler Data from the Western North Atlantic," *Am. Assoc. Petroleum Geol. Bull.* **61**, 698-707.
- Urick, R.J. (1975), *Principles of Underwater Sound* (McGraw-Hill, New York).
- U.S. Department of Energy (1987), DOE/MET, NTIS:DE 87001027, "Gas Hydrates. Technology Status Report."
- Vidmar, P.J. (1979), "The Effect of Sediment Rigidity on Bottom Reflection Loss," ARL-TR-79-49, Applied Research Laboratories, University of Texas at Austin.
- Vidmar, P.J., R.A. Koch, and D.W. Oakley (1988), "Review of Bottom Interaction Research: I. Effects on Broadband Signals. II. Propagation in Shallow Water," ARL-TR-88-40, Applied Research Laboratories University of Texas at Austin.
- Vidmar and Lindberg (1987), "Propagation to Buried Hydrophone in Two Shallow Water Environments," Annual Report Under Contract N00014-78-C-0113. Applied Research Laboratories, Austin, Texas ARL-TR-87-21 Report.
- Vogt, P.R. (1986), "Seafloor Topography, Sediments, and Paleoenvironments," in *The Nordic Seas*, B.G. Hurdle (ed.) (Springer, New York), pp. 237-410.
- Von Huene, R. (1980), "Leg 67: The Deep Sea Drilling Project Mid-America Trench Transect off Guatemala," *Geol. Soc. Am. Bull.* **91**, 421-432.
- White, R.S. (1985), "Frozen Energy in the Depths of the Oceans," *New Scientist* **107** (1463), 29.
- Widness, M.B. (1973), "How Thick is a Thin Bed?" *Geophys.* **38**, 1176-1180.

MICHAEL D. MAX

- Williams, H. and M.D. Max (1980), "Zonal Subdivision and Regional Correlation in the Appalachian-Caledonian Orogen." in *The Caledonides in the USA*, D.R. Wones (ed.), Proceedings IGCP Project 27 Symposium, Virginia Polytechnic Institute and State University Memoir 2, pp. 57-62.
- Wingfield, R.T.R. (1985), "Sea Bed Sediments and Quaternary Geology, Isle of Man," Sheet 54N-08W. 1:250,000, British Geological Survey.
- Wittebolle, R.J. and D.C. Sege (1985), "Analysis of a Production Well Through Sediments Containing Gas Hydrates," Conference Arctic '85 Proceedings, F.L. Bennett, and J.L. Machemehl (eds), *Am. Soc. Civil Eng.*, pp. 178-184.
- Yefremova, A.G. and B.P. Zhizhehenko (1975), "Occurrence of Crystal Hydrates of Gases in Sediments of Modern Marine Basins," *Doklady Academy of Sciences USSR*, English Translation 214, pp. 219-220.
- Zhou, J-x. and X-z Zhang (1987), "Geoacoustic Parameters in a Stratified Sea Bottom from Shallow-water Acoustic Propagation," *J. Acoustical Soc. Am.* 82, 2068-2074.
- Zonenshayn, L.P., I.O. Murdmaa, B.V. Baranov, A.P. Kuznetsov, V.S. Kuzin, M.I. Kuz'min, G.P. Avdeyko, P.A. Stunzhas, V.N. Lukashin, M.S. Barash, G.M. Valyashko, and L.L. Demina (1987), "An Underwater Gas Source in the Sea of Okhotsk West of Paramushir Island," *Oceanology* 27, 598-602.